Thesis for the Master of Science degree in

Molecular Biosciences

Investigation of p21 expression in melanoma

Sima Zolfaghari Golmakani

Department of Biosciences

Faculty of Mathematics and Natural Sciences

UNIVERSITY OF OSLO

June 2014

Oslo University Hospital

Table of Contents

ACKNOWLEDGEMENTS

The work presented in this thesis was carried out during the period from January 2013-June 2014 at the Department of Tumor Biology, Institute for Cancer Research, Oslo University Hospital. The thesis is a part of the master program Molecular Biosciences at the University of Oslo.

My sincere gratitude goes to my supervisor, Sigurd Leinæs Bøe. I am grateful for your excellent laboratory guidance, day-to-day assistance, patience, encouragement, and support. Thank you for your valuable experiences you shared with me not only in the lab work and writing process, but also in my life. You always have given me enthusiasm and motivation.

I am deeply grateful to Eivind Hovig, for providing me the opportunity to pursue my Master thesis in his laboratory. Your openess to my ideas, constructive feedback and our weekly seminars, which have broadened my scientific knowledge has been of great value.

To the "group members", specially Ane Sager Longva and Geir Frode Øy, thank you for all your enthusiasm, encouragement and technical support. It was a pleasure to be a part of such a vibrant and enthusiastic group. Thanks to Eyrun Thune, who always offered wonderful company during the breaks in my office.

I also would like to extend my gratitude to my friends Marie, Christel and Shadab for sharing with me great moments, encouragement and belief in me. A special thanks goes to Mehdi Tarabi for solving the computer application problems throughout this project. You always made me hopeful and tireless to confront various obstacles and difficulties, although you were far from me.

Last but not least, a great thank you to my family specially my beloved mother and father for their patience, support and helping me to come to Norway and follow my dreams. Thank you for always believing in me and providing me the love, optimism and comfort that can only come from family.

Oslo, June 2014

Sima Zolfaghari Golmakani

ABSTRACT

Melanoma is considered as one of the most aggressive forms of skin cancer and treatment is unsuccessful due to development of resistance. The complexity and different genetic alterations of melanoma makes it difficult to target. Therefore, finding the right treatment combination, attacking several signaling pathways at the same time might improve patient survival.

To understand melanoma progression and metastasis it is necessary to have insight into signaling pathways and their downstream effectors, such as p21 (WAF1/Cip1), a regulator of cell cycle progression. p21 is often deregulated in human cancers and has previously been shown to induce growth arrest/senescence. In the present study, we investigated the expression and regulation of p21 in a melanoma cell line panel consisting of 17 cell lines. We found a strong correlation between p21 mRNA and protein levels in all cell lines, except for the LOX cell line. We then correlated p21 expression levels against the progression of melanoma without detecting any obvious pattern. Furthermore, we detected a strong correlation between p21 expression levels and the p53 status in all of the cell lines. The correlation between p53 and p21 was also found after treating A375 and SKMEL28 with inhibitors against the MAPK- and cAMP-pathways. These latter results suggest that p21 is tightly controlled by the p53 tumor suppressor gene. However, p21 expression has also been shown to be regulated independently of p53. To address this, we investigated the expression of a number of transcription factors that previously have been reported to bind to the p21 promoter. When comparing these expression levels with p21 expression we did not find any obvious correlation, either positve or negative. The role of p53-independent transcriptional regulation of p21 is not fully understood and further studies needs to be carried out to disclose its role.

ABBREVIATIONS

AKT	Protein kinase B (PKB)
α-MSH	Alpha-melanocyte-stimulating hormone
AMPKα	AMP-activated protein kinase alpha
BCL-2	B-cell lymphoma 2
BMI1	Polycomb ring finger oncogene
B-RAF	Mitogen activated protein kinase kinase kinase (MAPKKK)
cAMP	Cyclic adenosine monophosphate
c-KIT	Proto-oncogene c-Kit, tyrosine-protein kinase Kit
Ct	Cycle threshold
ddH_2O	Double destilled water
DMSO	Dimethyl sulfoxide
DNA	Deoxyribonucleic acid
dNTP	Deoxyribonucleotide triphosphates
DTIC	5-[3,3-dimethyl-1-triazenyl]-imidazole-4-carboxamide. (Dacarbazine)
EDTA	Ethylenediaminetetraacetic acid
EGFR	Human epidermal growth factor receptor 1
CBX7	Chromobox homolog 7
CDC6	Cell division cycle 6
CDKN1A	Cyclin-dependent kinase inhibitor 1A
CDKN2A	Cyclin-dependent kinase inhibitor 2A
CEBPA	CCAAT/enhancer binding protein (C/EBP), alpha
CITED2	Cbp/p300-interacting transactivator, with Glu/Asp-rich carboxy-Terminal domain, 2
CREB	cAMP responsive element binding protein
EGF	Epidermal growth factor
ELK1	Member of ETS oncogene family
ELK4	Member of ETS oncogene family
EP300	E1A binding protein p300
ERK	Extracellular signal-regulated kinase

ETS 1	V-ets erythroblastosis virus E26 oncogene homolog 1 (avian)
FBS	Fetal bovine serum
FDA	US Food and Drug Administration
HRP	Horseradish peroxidase
IFN-α	Interferon alfa-2b
IL-2	Interleukin-2
ID1	Inhibitor of DNA binding 1, dominant negative helix-loop-helix protein
ID2	Inhibitor of DNA binding 2, dominant negative helix-loop-helix protein
ID3	Inhibitor of DNA binding 3, dominant negative helix-loop-helix protein
JNK	c-Jun N-terminal kinases
JUNB	Jun B proto-oncogene
KDa	Kilo Dalton
kHz	Kilohertz
LDS	Lithium dodecyl sulfate
LDS-PAGE	Sodium dodecyl sulfate-polyacrylamide gel electrophoresis
siRNA	Small interfering RNA
miRNA	Micro RNA
SKMEL28	Sloan-Kettering Institute melanoma cell line 28
Taq	*Thermos aquaticus*
TBS	Tris-buffered saline
UPL	Universal Probe Library
WM1366	Wistar institute melanoma cell line number 1366
WM983A	Wistar institute melanoma cell line number 983A
WM1341B	Wistar institute melanoma cell line number 1341B
WM239A	Wistar institute melanoma cell line number 239A
WM35	Wistar institute melanoma cell line number 35
WM115	Wistar institute melanoma cell line number 115
WM1382	Wistar institute melanoma cell line number 1382
WM852	Wistar institute melanoma cell line number 852
WM266-4	Wistar institute melanoma cell line number 266-4
WM9	Wistar institute melanoma cell line number 9

WM45.1	Wistar institute melanoma cell line number 45.1
FEMX-I	Human melanoma cell line
FEMX-V	Human melanoma cell line
A375	Human melanoma cell line
LOX	Human melanoma cell line
MEWO	Human melanoma cell line
MAPK	Mitogen-activated protein kinase
MAPK-pathway	Mitogen-activated protein kinase (MAPK) signal transduction cascade
MC1R	Melanocortin 1 receptor
MEK	MAPK extracellular kinase
MITF	Microphtalmia-associated transcription factor
mTOR	Mechanistic target of rapamycin
MYC	v-myc avian myelocytomatosis viral oncogene homolog
MOPS	3-(N-morpholino) propane sulfonic acid
mRNA	Messenger RNA
NRAS	Neuroblastoma ras viral oncogene homolog
nt	Nucleotides
p16	Cyclin-dependent kinase inhibitor 2A (p16) (CDKN2A)
p21	Cyclin-dependent kinase inhibitor 1A (P21, WAF1, CIP1) (CDKN1A)
p-AKT	Phosphorylated AKT
p-ERK1/2	Phosphorylated ERK1/2
p-AMPKα	Phosphorylated AMPKα
p-CREB	Phosphorylated CREB
p-STAT1	Phosphorylated STAT1
PCR	Polymerase chain reaction
PLX	Plexxikon, vemurafenib
UO126	Mek1/2 inhibitor
H-89	PKA inhibitor
BI-D1870	RSK inhibitor
PEA3	Ets variant 4 (ETV4)
PI3K	Phosphatidylinositol-3 kinase

PKA	Protein kinase A
PRMT6	Protein arginine methyltransferase 6
PTEN	phosphatase and tensin homolog deleted on chromosome 10
RTK	Receptor tyrosine kinase
RAS	Ras viral oncogene homolog protein
RNA	Ribonucleic acid
Rnase	Ribonuclease
RPMI	Roswell Park Memorial Institute
RT-PCR	Reverse transcriptase PCR
SALL2	Sal-like 2
SP1	Sp1 transcription factor
SP3	Sp3 transcription factor
SREBF1	Sterol regulatory element binding transcription factor 1
STAT1	Signal transducer and activator of transcription 1
TBX2	T-box 2
TBX3	T-box 3
TCF3	Transcription factor 3
TFAP2A	Transcription factor AP-2 alpha (activating enhancer binding protein 2 alpha)
TFAP2C	Transcription factor AP-2 gamma (activating enhancer binding protein 2 gamma)
TP53	Tumor protein p53, p53

SECTION I: INTRODUCTION

1.1 Cancer

Cancer is a genetic disease involving unregulated cell growth and cell divisions, forming malignant tumors, invading nearby tissues, and metastasizes to distant organs [1]. This disease is responsible for one in eight deaths throughout the world [1, 2]. It is known that cancer is difficult to treat and cure due to its genetic complexity and heterogeneity [2, 3]. Somatic mutations (such as point mutations, insertions and deletions of bases), DNA rearrangements (caused by DNA breakage), copy number changes (of DNA segments) and epigenetic alterations contribute to the complexity and heterogeneity of cancer [3, 4]. In general, no single mutation can cause cancer alone, but multiple mutations in key regulatory genes may put the cell at risk [5]. The tumor microenvironment (consisting of neighboring blood vessels, immune cells, fibroblasts, signaling molecules, the extracellular matrix (ECM) and other cells) have also been found to affect the process of tumor initiation, growth, progression and metastasis [6]. Deregulated signal pathways in and around tumor cells, as well as the absence of many regulatory checkpoints results in aberrant uncontrolled growth. A set of phenotypic properties essential for cancer development termed the hallmarks of cancer have been proposed by Hanahan and Weinberg (2011) and are presented in figure 1.1.

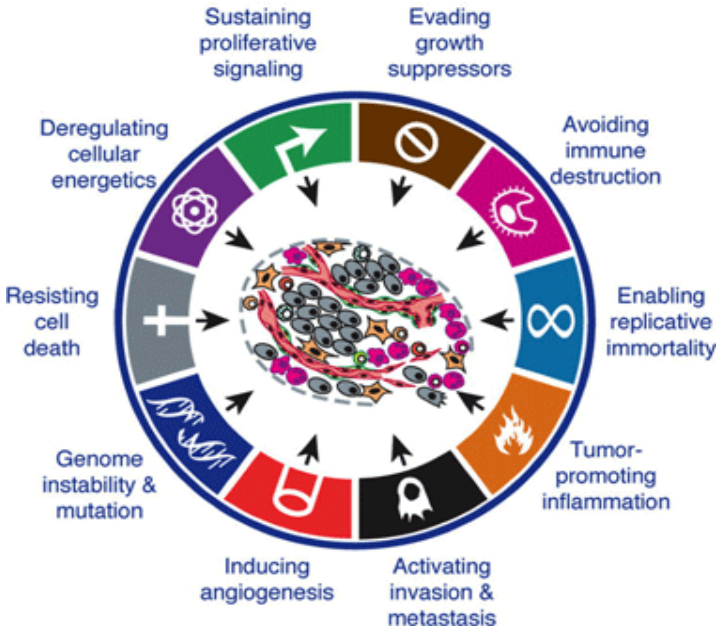

Figure 1.1. *The hallmarks of cancer. The figure is reproduced with permission from Hanahan and Weinberg, 2011 [6].*

Mutations promoting one (or multiple) of these hallmarks make the cell more likely to persist, survive, and divide uncontrolled [7]. Indeed, it is indicated that no two cancers are identical at the molecular level and that different cancers have diverse response to therapy [3, 8].

1.2 Melanoma

Melanoma is an aggressive form of skin cancer originating from melanocytes found in the skin and eyes. Skin is made up of two main layers: the epidermis (outer layer of skin) and the dermis (inner layer of the skin). The deepest layer of the epidermis, just above the dermis, contains melanocytes. The melanocytes can differentiate from embryonic stem cells and are responsible for producing the pigment melanin that plays a role in coloration of skin for protection against UV radiation [9]. Melanoma is considered to be the deadliest form of skin cancer and is known for its resistance to conventional therapy. However, development of novel personalized targeted therapy strategies may bring new hope [10-12]. An estimated number of 166.900 patients were diagnosed with melanoma in developed countries in 2011 [13]. According to the Cancer registry of Norway, melanoma is one of the most common types of cancer in Norway, with an increasing rate of incidence and mortality of 1718 and 325 in 2011, respectively [14]. Thereby, Norway is one of the countries with highest incidence and mortality rates of malignant melanoma in Europe [15]. Exposure to ultraviolet (UV) radiation from the sun, which makes alterations in the genome is a major risk factor for development of melanoma [9, 10]. People exposed to bright sunlight year-round, people who use tanning beds, those with fair skin and moles, and people with family disease history have an increased risk of developing melanoma. [15, 16].

1.2.1 Melanoma tumor progression

Melanoma can occur anywhere in the body where melanocytes (melanocytes are derived from the neural crest during development) are found. Melanoma begins when normal melanocytes change and grow uncontrollably, forming a mass called a tumor. A tumor can be benign (noncancerous) or malignant (cancerous, meaning it can spread to other parts of the body). The tumor progression from melanocyte to melanoma is illustrated in figure 1.2.

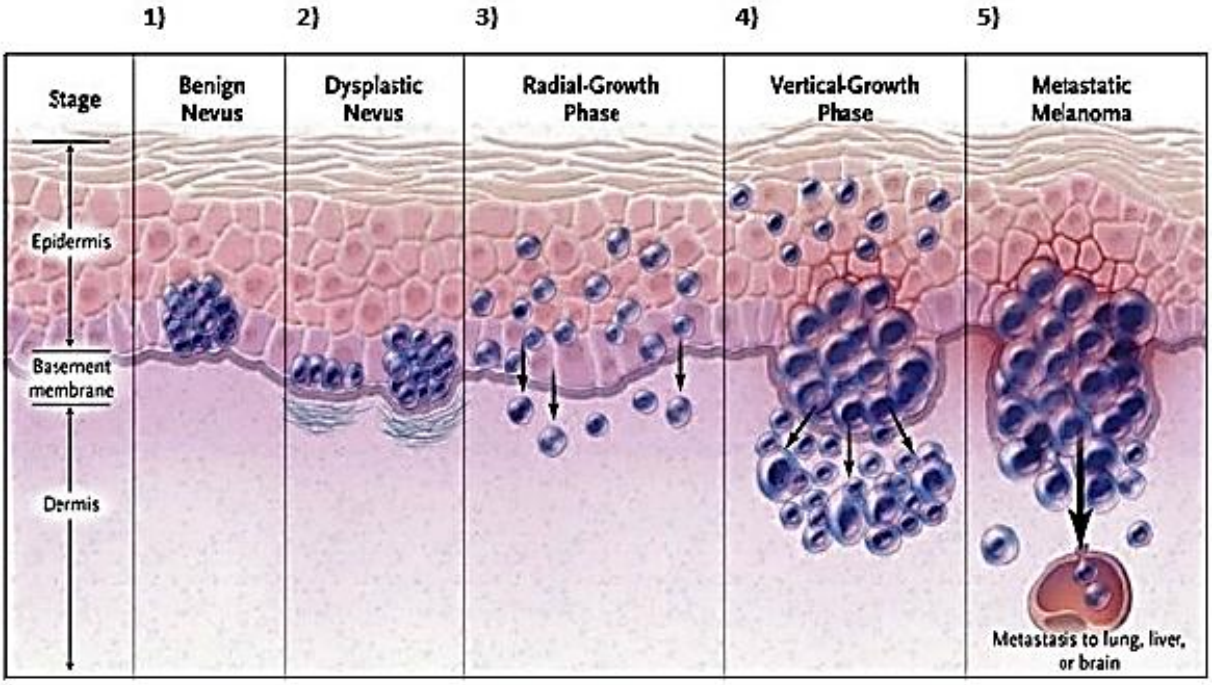

Figure 1.2. *The figure shows the steps of melanoma progression. 1) Benign nevus 2) Dysplastic nevus 3) Radial-growth phase 4) Vertical-growth phase 5) Metastatic melanoma. The figure is reproduced with permission from Miller and Mihm, 2006 [17].*

The steps of tumor progression from normal melanocyte to melanoma are as follows:

1) Mutations in normal melanocytes form benign nevus in epidermis.

2) Abnormal growth of melanocytes in a pre-existing nevus or new location resulting in a pre-malignant lesion, dysplastic/atypical nevi.

3) Radial growth: melanocytes acquire ability to proliferate horizontally in the epidermis (non-tumorigenic primary melanomas without metastatic competence).

4) Vertical growth: numerous biochemical events allow malignant cells to invade basement membrane and proliferate vertically in the dermis with metastatic potential (tumorigenic primary melanomas with competence for metastasis).

5) Metastasis: malignant melanocytes spread to other areas of the body by entering blood or lymphatic vessels and form tumors at distant sites. Spreading occurs usually first to lymph nodes, then to skin, subcutaneous soft tissue, lungs and the brain [17, 18].

1.2.2 Melanoma metastasis

The most dangerous aspect of melanoma is its ability, in later stages, to spread (or metastasize) to other parts of the body. The spread occurs through the lymphatic system and/or the blood vessels. Melanoma can spread to the subcutaneous tissue which lies underneath the skin, the lymph nodes, and to other organs such as the lungs, liver, to bone or to the brain [19]. Metastasis is typically described as a multistep process involving tumor cells ability to invade normal surrounding tissue through entering the blood circulation. The other steps of the metastasis include tumor cells which can adhere, extravagate, survive, and grow in the target organ [20, 21]. In order for a tumor cell to metastasize and form a clinically detectable and potentially lethal metastasis, it must complete a series of steps which is presented in figure 1.3.

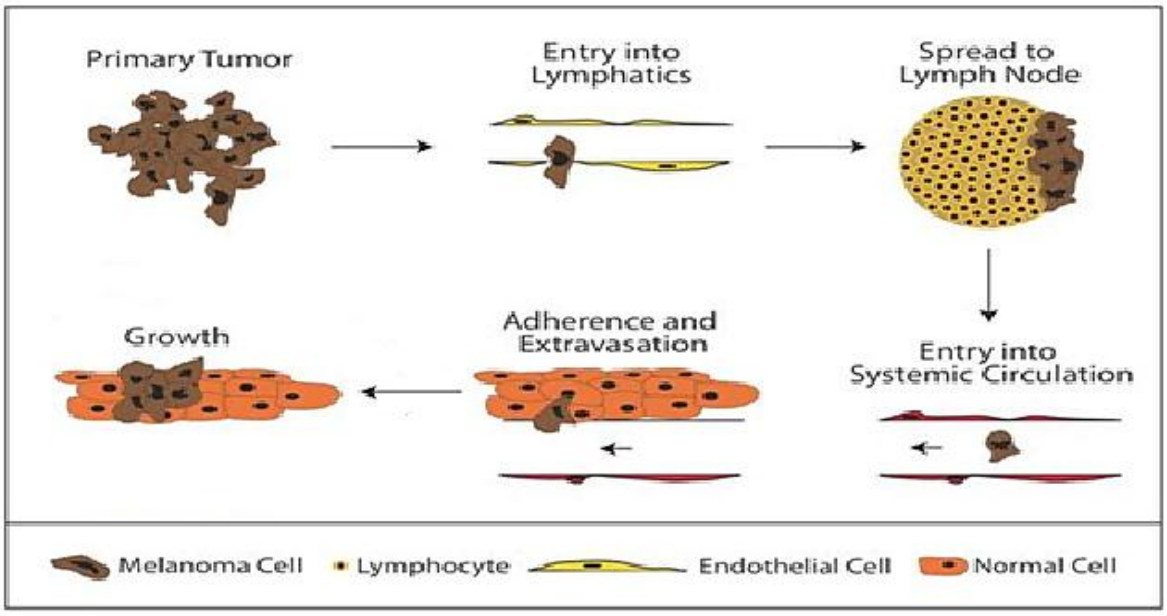

Figure 1.3. *The figure shows metastatic process of melanoma. The formation of a primary tumor is followed by tumor cells that are able to enter into the lymphatic vessels. Tumor cells then travel to the lymph node and subsequently enter into the systemic circulation via the thoracic duct. After that, tumor cells need to be able to survive in the circulation and they must adhere to the microvasculature of a target organ. The tumor cells then extravagate, and subsequently proliferate in order to develop into a secondary tumor and form a clinically relevant metastasis. Figure reproduced with permission from Damsky and Bosenberg, 2010 [20].*

The mechanisms regulating either success or failure at any step in the metastatic process are likely important and probably differ amongst different melanomas and different target organs [18, 20, 22].

1.2.3 Signaling pathways relevant for melanoma development

To understand melanoma development and metastasis it is necessary to have insight into signaling pathways that control proliferation and survival. Signaling pathways make cascades for transferring information from extracellular signals through receptors towards the nucleus where the expression of different genes is regulated. Complex changes in these pathways thus contribute to melanoma development and progression by deregulating genes that may lead to increased survival, proliferation, invasion, and angiogenesis [23]. The most prominent signaling pathways that are revealed to affect the melanoma development and progression are the MAPK- and PI3K/AKT-pathways, Wnt/β-Catenin, and the α-MSH signaling pathways [24]. The master regulator of melanocyte proliferation, survival and differentiation is Microphtalmia transcription factor (MITF). The MITF gene is strongly influenced by multiple upstream pathways, including c-KIT, Wnt/β-Catenin, and α-MSH [24, 25]. A simplified illustration of these pathways is shown in figure 1.4. c-KIT, Wnt and α-MSH signaling cascades are shown in purple, yellow and blue, respectively.

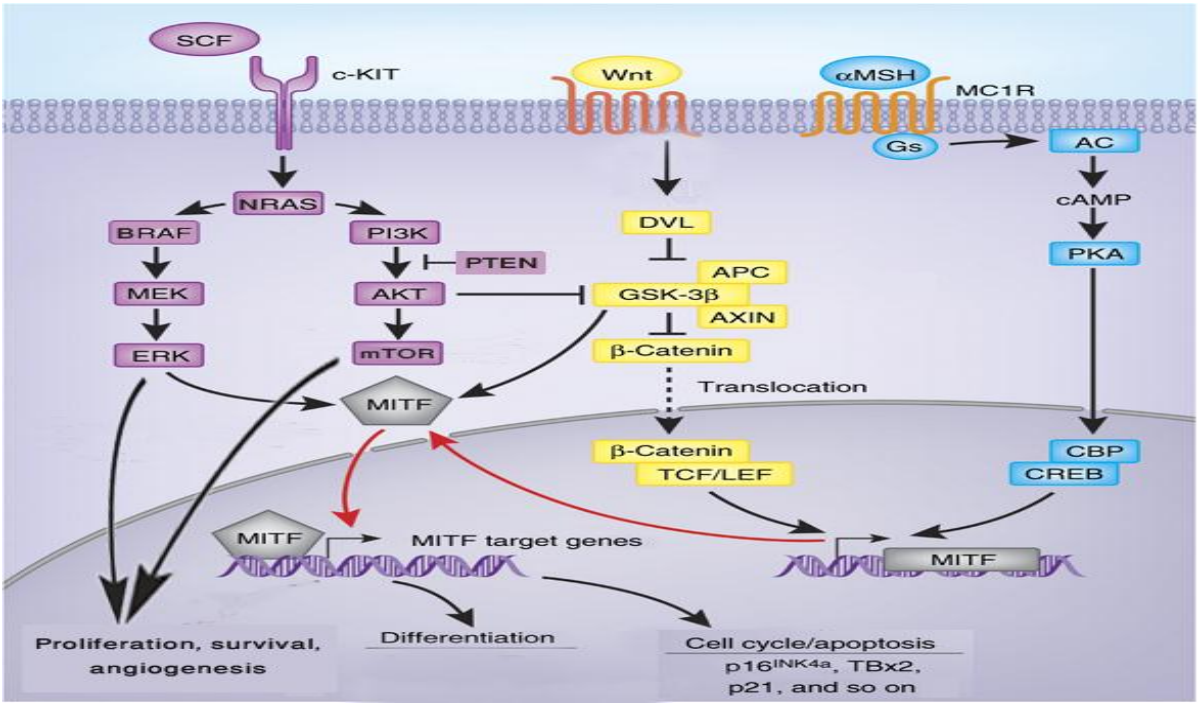

***Figure 1.4**. The figure shows signaling pathways often dysregulated in melanoma. Activation of c-KIT, by the stem cell factor (SCF) receptor tyrosine kinase triggers many downstream events, including activation of the MAPK and PI3K pathways. Activation of the Wnt/β -Catenin pathway results in the stabilization and nuclear translocation of β-Catenin. Activation of α-MSH/cAMP pathway results in MITF promoter activation. Activated MITF can then regulate a vast number of genes, including p21. Figure adapted and reproduced with permission from Hocker and Sing, 2008 [24].*

It is believed that deregulation of the PI3K/AKT-pathway, along with a constitutively active MAPK-pathway, promotes the development of melanoma by increasing cell proliferation and enhancing the resistance to apoptosis [23, 26].

1.2.4 Genetic alterations in melanoma

Understanding the molecular genetics underlying melanoma development and progression is necessary in order to develop rational treatments for the disease. Melanomas that occur in humans are usually deregulated in the RAS pathway, either by mutations or up-regulation of surface receptors (e.g. c-KIT and EGFR) or by mutations in intracellular signaling (e.g. NRAS, BRAF, and NF-1), which leads to elevated levels of activated ERK. In addition, mutations or epigenetically silencing of the CDKN2A (p16) gene is frequent. Since RAS also activates the phosphatidylinositol 3-kinase-PTEN-Akt pathway, NRAS mutations also results in elevated levels of activated Akt. Of note, melanoma cells have either NRAS or $BRAF^{V600E}$ mutation; they are never present within the same cell. In addition to NRAS, BRAF, and p16 mutations, a number of other genes have been found to be mutated in melanoma such as, PTEN, c-KIT, p53, CDK4, MC1R, and EGFR etc. Understanding the role of alterations in the pathways involved in melanoma and their interactions may provide important information that can be used in therapeutic settings. Table 1.5 shows the frequency of some important genetic mutations that are occurring in metastatic melanoma tumors.

***Table 1.5.** Genetic alterations and their incidences in melanoma tumor specimens.*

Mutation	**Incidence**	**Reference**
$BRAF^{V600E}$	~50%	[12]
NRAS	15-25%	[27]

CDKN2A (p16)	30-70%	[24]
PTEN	15-50%	[24]
p53	13%	[24]
c-KIT	0-39%	[24]
MITF amplification	21%	[25]

1.2.5 Melanoma treatment options

Melanoma is shown to be resistant to radiation therapy, chemotherapy and immunotherapy [26, 28]. Moreover, melanoma is a heterogeneous disease and the modifications within the tumors and metastases make it difficult to treat by targeted therapy [29, 30]. The study of tumor progression has been an important focus for the diagnosis of melanoma and is important for the prognosis prediction. If the tumor is detected at an early stage, before it has invaded into the dermis, it can usually be removed surgically or in combination with conventional chemotherapy, which provides a cure for about 99% of the patients [11, 31]. However, in 10% of the incidences the disease has developed into the late-stage melanoma, which rarely responds to existing therapies [26, 32]. An overview over some exciting melanoma treatment options and their mechanism of actions are shown in table 1.6.

Table 1.6 *shows an overview over various treatment options for the melanoma disease.*

Treatment	**Inhibition**	**Reference**
Imatinib	RTK (c-KIT)	[33]
Erlotinib, gefitinib	RTK (EGFR)	[33]
Trastuzumab	RTK (HER2)	[33]
Farnesyl transferase inhibitors	NRAS	[24]
Rapamycin	mTOR	[33]
Sorafenib	BRAF	[33]
Vemurafenib	$BRAF^{V600E}$	[34]
Mek inhibitors	MEK	[24]

CDK inhibitors	CDKN2A	[24]
Dacarbazine (DTIC)	Cell proliferation	[35]
Interleukin-2 (IL-2)	IL-2 receptor, AKT	[36]
Ipilimumab	CTLA4	[36]

Dacarbazine (DTIC), an alkylating agent, was until recent the standard treatment option for patients with advanced stage melanoma but unfortunately, the response rate for single agent treatment with DTIC is low (7-13%) with severe side effects [28, 31, 36]. Recently, approval of two promising more specifically targeted therapeutic approaches, ipilimumab and vemurafenib, have led to increasing understanding of melanoma characteristic and biology [31]. Ipilimumab is a monoclonal antibody that blocks cytotoxic T-lymphocyte-associated antigen 4 (CTLA4) on lymphocytes and thereby stimulating the immune system against the cancer cells. This strategy has been associated with enhanced overall survival [37], but the response rate is unfortunately low [31]. Another drug, vemurafenib, also called plexxikon (PLX4032), is a potent kinase inhibitor that shows selectivity against the $BRAF^{V600E}$ mutation. Vemurafenib has received FDA (US Food and Drug Administration) approval and is known to induce tumor regression in 70% of patients with late stage metastatic melanoma [34, 36, 38]. The $BRAF^{V600E}$ mutation is a good candidate for therapy in tumors with constitutive activated and deregulated $BRAF^{V600E}$ [39]. Unfortunately, the duration of the response is short and most patients develop resistance to the drug, which outcomes in relapse [31]. The drug resistance usually involves reactivation of the MAPK pathway, activation of receptor tyrosine kinases (RTKs) or activation of the PI3K/AKT-pathway [34]. However, ongoing studies have suggested that combination therapy targeting multiple pathways along with Vemurafenib may improve patients' survival [10, 34, 40].

1.3 $p21^{WAF1/CIP1}$ in melanoma

p21 / WAF1/ CIP1 (hereafter called p21) also known as cyclin-dependent kinase inhibitor 1 or CDK-interacting protein 1 (CIP1) or wild-type p53-activated factor (WAF1) is a protein that is encoded by the CDKN1A gene located on chromosome 6 (6p21.2) in the human genome [41, 42]. CDK inhibitors are negative regulators of cell proliferation and are

often deregulated in human cancers. The p21 protein binds and inhibits the activity of CDK4/6 complexes, cyclin E-CDK2 and cyclin B-CDK1, and thus functions as a regulator of cell cycle progression at G1 and S phase [42-45]. The ability of p21 to inhibit the cell cycle have been shown to induce growth arrest and in some occasions senescence [46, 47]. In addition, p21 may function as a tumor promoting factor by preventing apoptosis [46, 47].

Independently of p53 status, it is reported that p21 expression is absent in approximately 30% and 40% of the primary and metastatic melanomas, respectively. In most cases, there is a good correlation between p21 mRNA and protein expression, which might suggest that the protein expression is mainly regulated transcriptionally [48].

1.3.1 Transcriptional regulation of p21

The p21 promoter region

A number of transcription factor binding sites have been found in the p21 promoter region (see figure 1.7). Among these are binding sites for p53, which activates p21 transcription via two consensus binding sites located at -2285 and -1394 base pairs upstream from the transcription initiation site. In addition to p53, other stimuli such as growth factors, hormones, intracellular signaling molecules and tumor suppressors also regulate p21 transcription.

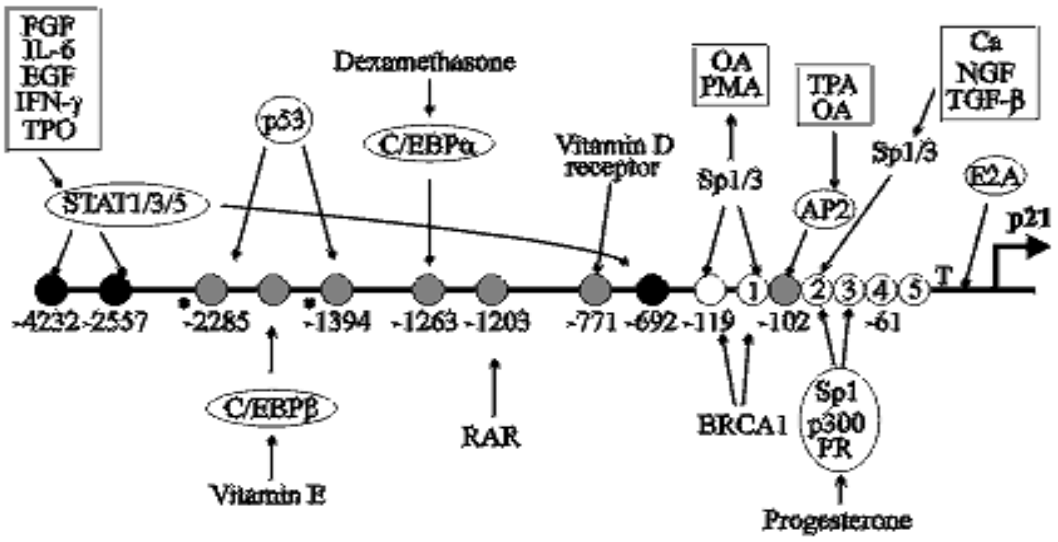

Figure 1.7. *Schematic drawing of the p21 promoter and its different response elements. Ca, calcium; C/EBP, CCAAT/enhancer binding protein; IL, interleukin; INF, interferon; OA,*

ocadaic acid; p300, cAMP-response element binding protein (CBP/p300); PMA, phorbol-12-myristate-13-acetate; PR, progesterone receptor; RAR, retinoic acid receptor; TPA, 12-O-tetradecanoyl-phorbol-13-acetate; TPO, thrombopoietin. The transcription factors Ap2, E2A, Sp1/3 and STATs are also presented. T, TATA-box; circles with an asterisk, p53-binding sites, which overlap distally with the Ets-binding sites; black circles, STAT-binding sites; white circles, Sp1 binding sites, of which the proximal five are numbered. Numbering of the base pairs correlates with the transcription start site at +1. Figure reproduced with permission from Gartel and Tyner, 1999 [49].

Known modulators of p21 expression

Many transcription factors have been shown to regulate p21 expression, and some of them are presented in table 1.8. How these transcription factors and signal pathways coordinately regulate p21 expression in response to intrinsic and extrinsic signals in melanoma is however not fully understood.

Table 1.8. *Transcription factors regulating p21 expression.*

Modulators	**Effect on p21**	**Cancer type**	**Reference**
ELK1	Activator	Colon cancer	[42]
ELK4	Activator	Prostate cancer	[50]
PEA3	Activator	Oesophageal adenocarcinoma	[51]
E1AF	Activator	Cervical cancer	[52]
ETS1	Activator	Vascular smooth muscle cells	[53]
ETS2	Activator	Fibroblast and the mink lung epithelial cells	[54]
AP-1 (JunB)	Activator	Endometrial cancer	[55]
AP-2 (TFAP2A/C)	Activator	Colorectal cancer	[56]
C/EBPα	Activator	Hepatocytes	[57]
C/EBPβ	Activator	Colorectal cancer	[58]
p300	Activator	Osteosarcoma	[59]
NF-kappaB	Activator	T-leukemia cells	[60]
E2A (E47 & E12)	Activator	B-cells	[61]
SREBP-1A/2	Activator	Liver carcinoma	[62]
SALL2	Activator	ovarian carcinoma	[63]
KLF4	Activator	Mesenchymal stem cell	[64]
RUNX1	Activator	Mesenchymal stem cell	[64]
MyoD	Activator	Myoblasts	[59]

MITF	Activator	Melanoma	[65]
CREB	Activator	Keratinocytes and myoblasts	[59]
STAT (1/3) proteins	Activator	Breast cancer	[66]
Sp1/3	Activator	Colon adenocarcinoma	[67]
Smad3/4	Activator	Liver carcinoma (hepatocytes)	[68]
TBX1	Repressor	DiGeorge syndrome	[69]
Bmi1	Repressor	Neural progenitor cells	[70]
c-Myc	Repressor	Normal kidney fibroblast	[71]
AP-1 (c-Jun)	Repressor	Liver cancer	[72]
CITED2	Repressor	Lung cancer	[73]
PRMT6	Repressor	Fibroblasts	[74]
CDC6	Repressor	Intestinal epithelium cells	[75]
CBX7	Repressor	Lung fibroblasts	[76]
SKP2	Repressor	Transformed cells	[77]
FOXM1	Repressor	Liver (hepatocytes)	[78]
ZNF76	Repressor	Osteosarcoma	[79]
Chk1	Repressor	Colorectal cancer	[80]
Brn-3a	Repressor	Neuronal cells	[81]
FBI-1	Repressor	Osteosarcoma	[82]
CUT	Repressor	Fibroblasts	[83]
DNMT1	Repressor	Breast cancer	[84]
ID (1/2/3) family	Repressor	Gastric epithelial cells	[85]
TBX2/3	Repressor	Breast cancer	[86]
Wnt1/4	Repressor	Liver cancer	[87]

1.3.2 Post-transcriptional regulation of p21

miRNAs, a group of noncoding RNAs of ~22 nucleotides long, regulate gene expression at the post-transcriptional level [88]. miRNAs can bind to the 5'- and/or 3'-untranslated region (UTRs) of a mRNA molecule and control the translational efficiency and stability of the target mRNA [89]. Several reports have previously demonstrated that miR-17, miR-20a, miR-20b, miR-93, miR-106a, and miR-106b can down-regulate the p21 expression through binding to the p21 3′-UTR mRNA. As a result, overexpression of these miRNAs has been found to increase cell proliferation and increase G1/S transition [90-94]. In contrast to these results, it has also been found that the let-7a miRNA can indirectly increase p21 protein expression by targeting NIRF (Np95 ICBP90 ring finger), but exactly how this occurs is not understood [95].

1.3.3 Post-translational regulation of p21

p21 can be phosphorylated by Cyclin E-CDK2 at Ser-130, which leads to decreased p21 stability via the ubiquitin-dependent degradation. In contrast, JNK and p38 phosphorylate p21 at Ser-130 and increase p21 stability and translation [96, 97].

1.3.4 Epigenetic regulation of p21

Epigenetic alterations include both DNA modifications (methylation of CpG islands), and alterations in DNA packaging (chromatin remodeling) by post-translational histone modifications. Methylation of CpG islands in promoter regions cause transcription repression and gene silencing [98], whereas histone deacetylation leads to transcriptionally inactivation of chromatin [99]. DNA hypermethylation of the p21 gene has been reported in p21-silenced cells in some cancer types i.e. in lung cancer [100]. In addition, CpG methylation across exon 1/intron 1 of the rat p21 gene has also been reported, which suggests defective p21 activation [100].

1.4 Aims of the study

The overall aim of the study was to evaluate expression and regulation of p21 in melanoma, with the benefit for potential therapeutic applications in the future.

The specific aims of the study can be summarized as follows:

- Measure the expression of p21 at mRNA and protein levels in a melanoma cell panel and compare levels against disease stage and mutational status.
- Measure mRNA levels of a number of genes previously reported to regulate p21 expression and compare with p21 expression levels.
- Investigate and study the effect of MAPK-, PI3K- and cAMP-pathway modulation and their effects upon p21 expression after treatments.

SECTION II: MATERIALS AND METHODS

2.1 Reagents and materials

Table 2.1. *Reagents and materials used in the study.*

Product	Company
2-Mercaptoethanol	SIGMA-ALDRICH (St Louis, USA)
Absolute alcohol Prima	Kemetyl (Norway)
Albumin from bovine serum (BSA)	SIGMA-ALDRICH (St Louis, USA)
ART TIPS	Thermo Scientific (USA)
Aprotinin 2.0 mg/ml	SIGMA-ALDRICH (St Louis, USA)
BD Matrigel™ Basement Membrane Matrix	BD Biosciences, VWR
BI-D1870 (RSK inhibitor)	Merck millipore (UK)
Bovine plasma gamma globulin (Protein standard 1)	BIO-RAD Laboratorios (USA)
Cell flasks 75 cm^2 and 175 cm^2 with filter cap	NUNC™, Thermo Scientific (Denmark)
Cell scraper S	TPP®, Techno Plastic Products AG (Switzerland)
Countess™ cell counting chamber slides	Invitrogen by Life Technologies (UK)
Dimethyl sulfoxide (DMSO)	SIGMA-ALDRICH (St Louis, USA)
Fetal bovine serum (FBS)	PAA, Fisher Scientific (USA)
GenElute™ Mammalian Total RNA Miniprep Kit	SIGMA-ALDRICH (St Louis, USA)
H-89 (PKA inhibitor)	Cell Signaling (Canada)
Hard-Shell PCR plates, 96 well Full C/C	BIO-RAD Laboratories (USA)
iBlot® Gel Transfer Stacks, Nitrocellulose, Regular	Novex® by life technologies (Norway)
IQ SYBR® Green Supermix	Quanta Bioscience (USA)
Isopropanol prima	ARCUS KJEMI AS (Norway)
Leupeptin 2.0 mg/ml	SIGMA-ALDRICH (St Louis, USA)
L-Glutamine	GibcoBRL (UK)
Lysis solution for total RNA kit	SIGMA-ALDRICH (St Louis, USA)
MOPS SDS running Buffer (20X)	Invitrogen Ltd, NuPAGE (UK)
NaAzid (NaN3) 25%	BIO-RAD Laboratories (USA)

Non-fat dry milk	TINE meierier (Norway)
Nunclon® Δ Surface, 6 well plate flat bottom	NUNCLON, Thermo Scientific (Denmark)
NuPAGE® 4-12 % Bis-Tris Midi Gel, 1.0 mm x20 well	Novex by life technologies (Norway)
NuPAGE® LDS (lithium dodecyl sulphate) sample buffer (4X)	BIO-RAD Laboratories (USA)
NuPAGE® Sample Reducing Agent (10X)	BIO-RAD Laboratories (USA)
Optical Tape	BIO-RAD Laboratories (USA)
PCR tubes (thin wall)	Axygen scientific, VWR (USA)
Pepstatin A 2.0 mg/ml	SIGMA-ALDRICH (St Louis, USA)
Phenylmethylsulfonyl fluoride (PMSF)	SIGMA-ALDRICH (St Louis, USA)
Phosphate Buffered Saline (PBS), 0.0067 M (PO4)	Lonza, Biowhittaker (Belgium)
Phosphate Inhibitor Cocktail Tablets (Phos STOP)	Roche (Germany)
Plexxikon 4032 (BRAFV600E inhibitor)	Merck millipore (UK)
Polyclonal Goat, Anti-Rabbit Immunoglobulins/HRP	Dako (Denmark)
Polyclonal Rabbit, Anti-Mouse Immunoglobulins/HRP	Dako (Denmark)
Protein Assay Dye Reagent	BIO-RAD Laboratories (USA)
qScript™ cDNA Synthesis Kit	Quanta, BIOSCIENCES (USA)
Real time PCR primers (human species specific (L+R)) (see Appendix B)	IDT® (Norway)
RPMI 1640 without L-Glutamine	Lonza, Biowhittaker (Belgium)
SafeSeal Micro Tubes	SARSTEDT (Germany)
SeeBlue® Plus2 Prestained Standard	Novex by life technologies (Norway)
Sodium chloride	Merck (Germany)
Super Signal West Dura Extended Duration Substrate	Thermo Scientific (USA)
Tris-HCL 1 M, PH 7.5	Gibco by life technologies (Norway)
TRYPSIN EDTA, 200 mg/l Versene (EDTA)	Lonza, Biowhittaker (Belgium)
Tween 20	Merck (Germany)
UO126 (MEK1/2 inhibitor)	Cell Signaling (Canada)
Venor™Gem Classic Mycoplasma detection kit	Minerva biolabs (Germany)

Cell lines

Human melanoma cell lines were obtained from the American Type Culture Collection (ATCC), the Coriell Institute (the Wistar collection) and the Norwegian Radium Hospital, see table 2.2.

Table 2.2. *Melanoma cell lines used in the study.*

Cell lines	Source	Melanoma site	Melanoma stage
WM35	Coriell Institute (Wistar collection)	Scalp/neck area	Radial Growth phase
WM1366	Coriell Institute (Wistar collection)	-	Vertical Growth Phase
WM1341B	Coriell Institute (Wistar collection)	Skin	Vertical Growth Phase
WM983A	Coriell Institute (Wistar collection)	Abdomen	Vertical Growth Phase
WM115	Coriell Institute (Wistar collection)	-	Vertical Growth Phase
FEMX-I	Norwegian Radium Hospital (established in house)	Lymph node	Metastatic
FEMX-V	Norwegian Radium Hospital (established in house)	Lymph node	Metastatic
LOX	Norwegian Radium Hospital (established in house)	Lymph node	Metastatic
WM852	Coriell Institute (Wistar collection)	Skin	Metastatic
WM9	Coriell Institute (Wistar collection)	Left axillary lymph node	Metastatic
WM239A	Coriell Institute (Wistar collection)	Right groin lymph node	Metastatic
WM45.1	Coriell Institute (Wistar collection)	-	Metastatic
WM266-4	Coriell Institute (Wistar collection)	Right thigh skin	Metastatic
A375	American Type Culture Collection (ATCC)	Skin	Metastatic
MEWO	American Type Culture Collection (ATCC)	Lymph node	Metastatic
SKMEL28	American Type Culture Collection (ATCC)	Skin	Metastatic
WM1382	Coriell Institute (Wistar collection)	Axillary lymph node	Metastatic

2.2 Cell culture

By using *in vitro* human cell cultures we can study cells that grow outside their natural environment under controlled conditions. This is a valuable tool for cancer research, permitting experiments on biological material in a simplified system but it also has some limitations for scientists working with cultured cells such as: cell line cross-contamination, nutrient depletion in the growth media, changes in pH of the growth media, accumulation of apoptotic/necrotic (dead) cells and etc.

2.2.1 Cell storage and retrieval of cells

All cell lines were stored in liquid nitrogen tanks (-180°C) to preserve them over a longer period of time, when not in use.

The procedure was as follows:

The cells were frozen in complete growth medium supplemented in FBS 20% and Dimethyl sulphoxide (DMSO) (SIGMA-ALDRICH) 10% (details in table A2, Appendix A). DMSO is a cryoprotective agent that lowers the freezing point, allowing a slow freezing, and thus prevents crystal formation which may harm the cells. The cells were frozen gradually, first in -80°C over night, before they were transferred to a liquid nitrogen tank for long term storage. When retrieved, the cells were thawed and resuspended in preheated complete growth medium (RPMI1640 medium supplemented with 10% fetal bovine serum (FBS) and 2mM L-glutamine 1%) as quickly as possible. The following day the medium was replaced to remove unattached cells and DMSO residues.

2.2.2 Culturing conditions

The cells were transferred from liquid nitrogen tanks to a water bath at 37°C (water BATH SWBD, Stuart Scientific). Once liquid, cells were added to cell culture flasks (175 cm^2 with a filter cap NUNC^{TM}, Thermo Scientific) containing 30 ml of complete growth medium (details in table A1, Appendix A). Next, cell culture flasks were kept at 37°C in a humidified 5 % CO_2 incubator (HERA cell, VWR), hereafter referred to as normal growth conditions. A correct CO_2 level is necessary to provide a buffering system for maintaining optimal pH conditions in the medium. The humidity is needed to prevent medium evaporation.

After 24 hours, the medium was replaced with fresh medium to remove residual DMSO from the freeze medium. The cells were typically grown for 2 weeks before used in experiments and they were detached and splitted each third or fourth day by using 1 ml trypsin with EDTA (TRYPSIN EDTA, 200 mg/l Versene (EDTA) Lonza, Biowhittaker). Cells were typically splitted in ratios between 1:3 to 1:10, depending on the growth rates of the different cell lines used. Cell detachment was confirmed visually and by a microscope (LEICA DMIL, Leica Microsystems TYPE 090-135.00). The cells were then resuspended in complete growth medium preheated to 37°C for further experiments (see section 2.2.4 for seeding out cells for treatment and experimental setup).

2.2.3 Quality control

The cells were always handled using sterile techniques to prevent contaminations like bacteria, yeast or fungus. Such contaminations can affect the cells and thus question the reliability of the experiments. The cells were inspected for bacterial infections and changes in morphology on a daily basis using a light microscope, and routinely tested for Mycoplasma infection (VenorGem Classic Mycoplasma detection kit) by laboratory staff. All the cell lines used in the study consistently tested negative for mycoplasma infection.

2.2.4 Seeding out cells for treatment and experimental setup

For the initial screening of p21 related genes, 17 melanoma cell lines were seeded out and grown in T175 culture flasks. As the size of the cells and their growth rates differed among cell lines we chose to use cell confluence as our standard when seeding out cells.
The procedure was as follows:

Kinase inhibitor studies:

A375 and SKMEL28 cells were seeded out and grown to 60-80% confluence in 6-well plates (Nunclon® Δ Surface, plate flat bottom, Thermo Scientific) containing 3ml complete growth medium (see table A1, Appendix A). Cells were treated as shown in figure 2.3 by replacing the culture medium with medium containing 10µM of the kinase inhibitors; Plexxikon ($BRAF^{V600E}$ inhibitor), UO126 (MEK1/2 inhibitor), H-89 (PKA inhibitor), BI-D1870 (RSK inhibitor), or combinations of 10µM of each of the respective inhibitors. The

cells were then incubated for 24 or 72 hours, followed by isolation of total RNA and/or protein. All 6-well plates contained a well with untreated control cells. Three independent biological experiments were used. Morphological changes caused by treatment with the inhibitors were captured using a Zeiss inverted microscope (ZEISS, Axiovert 200M, Germany) connected to an AxioCam CCD camera, and the images processed with the AxioVision software (see figure C1, Appendix C). A brief description of the inhibitors used in the experiment follows:

Vemurafenib/PLX4032 (Merck Millipore) is a highly selective inhibitor of BRAF kinase activity which targets the $BRAF^{V600E}$ mutation. PLX4032 was dissolved in DMSO to a concentration of 20 mM, aliquoted and stored at -20°C.

UO126/MEK 1/2 Inhibitor (Cell Signaling) is a highly selective inhibitor of MEK 1 and MEK 2. MEK 1 and MEK 2, also called MAPK or Erk kinases, are dual-specificity protein kinases that function in a mitogen activated protein kinase cascade controlling cell growth and differentiation. UO126 was dissolved in DMSO to a concentration of 10mM, aliquoted and stored at -20°C.

H-89/PKA inhibitor (Cell Signaling) is a potent selective inhibitor of cAMP dependent protein kinase (PKA). H-89 was dissolved in DMSO to a concentration of 20mM aliquoted and stored at -20°C.

BI-D1870/RSK inhibitor (Merck Millipore) is a potent and specific inhibitor of the p90 ribosomal S6 kinase (RSK) isoforms *in vitro* and *in vivo*, which inhibits RSK1, RSK2, RSK3 and RSK4 in vitro. BI-D1870 was dissolved in DMSO to a concentration of 10mM, aliquoted and stored at -20°C.

Figure 2.3. Overview of the kinase inhibitor experimental setup in 6-well plates.

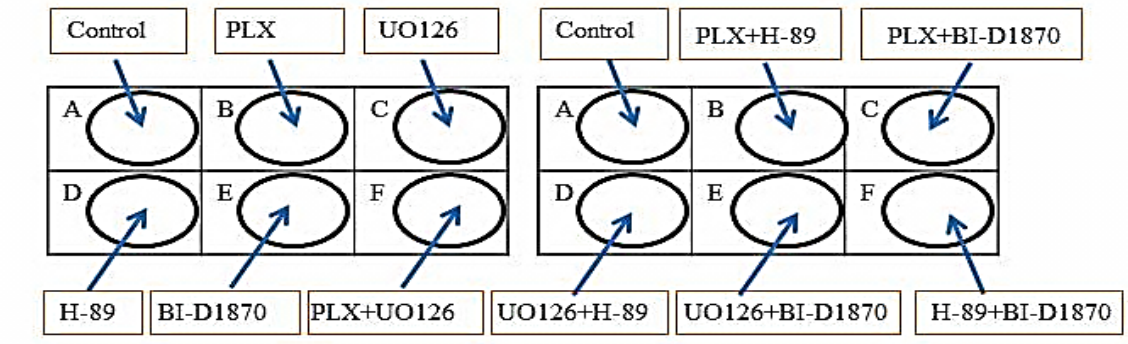

2.3 RNA analysis

2.3.1 Harvesting RNA

Cells were harvested for RNA by discarding the medium followed by a washing step with ice cold PBS before adding lysis solution (SIGMA-ALDRICH) containing 1% 2-Mercapto ethanol (SIGMA-ALDRICH). Cells were then lysed with 650 µl lysis buffer for 2-3 minutes at room temperature and the lysis suspension containing lysed cells were then added to eppendorf tubes (SafeSeal Micro Tubes, SARSTEDT). Cell tubes were stored at - 80°C until RNA isolation.

2.3.2 RNA isolation

Total RNA was extracted from cells using the GenElute™ Mammalian Total RNA Miniprep Kit (SIGMA-ALDRICH) according to the manufacturer's instructions.

The procedure was as follows:

- Transfer lysate to the blue filtration column and spin for 2 minutes at 14,000 × g.
- Add equal volume of 70% ethanol to filtrate (650 µl) and mix thoroughly.
- Transfer up to 700 µl lysate/ethanol mixture to clear binding column and spin for 15 seconds at 14,000 × g.
- Discard flow-through and repeat it for the rest of the solution.
- Add 500 µl Wash Solution 1 to the column and spin for 15 seconds at 14,000 × g.
- Transfer the column to a new collection tube.
- Add 500 µl Wash Solution 2 to the column and spin for 15 seconds at 14,000 × g. Discard the Wash Solution.
- Add second 500 µl Wash Solution 2 to the column and spin for 2 minutes at 14,000 × g to remove ethanol.
- Discard the remained solution and spin for 15 seconds.
- Transfer the column to a new collection tube.
- Add 50 µl of elution solution to the column and spin for 1 minute at 14,000 × g. Store the RNA solution at -80°C.

2.3.3 Measuring RNA concentration

The RNA concentration and purity were measured using a NanoDrop 2000 UV-VIS spectrophotometer (Thermo Scientific), which measures absorbance in small sample volumes. Absorbance was measured at the wavelengths of 260 nm, 280 nm and 230 nm. The absorption maximum of RNA is at 260 nm. These absorbance measurements provide data for calculating concentration and the ratios $A_{260/280}$ and $A_{260/230}$ give information about the purity of the RNA. The ratios were measured for each sample prior to using the RNA for further analysis.

The absorbance ratio of $A_{260/A280}$ is an important indicator of RNA purity and should be close to ~2 for optimal purity. A lower ratio may indicate presence of contaminants like proteins and phenol, which absorb near 280 nm. The RNA samples with $A_{260/280}$ ratio above 1.8 were considered to have acceptable purity. The $A_{260/230}$ ratio is used as a secondary measure of nucleic acid purity. Expected 260/230 values are commonly in the range of 2.0-2.2. If the ratio is lower, it may indicate the presence of contaminants like guanidine thiocyanate and phenol which absorb at 230 nm.

2.3.4 Isopropanol precipitation of RNA

To increase the quality of the RNA samples that did not meet the criteria mentioned above, they were purified by isopropanol precipitation.

The procedure was as follows:

- Add equal volume of isopropanol and 0.1 volume of 3M sodium acetate PH 5.2 to the RNA samples.
- Precipitate over night at -20°C.
- Centrifuge at 14,000 × g for 40 minutes (4°C).
- Discard the supernatant carefully.
- Wash the pellet with 100 µl 75 % ethanol to remove impurities.
- Centrifuge at 14,000 × g for 15 minutes.
- Remove the ethanol and dry the RNA pellet by keeping the lid open for a few minutes.
- Resuspend the pellet in 50 µl elution buffer and store at -80°C for further use.

2.3.5 cDNA synthesis (reverse transcriptase PCR)

Complementary DNA (cDNA) was synthesized from total RNA using qScript™cDNA Synthesis Kit (Quanta, BIOSCIENCES). Reverse transcriptase is a DNA polymerase which synthesizes a double stranded DNA from a single stranded RNA template. Primers hybridize to the mRNA and allow the reverse transcriptase to synthesize cDNA from the mRNA present in the sample.

The procedure was as follows:

The cDNA synthesis reaction containing 1 μg total RNA, 4.0 μl qScript Reaction Mix (5x) (containing 5x concentrated solution of optimized buffer, magnesium, Oligo (dT), random primers, and dNTPs), 1.0 μl qScript Reverse Transcriptase (50x) and nuclease free water were added to give a total reaction volume per sample of 20μl. The cDNA synthesis was carried out in a GeneAmpPCR System 9700 thermal cycler (Applied Bioscience, USA). It was assumed that the conversion from RNA to cDNA had an efficiency of 100%. To obtain a concentration of 10ng/μl, the cDNA was diluted to 100μl in nuclease free water. Diluted cDNA was stored at -20°C. The cDNA temperature cycling program is shown in table 2.4.

Table 2.4. *Temperature cycle program for the cDNA synthesis.*

Temperature	**Time**	**Function**
22 °C	5 min	Stabilizing samples
42 °C	30 min	cDNA synthesis
85 °C	5 min	Deactivation of enzyme
6 °C	∞	Hold

2.3.6 Gene panel

A list of 18 genes associated with p21 regulation was generated based on the literature studies, and is shown in table 2.5.

Table 2.5. *List of p21 associated genes and their function.*

Gene	Associated with
CBX7	Cell-cycle control
CDC6	Cell-cycle regulation
CEBPA (C/EBPalpha)	Interacting with CDK2 and CDK4 and causing growth arrest
CITED2	p53-dependent apoptosis
c-Myc	Cell-cycle progression, apoptosis and cellular transformation
ELK4	Ras-Raf-MAPK signaling cascade
EP300	Cell proliferation and differentiation
ID2/3	Cell growth, senescence and differentiation
MITF	Differentiation, development of melanocytes retinal pigment epithelium and pigmentation
PRMT6	Transcriptional repression
SALL2	p53-independent regulation of p21
SP1/3	Cell differentiation, cell growth and apoptosis
TBX2/3	Tumorigenesis, cell proliferation, developmental processes and senescence
TFAP2A (AP-2alpha)	Transcriptional activation/repression
TFAP2C (AP-2gamma)	Cell differentiation and developmental processes

2.3.7 Quantitative polymerase chain reaction (qPCR)

Quantitative PCR is a method that allows quantification of gene expression based on mRNA levels. RNA is isolated from cells, cDNA is made by reverse transcription and real time PCR is run to detect the expression of genes of interest. The iQ SYBR Green Supermix kit (Quanta Bioscience) was utilized for monitoring both the generation of PCR products during amplification in real time and the denaturation of PCR products in the melting curve analysis.

The procedure was as follows:

A master mix for each primer pair was prepared in a clean template free pre-PCR hood to prevent contamination. The PCR reaction contained 30 µl SYBR Green SuperMix (Quanta Bioscience), 1.6 µl of forward primer (10 pmol/µl), 1.6 µl of reverse primers (10 pmol/µl), and 16.4 µl PCR-graded water. For each sample, 50 µl of the master mix was added to 10 µl cDNA (10ng/µl) and mixed by vortexing. 25 µl of each sample was run in duplicates in a 96-well Hard-Shell PCR plate. In addition, no template controls (blanks) were included for each primer pair (a reaction mix without cDNA template) as quality control for template contamination of the master mix. The qRT-PCR amplification was performed using the iCycler PCR machine (BIO-RAD) and the temperature cycling program is shown in table 2.6.

Table 2.6. *qRT-PCR temperature cycling.*

Step #	**Temperature**	**Hold time**	**Cycles**	**Function**
1	95°C	3 minutes	1	Initial denaturation
2	95°C 60°C	10 seconds 35 seconds	42	Denaturation, annealing and extension
3	95°C	20 seconds	1	Denaturation
4	55°-95°C (in 0.5°C increments)	10 seconds	1	Melt curve
5	6°C			Hold

The initial denaturation of cDNA and activation of the DNA polymerase were performed in step 1, followed by 42 cycles of denaturing, annealing and extension in step 2. Melting curves were generated in step 4 by increasing the temperature in increments of 0.5°C. Fluorescent signal was monitored in step 2 (amplification reaction) and in step 4 (the melt curve analysis). In the final step the samples were cooled down to 6°C. The data was analyzed using the iCycler software.

qPCR primer design and efficiency

A successful real-time PCR reaction requires efficient and specific amplification of the product. Quantitative real time PCR primers specific for the 18 genes in table 2.5 were designed using the Roch Universal Probe Library (UPL) software. The specificity of each primer pair was assessed by gel-electrophoresis of the PCR products generated during amplification. This was done by running 5µl aliquots of PCR product from each assay mixed with 1.2 µl loading dye on a TBE gel. The molecular weight of the PCR products were estimated with the aid of a molecular weight standard and compared to the theoretical weight of the respective PCR products. The primers were considered specific only if a single PCR product with the correct molecular weight was detected on the gel. Next, in order for the primers to be considered in a quantitative real-time PCR assay, the efficiency of the primers had to be assessed. Small differences in amplification efficiency between sample and reference genes can generate false expression ratios, ultimately leading to over-/under estimation of the initial mRNA amount. Thus, primer efficiency tests were performed for all primers using cDNA from the MEWO cell line as template. A primer efficiency of 92-105% was considered satisfactory. The qPCR primer sequences and amplification efficiency are shown in table B1, figure B2 and table B3, Appendix B.

Relative quantification and melting curve analysis

SYBR green is a double-stranded DNA binding dye, which unbound exhibits minimal fluorescent. However, in PCR reactions its signal increases proportional to the amount of double stranded nucleic acids generated during amplification. The Ct-values of test samples were compared to those of control samples, yielding the fold difference of target nucleic acids in the test sample relative to control sample. The Ct (cycle threshold)-value is defined as the number of cycles required for the fluorescence signal in the PCR reaction to reach this threshold. The expression of housekeeping genes were used to ensure that the target quantities were compared from equivalent amount of sample. In the present study TATA-binding protein (TBP) and large ribosomal protein (RPLPO) were selected as appropriate housekeeping genes. The melting curve analysis was primary used to monitor the uniformity of the amplified PCR products. As the temperature is raised, the PCR products incorporated with the SYBR green dye begins to dissociate, leading to decreased fluorescent signal. Figure

2.7 shows the negative differentiated fluorescent signal as a function of temperature plotted against the temperature. The peaks observed in the diagram represent the melting temperature (Tm) of a product generated in the assay.

Figure 2.7. *Temperature plot displaying melting peaks of an amplified PCR product.*

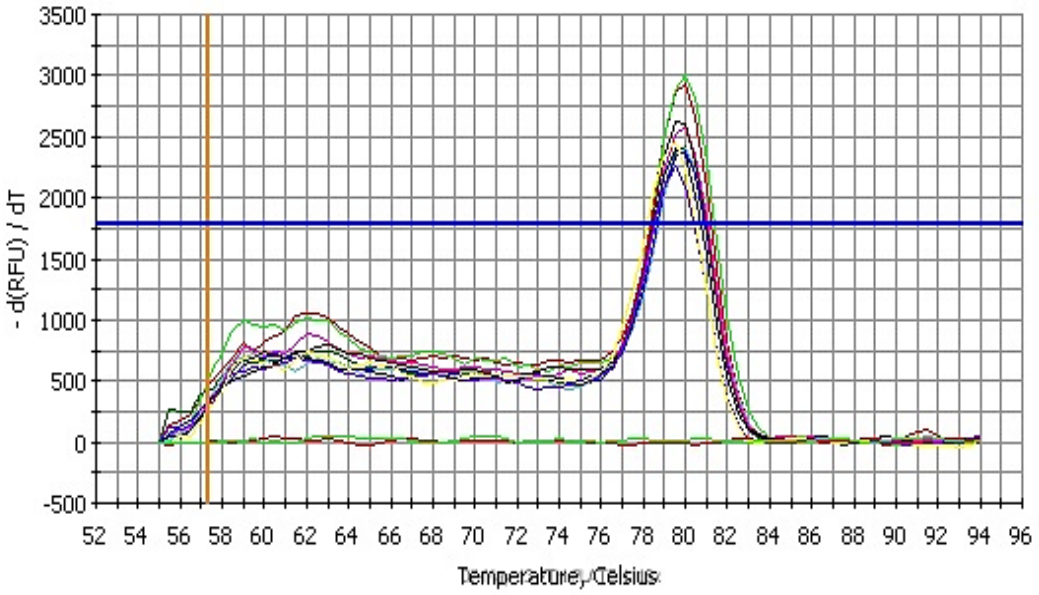

2.4 Protein analysis

2.4.1 Harvesting protein

The procedure was as follows:

Culture medium was discarded from 6-well plates and cells were washed with ice cold PBS to remove serum residual. Cells were then detached in ice cold PBS using a cell scraper (cell scraper S (TPP®, Techno Plastic Products AG) and transferred to a 15 ml centrifuge tube. The tubes were then centrifuged at 4°C by using a PICO 21 Centrifuge (THERMO SCIENTIFIC), at 3000 g for 5 minutes. The supernatant was discarded and the cells washed in 1 ml of cold PBS and transferred to eppendorf tubes (SafeSeal Micro Tubes, SARSTEDT) on ice. After a new centrifugation at 4°C by using an eppendorf Centrifuge 5810 R at 3000 g for 5 minutes, the supernatant was discarded and cell pellets were immediately frozen at -80°C until protein isolation.

2.4.2 Protein isolation

To extract proteins from cells, the cells need to be disrupted without altering the proteins of interest.

The procedure was as follows:

Cell pellets stored at -80°C were immediately placed on ice and lysis buffer containing a cocktail of protease inhibitors and phosSTOP (Phosphate Inhibitor Cocktail Tablets, Roche) (see table 2.8 for details) was added to the samples. A mild non-ionic detergent solubilizes the cell membranes and lyses the cells, liberating the cell contents. Protease inhibitors were added to prevent proteases from degrading the proteins and phosphatase inhibitor was added to preserve phosphorylation status of the phosphorylated proteins. The amount of lysis buffer used depended upon the size of the pellets, ranging from 25 µl to 500 µl. The samples were then incubated on ice for 30 minutes and vortexed every tenth minute for at least 3 times to lyse the cells. Next, cell lysates were ultrasonicated at 4°C in short bursts by dipping the probe in the tubes three times for 3 seconds to disrupt the cells by high-frequency sound waves (20-50 kHz) in order to ensure complete extraction of proteins. After sonication, the samples were centrifuged at 14000 g for 15 minutes (4°C) before the supernatants were transferred to new eppendorf tubes and stored at -80 °C.

Table 2.8. *Constituents of stock lysis buffer and lysis buffer with inhibitors.*

Lysis Buffer (50 ml):	**Lysis Buffer with inhibitors:**
1.5 ml 5M NaCl	900 µl lysis buffer
2.5 ml 1M Tris-HCl	10 µl 2 mM aprotinin
50 µl Nonidet P40 (NP-40)	10 µl 2 mM leupeptin
45 ml ddH_2o	10 µl 2 mM pepstatin A
	10 µl 2 mM PMSF
	100 µl PhosSTOP 10X (1 tablet dissolved in 1 ml ddH_2o)

2.4.3 Measuring protein concentration

Protein concentrations were measured using BIO-RAD Protein Assay (Bradford assay) which utilizes a color reaction and can be quantified by the WALLAC 1420 MULTILABEL COUNTER (WALLAC VICTOR^2, Finland) at 595 nm. The Bio-Rad solution contains the dye Coomassie brilliant blue G-250, which will change color when it is in contact with proteins. By using a dilution curve of a reference protein with a known concentration, the concentration of the protein in the sample can be quantified. The dye binds primarily to Arginine side chains, and slightly to other basic and aromatic residues. The amino acid composition of the protein therefore influences the level of dye binding. The protein lysate was assumed to have similar overall amino acid composition as the reference protein bovine gamma globulin (BGG).

The procedure was as follows:

- Bio-Rad Protein Assay Dye Reagent Concentrate was diluted 1:5 in water.
- A dilution series of 0, 1, 2, 3, 4 and 5 µg of the reference protein was added in 3 parallels in a 96-well plate and ddH_2O was added to obtain a total volume of 10 µl (see table B4, Appendix B).
- 1 µl of each lysate sample was pipetted on the plate in 3 parallels and ddH_2O was added to obtain a total volume of 10 µl.
- 100 µl of Bio-Rad solution was added to each well.
- After a minimum of 5 minutes of incubation in room temperature, the absorbance at 595 nm was measured by a WALLAC VICTOR^2 plate reader.
- The protein concentration of the samples were calculated based on the standard curve that was generated by plotting the absorbance at 595nm against reference protein (bovine gamma globulin) concentration (1.37 mg/ml), (see figure B5, Appendix B).

2.4.4 LDS-PAGE (Lithium Dodecyl Sulphate Poly Acrylamide Gel Electrophoresis)

Proteins are separated according to their size (molecular weight) by the use of an electric current in electrophoresis. The secondary structures of the proteins are denatured by heat and the anionic detergent LDS (lithium dodecyl sulphate) binds to hydrophobic groups

along the polypeptide, giving it a uniform negative charge. Proteins will then be distributed according to mass. Adding a reducing agent cleaves disulfide bonds and disrupts the tertiary and quaternary structure, and thus denatures the proteins further. The resulting denatured linearized protein with uniform mass/charge ratio makes it possible to separate the proteins based on size only, not influenced by native 3D structure and charge. Smaller proteins migrate faster than larger proteins, which are delayed in a porous matrix such as a polyacrylamide gel.

The procedure was as follows:

Preparing samples

Protein samples were prepared on ice as follows: 2.5 µl NuPage sample buffer (LDS 4X), 1 µl NuPage reducing agent 10X and 20-30 µg protein were mixed with de-ionized water to make a total volume of 10 µl. The sample buffer (LDS) contains glycerol which increases the density of the samples and makes them sink into the wells. It also contains bromophenol blue which enables visualization and tracking of the sample migration through the gel. The samples were then heated to 70°C for 10 minutes on a heat block to promote denaturation, followed by incubation on ice. Samples were then centrifuged to spin down all the liquid before application on the gel.

Gel electrophoresis

The gel system was assembled and filled with running buffer 3-(N-morpholino) propane sulfonic acid, 20mM (MOPS) which separates the proteins over a molecular weight ranging from 1-200 kDa. The gels used were NuPAGE Novex 4-12% Bis-Tris Midi Gel 1.0 mm with 20 wells (Life technologies). The gels had an increasing density from 4-12% of polyacrylamide. Before samples were applied, the wells were rinsed with running buffer to remove possible unwanted gel material and bubbles. To be able to estimate the sizes and identify the proteins in gel, 2.5 µl of the protein marker, Sea Blue Plus2 Pre-stained Standard was used on each gel in the first well, and in the remaining wells 10 µl of each sample were applied. The electrophoresis was assembled in an XCell4 Surelock^{TM} Midi-Cell chamber on 160 V for ~1-1.5 hours.

2.4.5 Western blotting

Western blotting is a widely used method for separation and detection of specific proteins. Proteins in the gel are transferred to a membrane and incubated with antibodies to detect the specific protein of interest.

Blotting

The procedure was as follows:

After the running procedure was completed, proteins were transferred from the gel matrix to a nitrocellulose membrane using a dry blotting system (iBlot, Invitrogen). The gel was assembled on a nitrocellulose membrane in between a top and bottom stack (iBlot Gel Transfer Stacks Nitrocellulose). Using an iBlot Gel Transfer Device, the gel was blotted onto the nitrocellulose membrane by applying 23 V for 9 minutes. High field strength and current during blotting make the transfer of proteins efficient and fast.

Blocking

The procedure was as follows:

To reduce non-specific binding of primary or secondary antibody to the membrane, the membrane is blocked by agents that occupy space that is not already occupied by proteins. Hence, each membrane was specifically blocked with a blocking solution usually 5% dry milk in 0.1% TBS-T (Appendix A, table A4) or 5% BSA in 0.1% TBS-T for at least 1 hour at 37°C.

Primary antibodies

The procedure was as follows:

Membranes were incubated with primary antibodies diluted in 5% dry milk in 0.1% TBS-T or 5% BSA in 0.1% TBS-T over night at 4°C with continuous gentle movement. The primary antibodies were used several times and conserved by adding 0.05% sodium azide (preservative) to prevent bacterial growth. All of the antibodies were purchased from Cell Signaling Technology (Canada) except the p53 antibody, which was purchased from Santa Cruz Biotechnology (USA). An overview of the conditions used for antibody specifications in this study is presented in table 2.9.

Table 2.9. *Antibody conditions used for Western Blot.*

Primary Ab name	**Size (kDa)**	**Blocking conditions**	**Primary Ab dilution**	**Secondary Ab dilution**	**Buffer for Ab dilution**
Histone H3	17	5% dry milk	1:3000	1:8000 (rabbit)	5% Dry milk in TBS-T
p21 Waf1/Cip1	21	5% BSA	1:1000	1:5000 (rabbit)	5% BSA in TBS-T
AKT	60	5% BSA	1:1000	1:5000 (rabbit)	5% BSA in TBS-T
p-AKT (Ser473) XP	60	5% BSA	1:2000	1:6000 (rabbit)	5% BSA in TBS-T
ERK 1/2 (Thr202/204)	44/42	5% BSA	1:2000-1:3000	1:7000 (rabbit)	5% BSA in TBS-T
p-ERK 1/2	44/42	5% BSA	1:2000	1:7000 (rabbit)	5% BSA in TBS-T
CREB (48H2)	43	5% BSA	1:1000	1:5000 (rabbit)	5% BSA in TBS-T
p-CREB (Ser133)	43	5% BSA	1:1000	1:5000 (rabbit)	5% BSA in TBS-T
p-STAT1 (Ser727)	91	5% BSA	1:1000	1:5000 (rabbit)	5% BSA in TBS-T
p53 (FL393)	53	5% Dry milk	1:500	1:2000-1:3000 (rabbit)	5% Dry milk in TBS-T
MITF	50-75	5% BSA	1:1000	1:5000 (rabbit)	5% BSA in TBS-T
AMPKα	62	5% BSA	1:1000	1:5000 (rabbit)	5% BSA in TBS-T
p-AMPKα (Thr 172)	62	5% BSA	1:1000	1:5000 (rabbit)	5% BSA in TBS-T

Washing step 1

The procedure was as follows:

The membranes were washed 3x for 10 minutes with wash buffer (TBS buffer containing 0.1% Tween 20 (Appendix A, table A4)).

Secondary antibodies

The procedure was as follows:

Membranes were incubated with secondary antibody diluted with 5% dry milk in 0.1% TBS-T or 5% BSA in 0.1% TBS-T at room temperature for 1 hour using a shaker with gentle movement. See table 2.9 for secondary antibodies used in this study.

Washing step 2

The procedure was as follows:

The membranes were then washed 3x for 10 minutes with wash buffer (TBS buffer containing 0.1% Tween 20 (Appendix A, table A4)).

Detection

The protein of interest is detected by a primary antibody specific to the protein. This antibody is in turn detected by a secondary antibody, targeting the constant region of the primary antibody. The secondary antibodies carry a label, typically horseradish peroxidase (HRP), which by oxidizing a substrate emits a measurable signal proportional to the amount of target protein present (figure 2.10). Due to the specificity of immunodetection, it is possible to detect small amounts of a specific protein in a sample with many different proteins. Chemiluminescence occurs when a chemical reagent containing stored energy releases light. The reagent is normally stable and does not emit light, but can be converted into a light emitting product, for example after interaction with a specific enzyme.

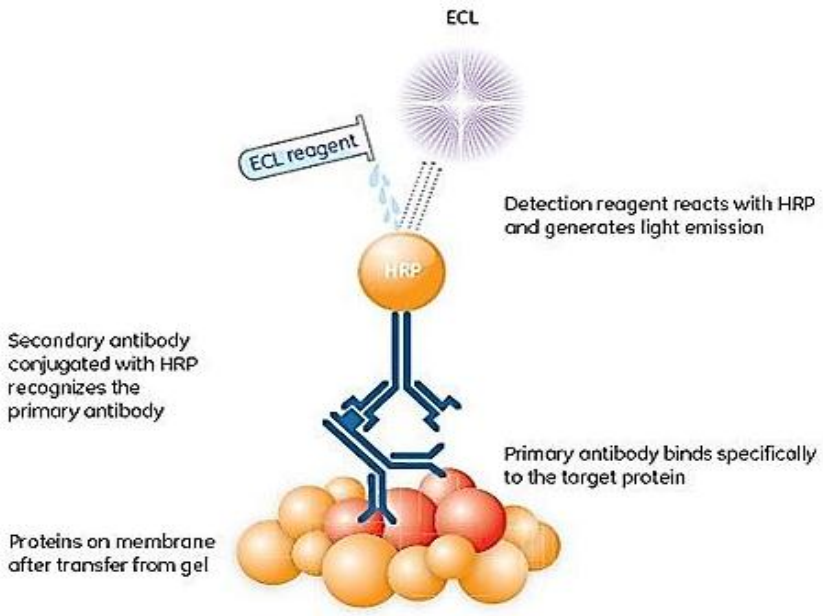

Figure 2.10. *Detection by antibodies. The protein of interest is bound by a specific primary antibody, which in turn is detected by a HRP-linked secondary antibody, which enables electrochemiluminescence (ECL) detection. Figure reproduced with permission from "Western blotting, Principle and Methods, 28-9998-97AA GE Healthcare Life Science" [101].*

The procedure was as follows:

The proteins on the membranes were visualized using Super Signal West Dura Extended Duration Substrate reagent (Thermo Scientific). The HRP on the secondary antibodies oxidizes the added substrate in the presence of hydrogen peroxide, and chemiluminescence was detected by a light sensitive camera G: box iChem (Syngene, UK) with the associated GeneSnap version 7.12 software. Image analysis was carried out with GeneSnap version 7.12 and GeneTools.

Loading control

For each membrane, the amount of protein loaded in each well was controlled by detection of a housekeeping protein, which is supposed to be present at approximately equal amount in all cells. For this purpose, the housekeeping protein Histone H3 was used as the loading control.

SECTION III: RESULTS

3.1. Characterization of melanoma cell lines

In order to be able to compare p21 expression levels against the disease stage and the mutational background of each cell line used in the study, a table was made (see table 3.1). Information about the disease stage and the mutational background of each cell line was obtained from the literature, the Wistar Institute webpage (link: http://www.wistar.org/lab/meenhard-herlyn-dvm-dsc/page/melanoma-cell-lines-0) and the Coriell Institute webpage (link: http://ccr.coriell.org/Sections/Collections/WISTAR/CellLines.aspx?PgId=572&coll=WC).

Cell line	Stage	BRAF	H/N-Ras	p53
WM35	RGP	V600E*	WT	WT
WM115	VGP	V600D*	WT	WT
WM1341B	VGP	V600R*	WT	WT
WM1366	VGP	WT	61L*	Y220C*
WM983A	VGP	V600E*	WT	P278F*
WM45.1	Metastatic	V600E*	WT	Y220C*
WM239A	Metastatic	V600D*	WT	WT
WM266-4	Metastatic	V600D*	WT	WT
WM852	Metastatic	WT	61R*	S241F*
WM1382	Metastatic	WT	WT	WT
LOX	Metastatic	V600E*	WT	WT
FEMX-I	Metastatic	WT	Mut*	WT
FEMX-V	Metastatic	WT	Mut*	WT
SKMEL28	Metastatic	V600E*	WT	L145R*
MEWO	Metastatic	WT	NF1/Q1336*	Q317/E258K*
A375	Metastatic	V600E*	WT	WT
WM9	Metastatic	V600E*	WT	WT

Table 3.1. The table shows the disease stage and BRAF, H/N-Ras, and p53 mutations in our melanoma cell panel. *RGP and VGP are short for Radial Growth Phase and Vertical Growth Phase, respectively. Mutated genes are shown with stars (*). Abbreviations: WT, wild-type; Hem Del, hemizygous deletion; Hom, homozygous; Het, heterozygous; Mut, mutant; R, arginine; Q, glutamine; E, glutamic acid; K, lysine; L, leucine; V, valine; Y, tyrosine; C,*

cysteine; D, aspartic acid; T, threonine; A, alanine; S, serine; P, proline; F, phenylalanine: NF1 (gene), Nuclear factor I.

3.2 p21 expression in melanoma cell lines

3.2.1 Expression of p21 mRNA levels in the cell panel

To investigate p21 mRNA expression levels in the melanoma cell panel we used the Real-Time RT-PCR method. Results showed variable amount of p21 mRNA in the cell panel. When we arranged the cell lines after the progression of the disease we found no obvious expression pattern (see figure 3.2). Highest level of p21 mRNA, compared to WM35 (control), was measured in the LOX cell line. However, high p21 mRNA expression levels were also detected in WM115, WM1341B, WM266.4, WM239A, and WM1382, compared to WM35. Cell lines such as WM983A, WM1366, FEMX-I, SKMEL28, MEWO, and WM45.1 displayed low levels of p21 mRNA compared to WM35, while WM852, WM9, A375, and FEMX-V showed more or less comparable levels as WM35. Together, these data suggests that there is no general increase or decrease in p21 mRNA levels when comparing against the progression of the disease from RGP to VGP and metastatic stages in our melanoma cell line panel.

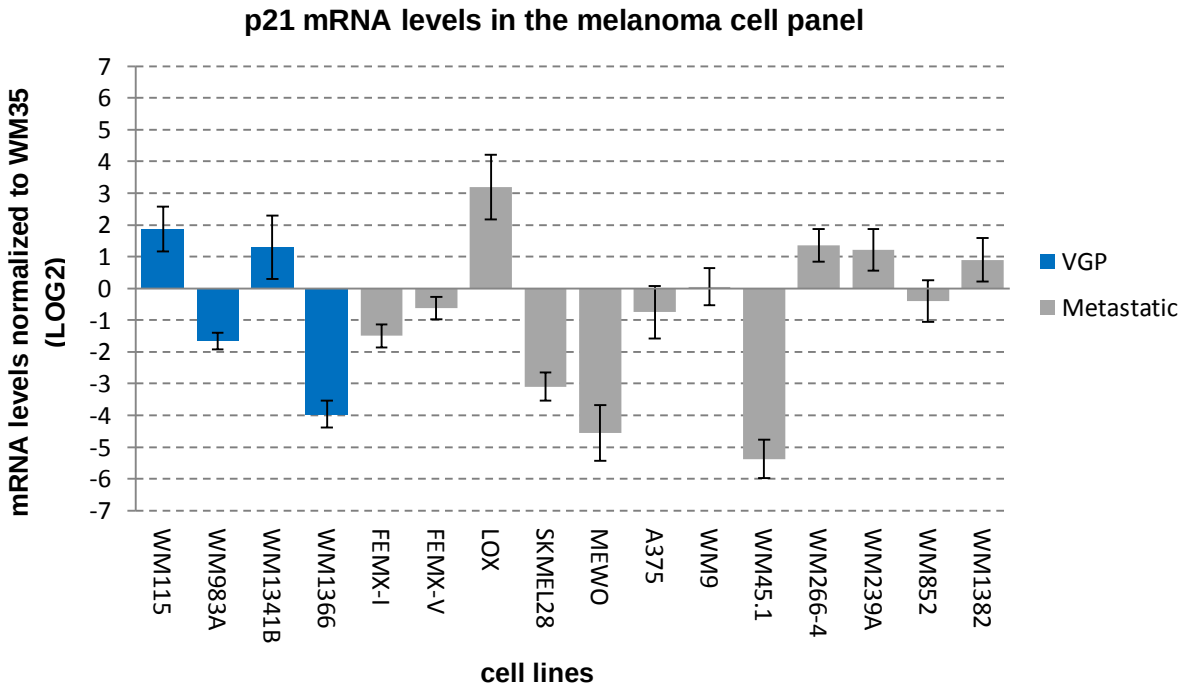

Figure 3.2. *The graph shows p21 mRNA expression levels in our melanoma cell panel. Data is presented as LOG2 and cell lines were normalized to WM35 (a cell line from the RGP stage). Blue bars represent VGP cell lines, while grey bars represent metastatic cell lines. Error bars represent standard deviation (SD) from three biological parallels.*

3.2.2 Expression of p21 protein levels in the cell panel

To investigate p21 protein expression levels in our melanoma cell line panel, we used the western blotting method. As for p21 mRNA expression levels, we did not see any correlation between the p21 protein levels and the various stages of the disease (RGP, VGP, and metastatic) (see figure 3.3). High levels of p21 protein levels were found in WM115, WM1341B, WM239A and WM1382. In cell lines such as LOX, WM266.4, WM9 and WM35, we detected low or very low levels of p21. No p21 protein was detected in WM983A, WM1366, FEMX-I and V, SKMEL28, MEWO, A375, WM45.1 and WM852.

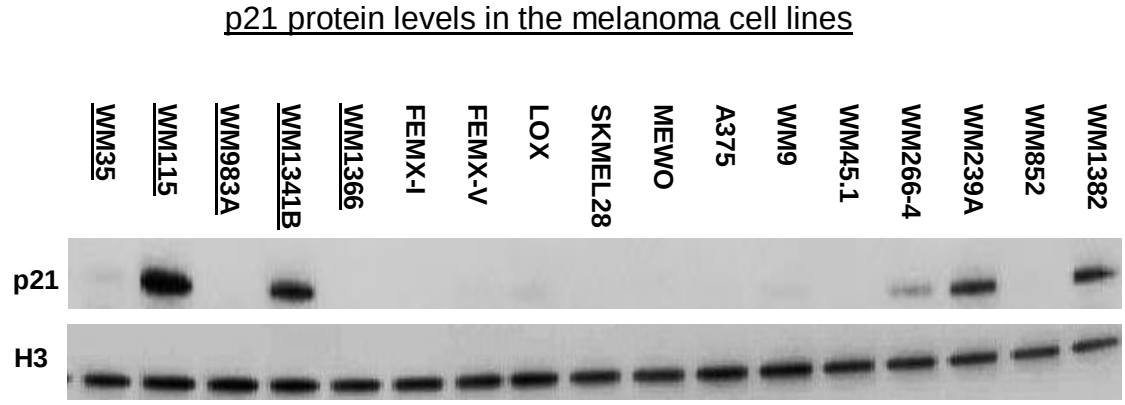

Figure 3.3. *Western blot shows p21 protein expression in our melanoma cell panel (cell lines are arranged after disease stage). Cell lines from the RGP and VGP stages are underlined. Histone H3 (H3) was used as a loading control. The western blot pictures shown are representative for one out of two parallels.*

3.2.3 Comparing p21 mRNA levels with p21 protein levels

To investigate a potential role of microRNAs (miRNAs) in post-transcriptional regulation of p21, we compared p21 mRNA expression levels (figure 3.2) with the p21 protein expression levels obtained from the western blotting (figure 3.3). Together, these results showed that there was a strong positive correlation between p21 mRNA levels and the respective protein levels for all the cell lines except LOX.

3.3 p53-dependent regulation of p21 expression

3.3.1 Comparing p21 mRNA levels upon the p53 status

According to the literature, p53 is a major transcriptional regulator of p21 expression. Here, we wanted to investigate the correlation between p21 mRNA expression and the p53 status in our melanoma cell line panel. Our results showed that cell lines with mutated p53 (WM1366, WM983A, WM45.1, WM852, SKMEL28 and MEWO) have in general much lower levels of p21 mRNA compared to WM35, which contain wild-type p53 (figure 3.4). Cell lines with wild-type p53 such as WM115, WM1341B, WM239A, WM266-4, WM1382, and LOX had higher p21 mRNA levels than WM35, while the p53 wild-type cell lines like FEMX-I and V, A375 and WM9 had comparable or lower levels. Together, these results showed that there is a good correlation between p21 mRNA expression levels and the p53 status.

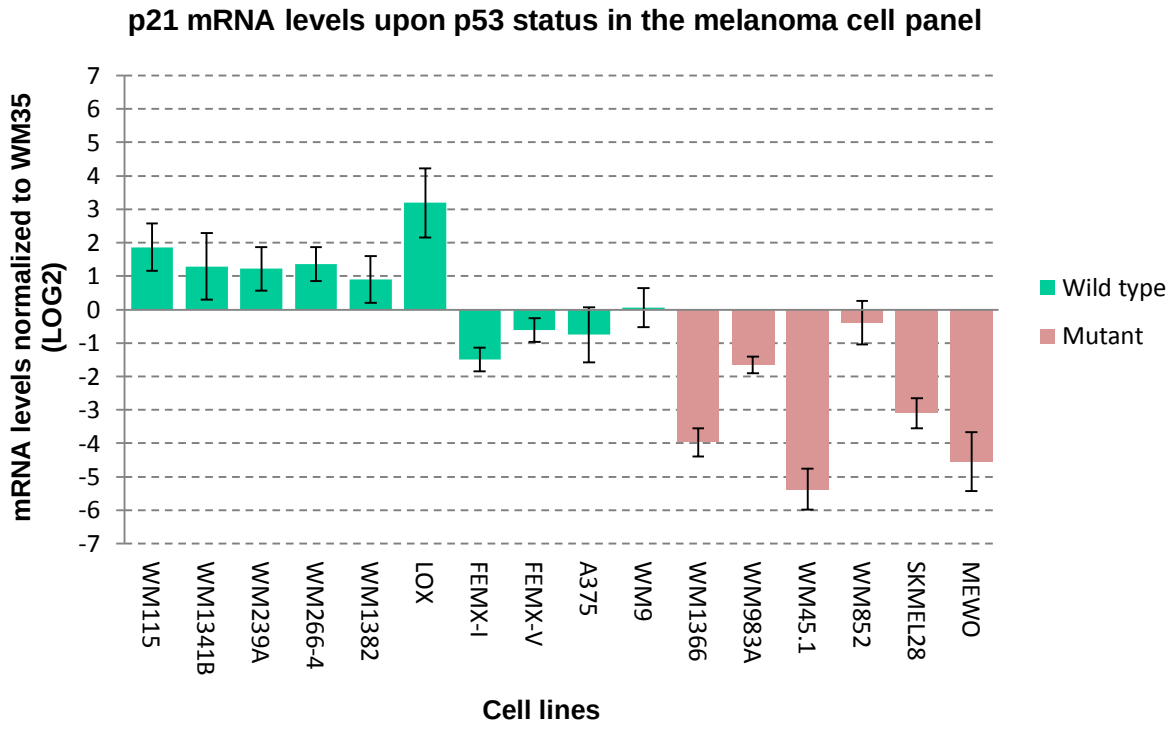

Figure 3.4. *The graph shows p21 mRNA expression levels in our melanoma cell panel. Data is presented as LOG2 and cell lines were normalized to WM35 (a cell line from the RGP stage). Green bars represent p53 wild-type cell lines, while red bars represent p53 mutated cell lines. Error bars represent standard deviation (SD) from three biological parallels.*

3.3.2 Comparing p53 protein levels with p21 protein levels

After studying the correlation between p21 mRNA levels and p53 status we were interested in comparing p21 protein levels with p53 protein levels. For this, we used the western blot procedure and our results are shown in figure 3.5. Interestingly, our results showed that melanoma cell lines which were mutated for p53 had much higher expression of p53 than wild-type p53 cell lines. None of the cell lines with mutated p53 had any detectable level of p21, which was in agreement with our Real-Time RT-RCR data. All the cell lines with high p21 protein levels had low or close to undetectable levels of p53 protein.

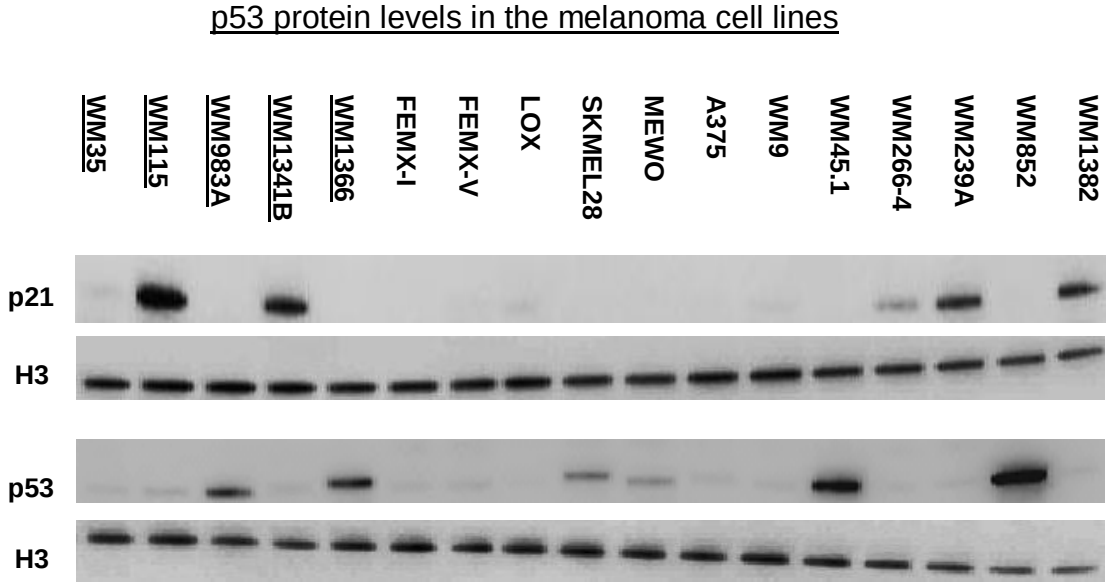

Figure 3.5. *Western blot shows p21 and p53 protein expression in our melanoma cell panel (cell lines are arranged after disease stage). Cell lines from the RGP and VGP stages are underlined. Histone H3 (H3) was used as a loading control. The western blot pictures shown are representative for one out of two parallels.*

3.3.3 Comparing p21 protein levels upon the p53 status after treatment with inhibitors

To further address the correlation between p21 and p53, we measured protein levels of p21 and p53 after inhibitor treatments (72 hours) in A375 (p53 wild-type) and SKMEL28 (p53 mutated) respectively (figure 3.6). Our data showed that p21 protein levels decreased dramatically in the A375 cell line after single treatments like PLX4032 ($BRAF^{V600E}$) and

UO126 (MEK1/2). A strong decrease in p21 protein levels was also detected after combination treatments such as: PLX+UO126, PLX+H-89 (PKA), and PLX+BI-D1870 (RSK), while a minor decrease was observed in UO126+BI-D1870 and H-89+BI-D1870. Our results showed that p21 protein levels are comparable to p53 protein levels after inhibitor treatments. The exceptions were PLX+H-89 and H-89+BI-D1870 treatments, which showed an increase in p53 protein levels compared to untreated control. In treatments like H-89, BI-D1870 and UO126+H-89 we observed an increase for both p21 and p53, compared to untreated control. For the SKMEL28 cell line we observed comparable changes in both p21 and p53 protein levels as for A375 after the various treatments. Exceptions were the decline observed in both p21 and p53 protein levels after UO126+H-89 treatment, together with the decline in p53 protein levels in PLX+H-89 and H-89+BI-D1870. Together, the data showed that there is a strong positive correlation between p53 and p21 protein levels in both A375 and SKMEL28 after inhibitor treatments.

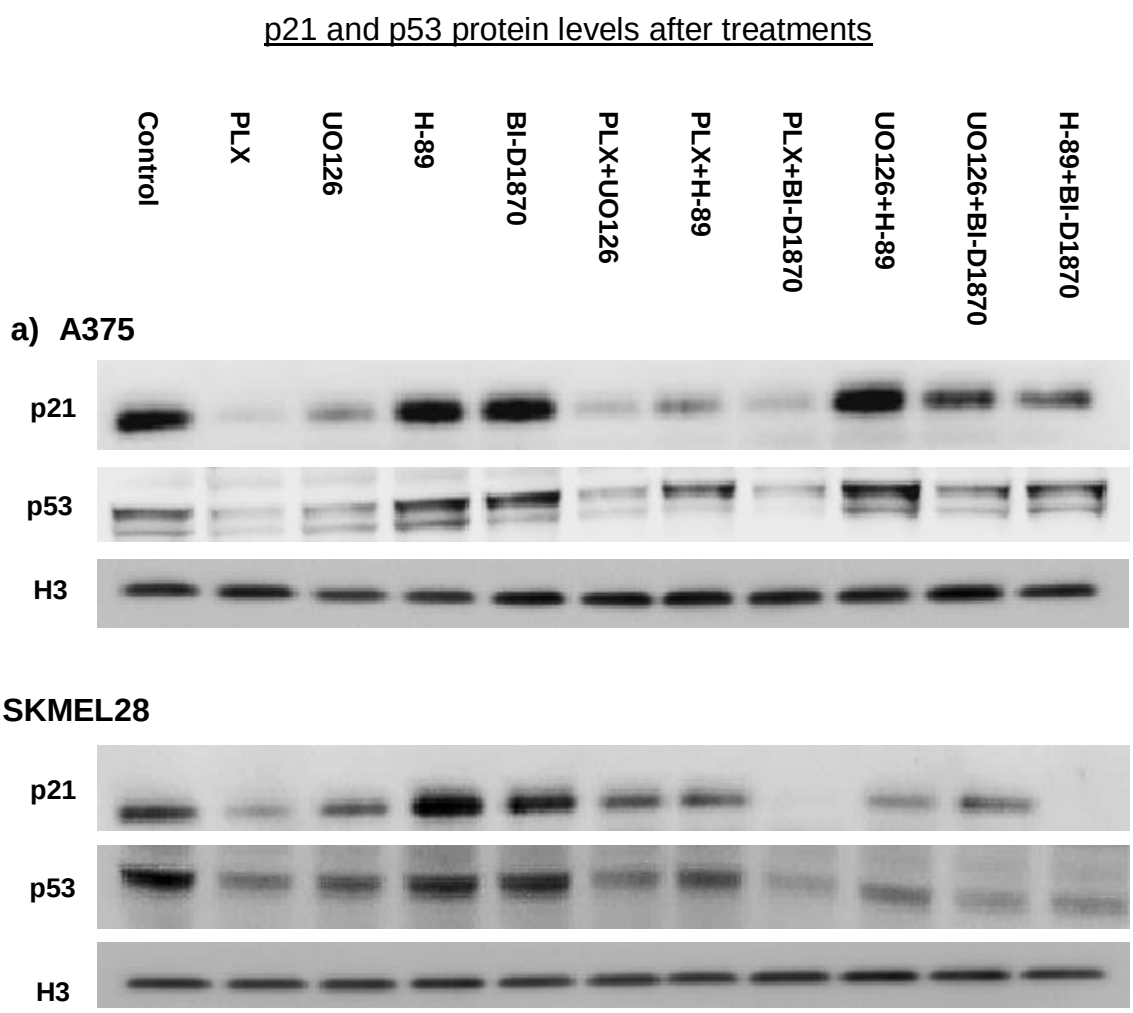

Figure 3.6. *Western blot showing protein expression of p21 and p53 after treatment (72 hours) with 10 µM of PLX4032, UO126, H-89, BI-D1870 and the combinations PLX+UO126, PLX+H-89, PLX+BI-D1870, UO126+H-89, UO126+BI-D1870 and H-89+BI-D1870 in a) A375 and b) SKMEL28. Histone H3 (H3) was used as a loading control. The western blot pictures shown are representative for one out of three parallels.*

3.4 p53-independent regulation of p21 expression

3.4.1 mRNA expression of various p21 modulators

Not only p53, but a large number of genes have been shown in previous articles to regulate p21 at the transcriptional level in different types of cancers and disorders (section 1.3.1, table 1.8). Some of these regulators modulate p21 expression directly for instance, Sp1, c-Myc, MITF, AP-2α and TBX2, while others like p300 regulate p21 indirectly through MITF by CREB activation (see figure 3.7).

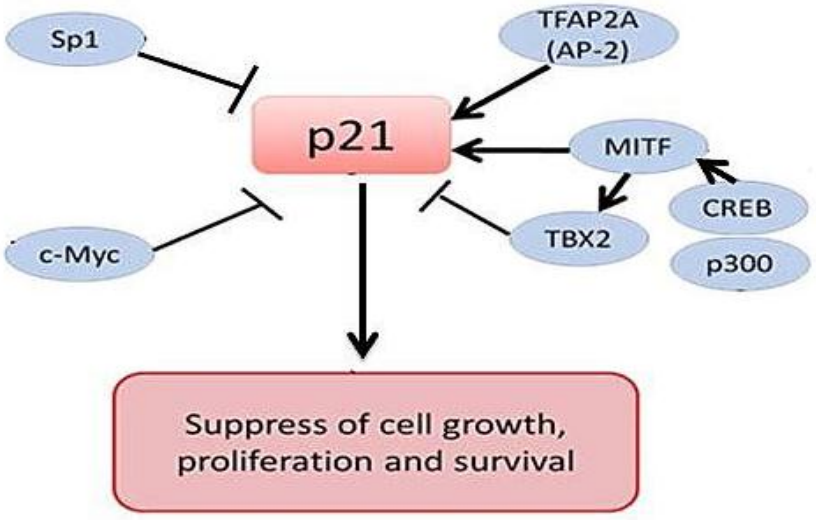

Figure 3.7. *An illustration over a proposed transcriptional network representing some potential p21 regulators in melanoma.*

A number of transcription factors can bind to the p21 promoter besides p53 (see figure 1.7). In order to investigate potential p53-independent regulation of p21 transcription, we measured mRNA levels of the genes presented in figure 3.7, which previously have been reported to regulate p21 (see figure 3.8).

a)

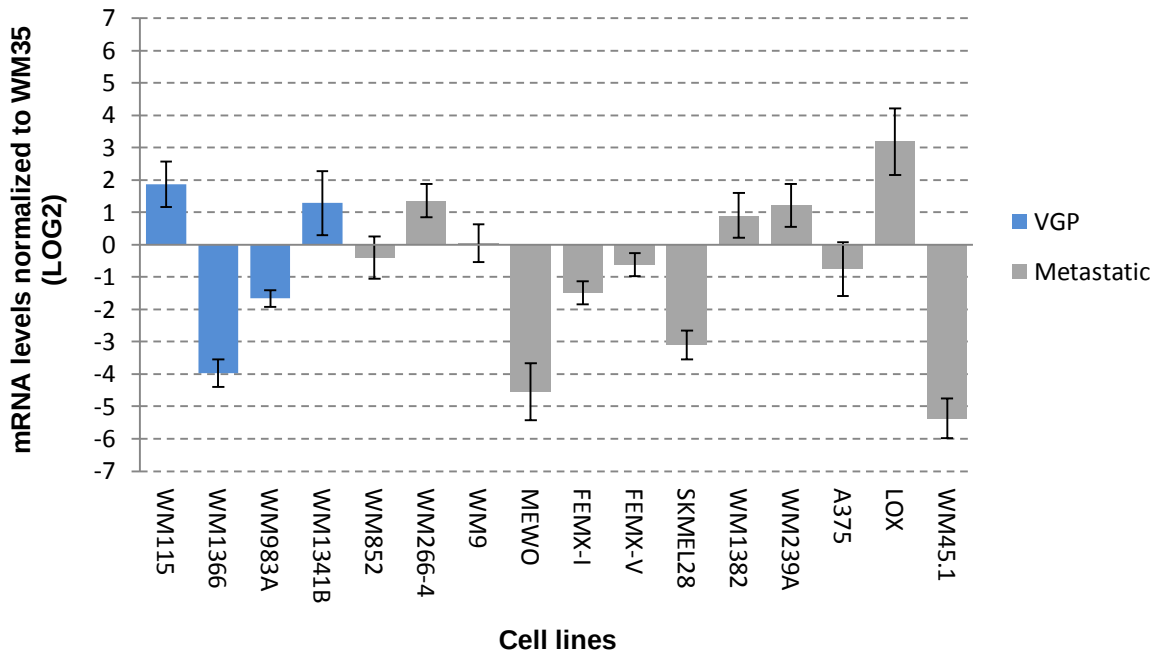
p21 mRNA levels in the melanoma cell panel
mRNA levels normalized to WM35 (LOG2)
7
6
5
4
3
2
1
0
-1
-2
-3
-4
-5
-6
-7
WM115
WM1366
WM983A
WM1341B
WM852
WM266-4
WM9
MEWO
FEMX-I
FEMX-V
SKMEL28
WM1382
WM239A
A375
LOX
WM45.1
Cell lines
VGP
Metastatic

b)

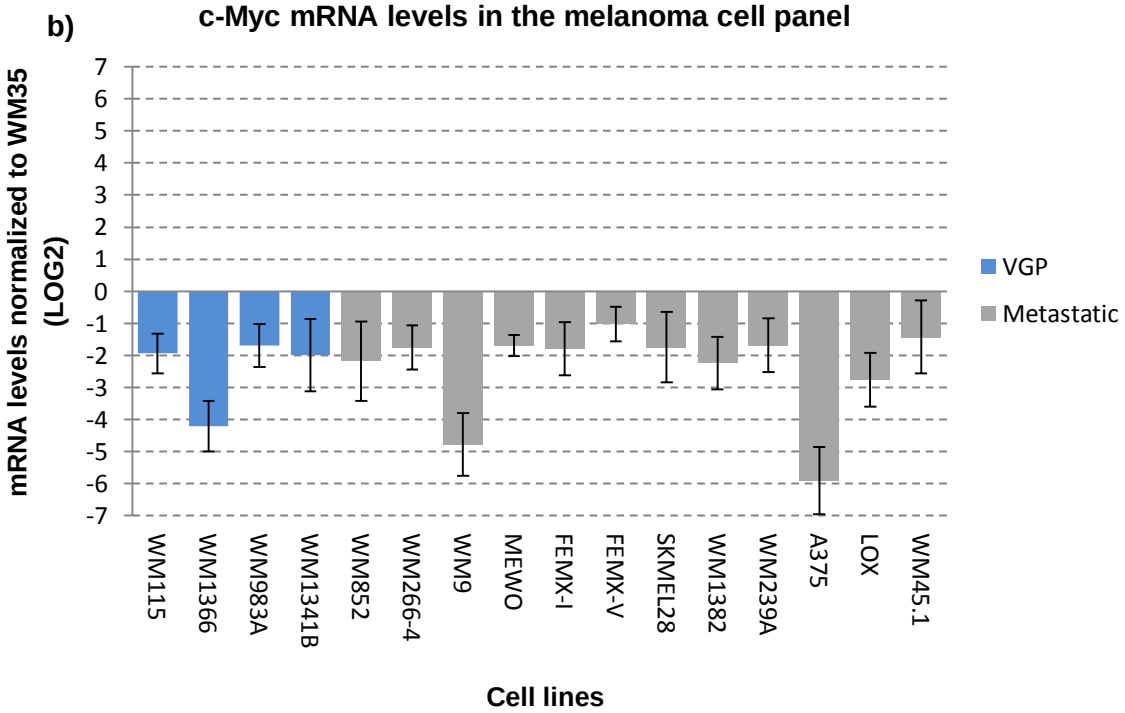
c-Myc mRNA levels in the melanoma cell panel
mRNA levels normalized to WM35 (LOG2)
7
6
5
4
3
2
1
0
-1
-2
-3
-4
-5
-6
-7
WM115
WM1366
WM983A
WM1341B
WM852
WM266-4
WM9
MEWO
FEMX-I
FEMX-V
SKMEL28
WM1382
WM239A
A375
LOX
WM45.1
Cell lines
VGP
Metastatic

c)

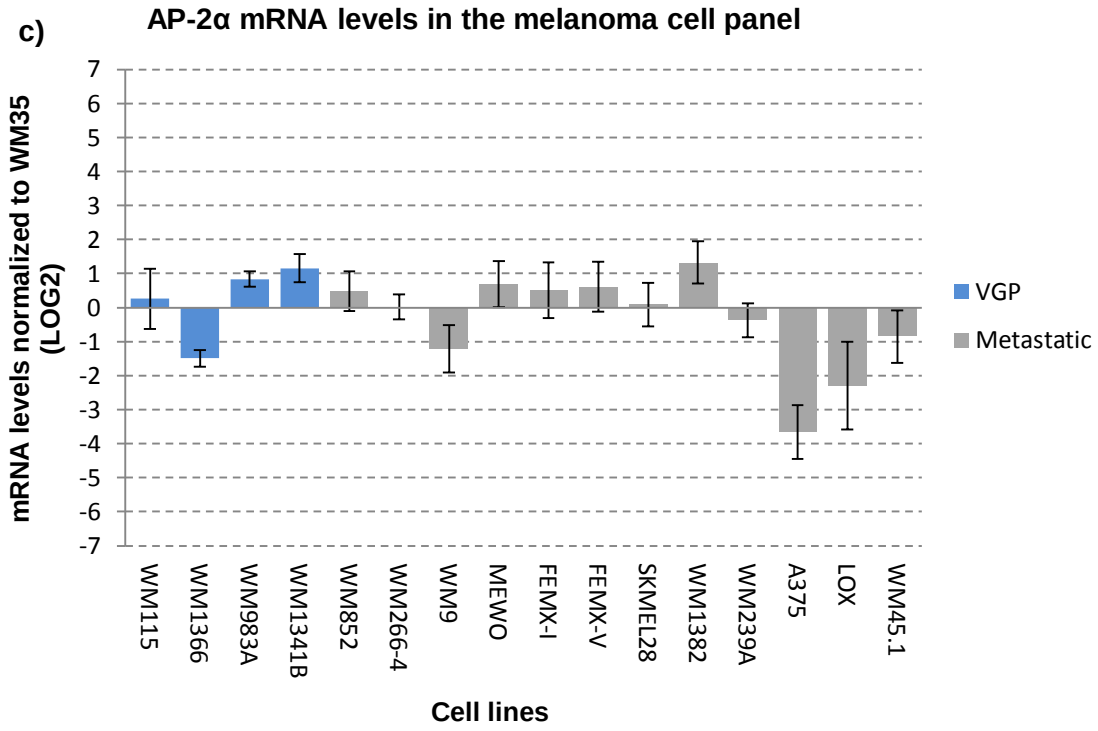
AP-2α mRNA levels in the melanoma cell panel
mRNA levels normalized to WM35 (LOG2)
7
6
5
4
3
2
1
0
-1
-2
-3
-4
-5
-6
-7
WM115
WM1366
WM983A
WM1341B
WM852
WM266-4
WM9
MEWO
FEMX-I
FEMX-V
SKMEL28
WM1382
WM239A
A375
LOX
WM45.1
Cell lines
VGP
Metastatic

d)

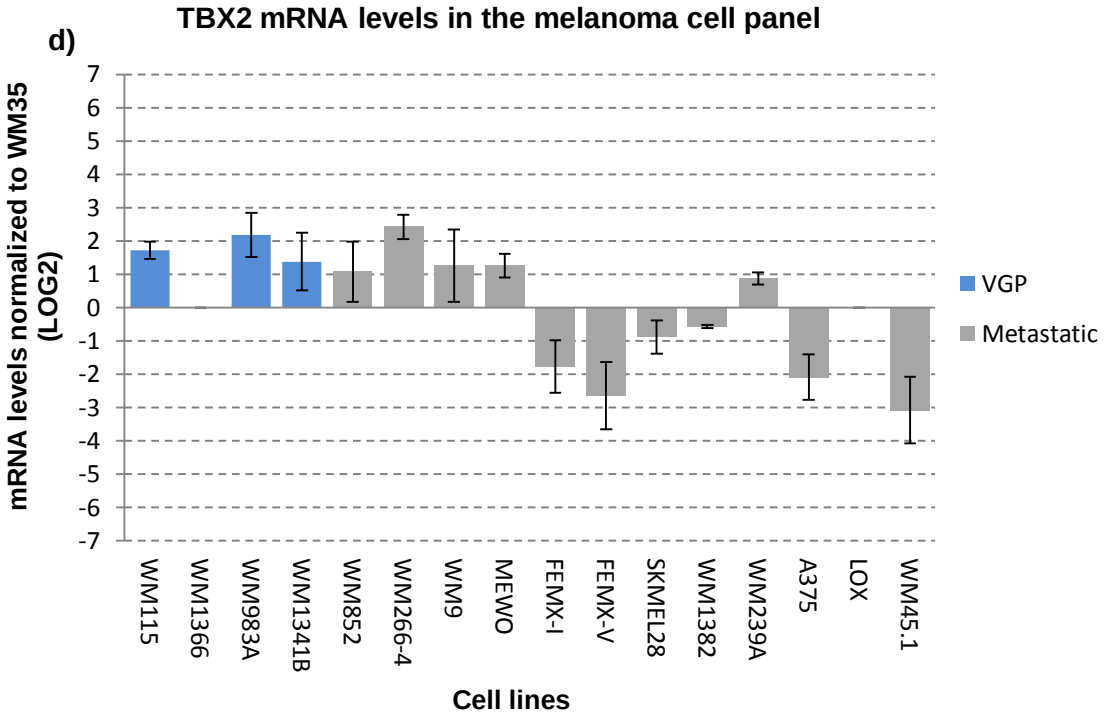
TBX2 mRNA levels in the melanoma cell panel
mRNA levels normalized to WM35 (LOG2)
7
6
5
4
3
2
1
0
-1
-2
-3
-4
-5
-6
-7
WM115
WM1366
WM983A
WM1341B
WM852
WM266-4
WM9
MEWO
FEMX-I
FEMX-V
SKMEL28
WM1382
WM239A
A375
LOX
WM45.1
Cell lines
VGP
Metastatic

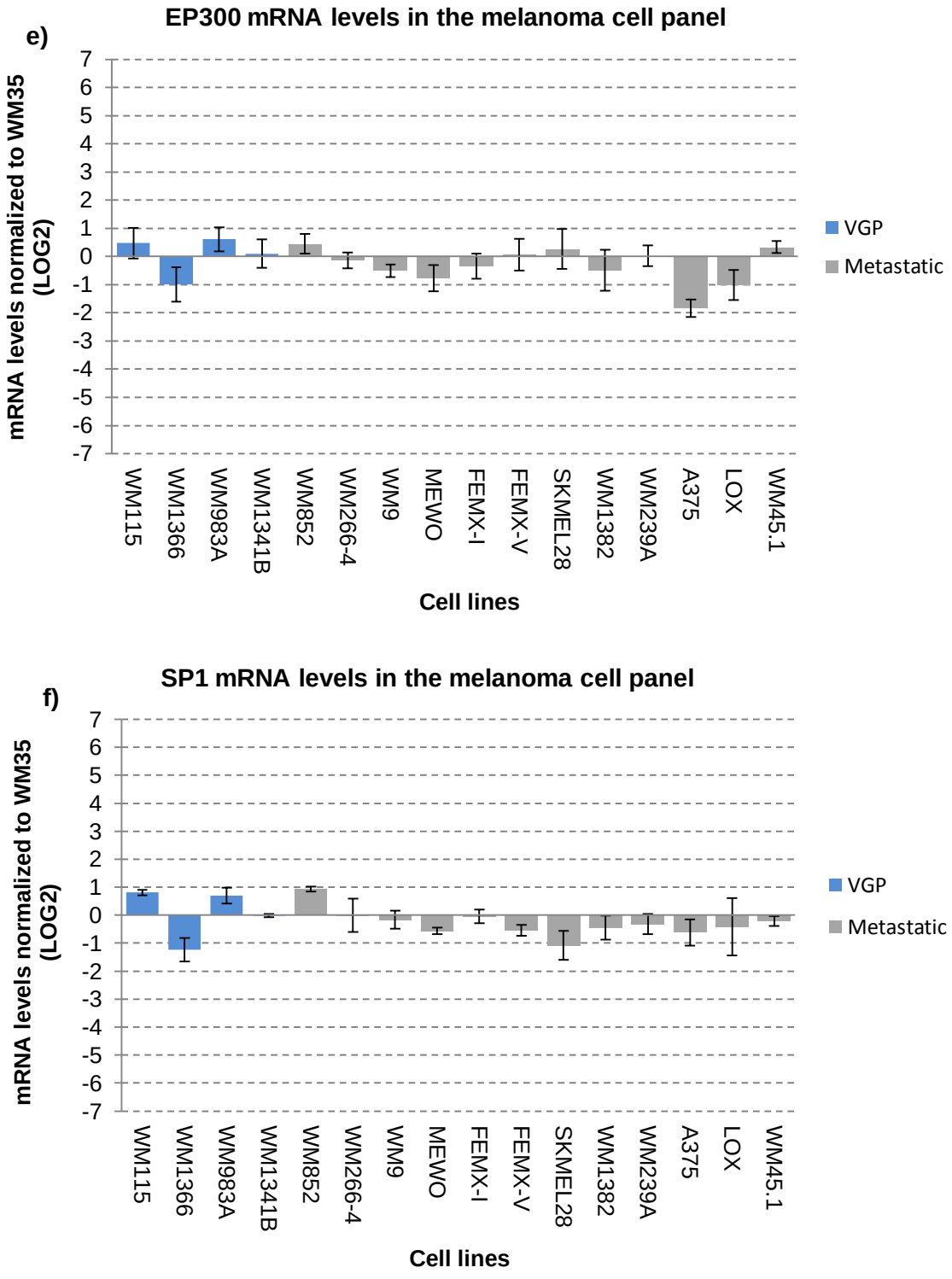

Figure 3.8. *Real-time RT-PCR data showing mRNA expression levels of a) p21, b) c-Myc, c) AP-2α, d) TBX2, e) EP300, and f) SP1 in our melanoma cell panel. The blue bars represent cell lines from the vertical growth phase (VGP) and the grey bars represent cell lines that are in the metastatic stage. Results are presented as LOG2 and values from all cell lines are*

normalized to WM35. Error bars represent standard deviation (SD) from three biological parallels.

Our data showed that c-Myc is down-regulated in the whole melanoma cell panel in comparison to WM35 (used as control). AP-2α is down-regulated in WM1366, WM9, WM239A, A375, LOX and WM45.1, and up-regulated in the rest of the cell lines. Furthermore, the TBX2 gene is not expressed in WM1366 and LOX, and is down-regulated in FEMX-I, FEMX-V, SKMEL28, WM1382, A375 and WM45.1 and up-regulated in the rest of the cell lines. EP300 is up-regulated to some extent in WM115, WM983A, WM852 and WM45.1, while down-regulated moderately in WM1366, MEWO, A375 and LOX, and shows about unchanged expression levels in the rest of the cell lines. Finally, SP1 is down-regulated in WM1366 and SKMEL28, up-regulated in WM115, WM983A and WM852 and shows about unchanged expression in the rest of the cell lines.

When comparing the various mRNA expression levels of these transcription factors with the p21 mRNA levels throughout the cell panel we do not find any obvious correlation. As seen from figure 3.8, p21 mRNA is up-regulated in WM115, WM1341B, WM266-4, WM1382, WM239A and LOX and down-regulated in WM1366, WM983A, WM852, WM9, MEWO, FEMX-I, FEMX-V, SKMEL28, A375 and WM45.1. Data from other genes validated at the mRNA level are shown in Appendix C, Supplementary data, figure C2.

3.4.2 Modulation of p21 regulators by chemical inhibitors

To investigate the possible role of TBX2 and c-Myc as repressors, and AP-2α and MITF as possible activators of p21 transcription, we treated A375 and SKMEL28 with chemical inhibitors and analyzed their mRNA levels by real time RT-PCR (figure 3.9). Our results showed that the mRNA levels of p21 expression after treatment with PLX, UO126, H-89 and BI-D1870 was in agreement with protein levels of p21 (figure 3.6) after 72 hours incubation in both cell lines; PLX and UO126 showed down-regulation of p21, while H-89 and BI-D1870 showed a minor up-regulation. We then compared mRNA and protein expression levels of p21 with changes in TBX2, c-Myc, AP-2α and MITF mRNA levels.

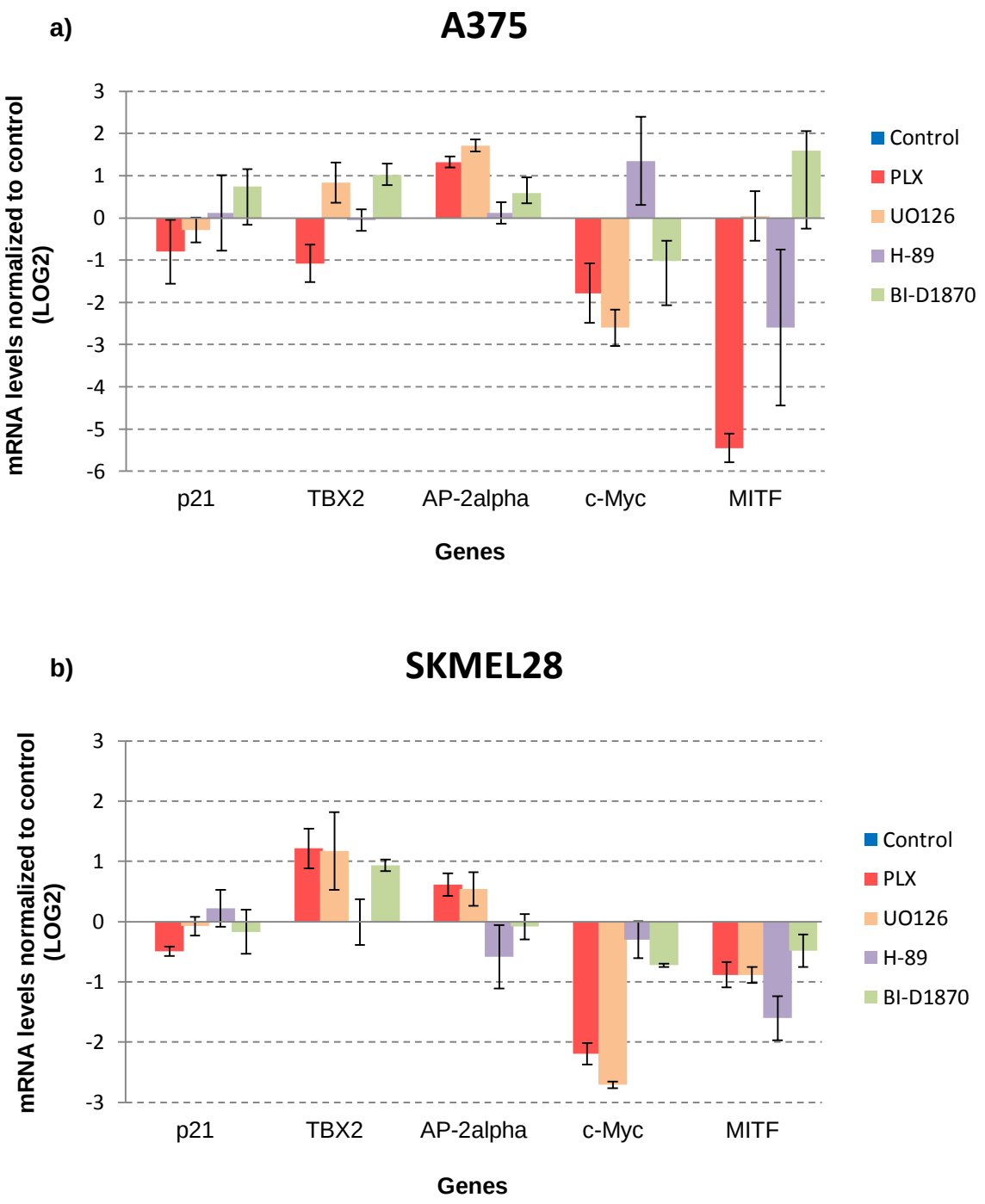

Figure 3.9. *Real-time RT-PCR data showing mRNA expression levels of p21, TBX2, AP-2α, c-Myc and MITF in a) A375 and b) SKMEL28 after treatment with 10 µM PLX4032, UO126, H-89, and BI-D1870. Results are presented as LOG2 and values from all cell lines are normalized to untreated control. Error bars represent standard deviation (SD) from three biological parallels.*

TBX2 mRNA levels were decreased in response to PLX, increased in response to UO126 and BI-D1870 and unchanged in response to H-89, in A375. This was in contrast to SKMEL28, where TBX2 was up-regulated in response to PLX, UO126 and BI-D1870, and unchanged in response to H-89. No correlation between TBX2 and p21 was found in A375, while a negative correlation was observed for SKMEL28. Furthermore, AP-2α mRNA expression levels were increased in response to PLX and UO126 in both cell lines, while less affected after H-89 and BI-D1870 treatment. The c-Myc transcription factor was down-regulated in response to PLX and UO126, almost unchanged in response to H-89, and down-regulated in response to BI-D1870 in both cell lines. Finally, we investigated MITF mRNA levels as a regulator of p21 mRNA production. MITF mRNA was down-regulated in response to all four treatments (approximately unchanged in response to UO126) in A375, which is in accordance with protein levels of MITF (figure 3.10 a). In SKMEL28, MITF mRNA was also down-regulated in response to all four treatments, however it was inconsistent with protein levels of MITF, indicating up-regulation in response to PLX and UO126 (figure 3.10 b). When we compared the MITF mRNA levels with the p21 mRNA levels we were not able to detect any correlation.

3.5 Signal pathway modulation and p21 expression

To investigate the effect of pathway modulation upon p21 expression we used small chemical inhibitors against the MAPK- and cAMP-pathways. We next analyzed phosphorylation status of a number of key genes in MAPK-, PI3K/AKT-, JAK/STAT- and cAMP- pathways that are believed to regulate melanoma development when deregulated. Figure 3.10 shows protein levels of ERK1/2 and AKT and their activated, phosphorylated forms p-ERK1/2 and p-AKT. In addition, the levels of MITF and p-STAT1, p21 and H3 (loading control) were analyzed. Our data showed changes in pathway signaling in response to $BRAF^{V600E}$, MEK1/2, PKA, and RSK inhibition as expected. When comparing changes in p21 protein levels after single treatments against the p-AKT/AKT we observed a strong positive correlation in the A375 cell line (Figure 3.10 a). A comparable strong positive correlation is detected when comparing p21 levels to ERK1/2 levels after single treatments. Surprisingly, the correlation was less obvious when comparing to p-ERK1/2, which showed strong down-regulation with both PLX and UO126 treatment. This was in contrast to the p21 levels that showed strong down-regulation with PLX, and more moderate down-regulation

with UO126. The phosphorylation status of STAT1 was comparable to p-ERK1/2 after single treatments and MITF expression was more or less absent. When comparing p21 protein levels with the combination treatments for A375, we did not see any convincing correlation in either of the genes tested. For the SKMEL28 cell line, we did not observe any strong positive correlation between p21 protein levels and the genes investigated (figure 3.10 b). However, we observed a detectable negative correlation between p21 protein levels and MITF levels after single treatments. When we compared the pathway signaling after inhibitor treatment between the two cell lines SKMEL28 and A375, we observed substantial differences in phosphorylation status and protein amounts. Our results showed that the phosphorylation status of ERK1/2 was the only obvious common factor between the two cell lines in the tested genes.

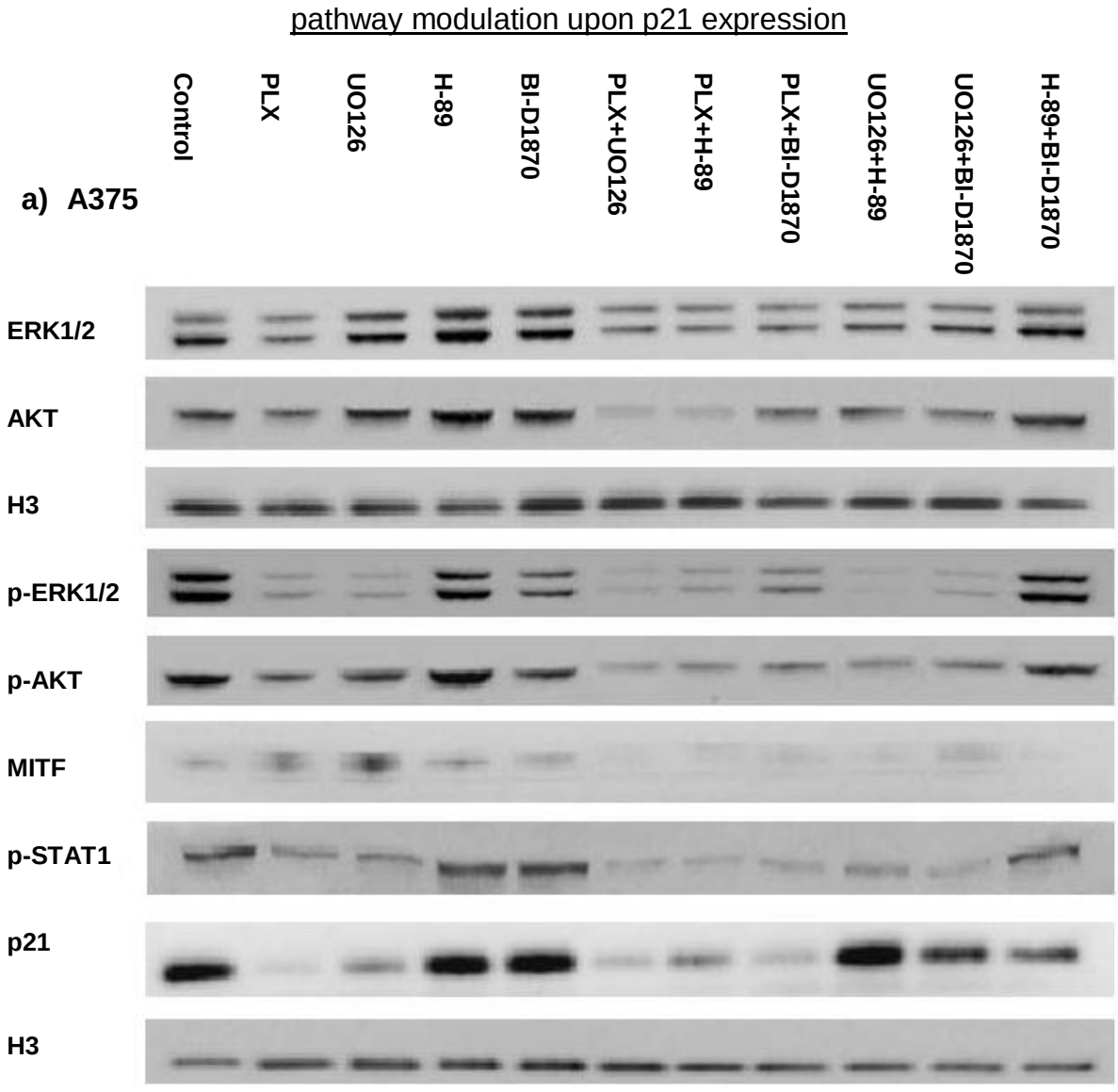

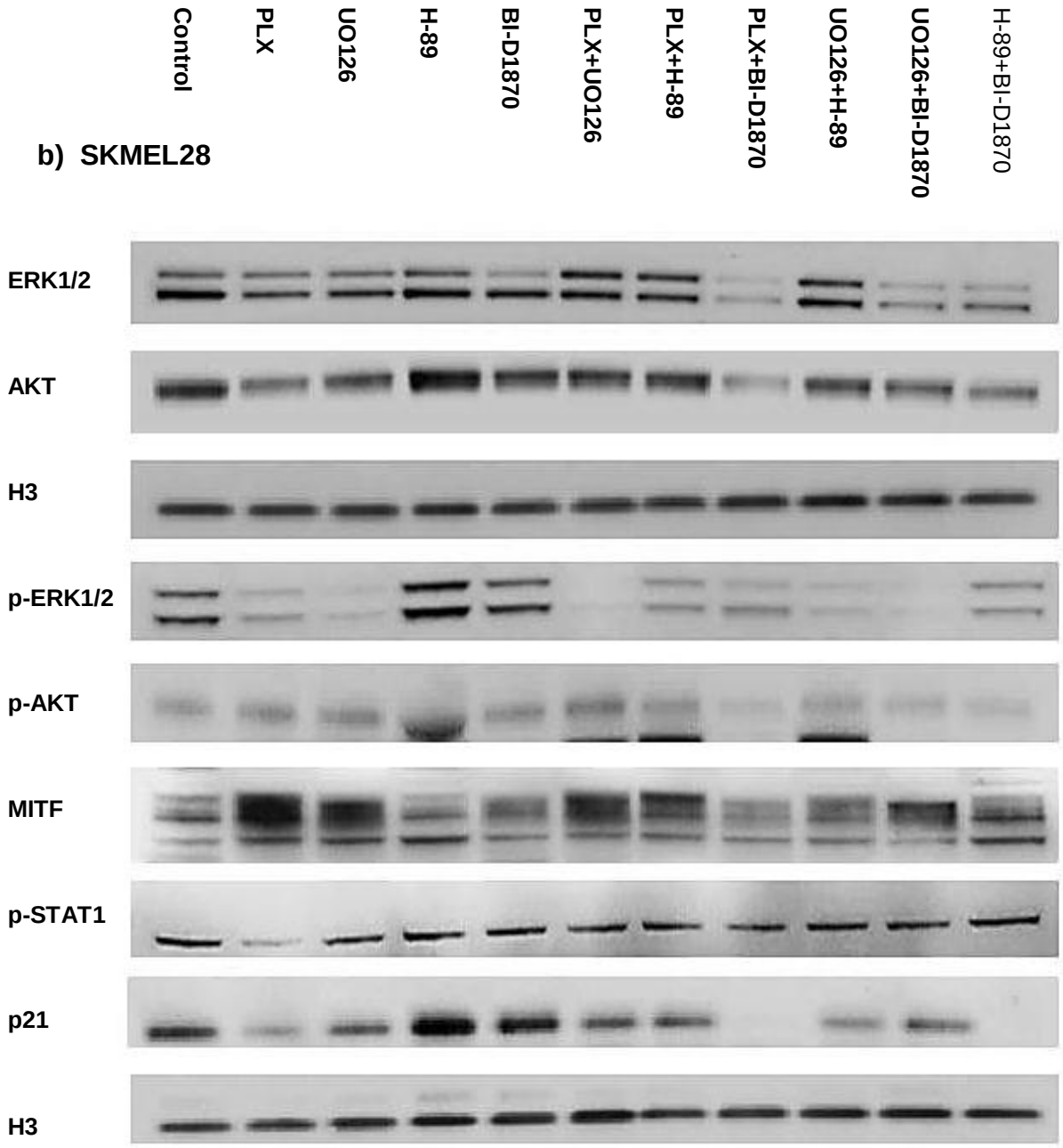

Figure 3.10. *Western blot showing the expression of proteins involved in melanoma signal pathways after treatment with 10 µM PLX4032, UO126, H-89, BI-D1870 and combinations PLX+UO126, PLX+H-89, PLX+BI-D1870, UO126+H-89, UO126+BI-D1870 and H-89+BI-D1870 in a) A375 and b) SKMEL28. Western blotting was performed to detect levels of ERK, AKT, their phosphorylated forms, in addition to MITF, p-STAT1, p21 and Histone H3 (loading control). The western blot pictures are representative for three independent biological parallels.*

SECTION IV: DISSCUSSION

4.1 p21 expression in the melanoma cell panel

The expression of p21 has previously been investigated both *in vitro* and *in vivo* in many different cancer cell types [22, 38, 102]. However, there are few studies that have investigated p21 expression in a large cell line panel, spanning the different stages of melanoma [25, 69, 95]. In this study, we aimed to investigate p21 expression at both the mRNA and protein level. In addition, we compared the expression levels of p21 against the stages of the disease and the mutational background of each cell line. From our Real-Time RT-PCR data we could not find any correlation between the mRNA values of p21 and the different stages of the disease. This result is in contrast to Mealandsmo *et al*. that measured low levels of p21 in benign nevi and high levels in metastatic melanoma [103]. The fact that our results are obtained from human melanoma cells *in vitro*; while Mealandsmo *et al.* investigated *in vivo* samples, may explain the discrepancy. Next, we compared the p21 mRNA values obtained from our cell line panel with the mutational background of each cell line. Of note, only a few mutations for these cell lines have been described in the literature, including mutations in BRAF, RAS, and p53 (Table 3.1). Among the mutations in these genes, we detected a good correlation between the mutational status of p53 and p21 mRNA expression in our cell line panel. No correlation was found between p21 and BRAF, RAS status. This result is in agreement with previous studies, showing the regulatory role of p53 upon p21 transcription [103-105]. All the cell lines containing the Y220C, L145R and Q317/E258K mutations had very low levels of p21 mRNA compared to the wild-type p53 cell line WM35 (used as control). A marked reduction of p21 mRNA was also measured in WM983A, which contains a P278F mutation in p53. Among the 6 cell lines in the cell panel with p53 mutation, only WM852 contained comparable levels of p21 as the wild-type p53 cell line WM35. The WM852 cell line has been described to have a S241F mutation in p53 [106]. Based on our results, it appears like the p53 mutation in WM852 does not affect p53-dependent regulation of p21. Alternatively, other transcription factors in the p21 promoter region compensate for the loss of p53 by keeping p21 mRNA levels at comparable levels to the p53 wild-type cell line WM35.

Of interest, the p53 wild-type cell line LOX contained 8-fold more p21 mRNA than WM35 and around 16-fold more than the FEMX-I cell line (also wild-type for p53). These results, suggest that there are large differences in p21 mRNA levels within the group of cell lines that are p53 wild-type. This may suggest that not only p53, but also p53-independent regulation of p21 transcription is occurring. Alternatively, p53 is more active in LOX than in the other cell lines.

A few previous reports have shown that there is a good correlation between p21 mRNA and protein expression levels [47, 103]. This is in agreement with our data, which show high expression of p21 protein in the cell lines that contain high levels of p21 mRNA (figure 3.2 and 3.3). The exception is LOX, showing very high levels of p21 mRNA, but close to no p21 protein (figure 3.2 and 3.3). This latter result implies possible post-transcriptional or post-translational regulation of p21 in LOX. Several miRNAs (miR-17, miR-20a, miR-20b, miR-93, miR-106a, and miR-106b) have been found to decrease p21 protein levels by binding to the 3`UTR of p21 [90-94]. Furthermore, post-translational regulation by GSKβ (Glycogen synthase kinase beta) may occur. GSKβ have been found to phosphorylate Thr-57 at p21 and subsequently decreases protein stability [70]. Of note, cyclin E-CDK2 have also been found to decrease p21 stability by phosphorylation of p21 at Ser-130 [107]. The expression levels of p21 mRNA and protein can be modulated by several processes and in the next chapter we will discuss p53-dependent regulation of p21 transcription.

4.2 p53-dependent transcriptional regulation of p21

It has for a long time been well-known that p53 is a major regulator of p21 transcription [71, 72, 108]. In this study we aimed to investigate whether this also was the case for our human melanoma cell lines. In our cell panel we had 6 cell lines that were p53 mutant, while the remaining 11 cell lines contained p53 wild-type. As mentioned previously in this discussion under “p21 expression in the melanoma cell panel”, low or non-present levels of p21 mRNA and protein were detected in p53 mutated cell lines, respectively. These results imply that p53 status is important for p21 transcriptional regulation. The exception was WM852, which contained comparable p21 mRNA levels to the control p53 wild-type cell line WM35. The highest levels of p21 mRNA and protein was detected in WM115, WM1341B, WM239A, WM266-4 and WM1382, all of them p53 wild-type. These cell lines showed

higher p21 mRNA levels than other wild-type p53 cell lines such as WM35, FEMXI and V, A375, and WM9. A relevant question is then whether this difference in p21 mRNA levels is a consequence of p53-independent regulation or just an increase in p53 activity. Then investigating the amount of p53 protein between the two groups of p53 wild-type we were unable to detect any difference when inspecting the western blot pictures. This result implies that observed discrepancy in p21 mRNA levels is at least not due to the amount of p53 protein. Interestingly, the amount of p53 protein was much higher in p53 mutated vs. wild-type cell lines. This is consistent with other reports, showing high expression of p21 in the absence of p53 and on the contrary in *in vitro* and immunohistochemistry analysis [48, 109]. Our results support the suggestion that there also exist p53-independent regulation of p21 (which will be discussed in more details in the next chapter). The significance of p53-independent regulation of p21 in melanoma is nevertheless less understood. When using small molecular chemical inhibitors against the MAPK- and cAMP-pathway, we measured their effects upon p21 and p53 protein levels. In both the mutated p53 cell line (SKMEL28) and in the p53 wild-type cell line (A375), we observed a strong positive correlation between the two genes after single treatments with inhibitors. A good positive correlation was also detected after combination treatments in A375 and SKMEL28, however not as strong as for the single treatments. No differences between the cell lines (A375 and SKMEL28) were detected in response to chemical inhibitors after single treatments, while minor differences were observed after combination treatments. Interestingly, we observed down-regulation of both p53 and p21 after inhibiting $BRAF^{V600E}$, in contrast to up-regulation of p53 and p21 when inhibiting RSK, both mediators in the same signal pathway (MAPK). At the present we do not have any explanation for these latter results and suggest that further evaluation by siRNA knock-down of the respective genes would be useful to disclose the different role of $BRAF^{V600E}$ and RSK in the regulation of the p53/p21 pathway.

In summary, p21 transcription has been found to be controlled by a vast number of different transcription factors; however, our results suggest a major role for p53 as a transcriptional activator of p21 in melanoma. In p53 mutated cell lines we detected a marked reduction in p21 mRNA levels compared to p53 wild-type cell lines. However, p21 mRNA could still be detected with Real-Time RT-PCR in these cell lines, suggesting that other transcription factors also contribute to transcriptional regulation of p21. In the next chapter, p53-independent transcriptional regulation of p21 will be discussed.

4.3 p53-independent transcriptional regulation of p21

The promoter region of p21 has been characterized and a number of binding sites for various transcription factors have been previously described [110]. A list over potential regulators of p21 transcription is shown in Table 1.8, section 1.3.1. Preferably, all of these potential regulators of p21 should be screened at the protein level with additional gain- and loss of function studies to elucidate their possible role in p21 transcriptional regulation of melanoma. However, due to limited number of antibodies available, combined with the time limitation of this study, we chose to validate around 17 potential transcription factors at the transcriptional level in 17 cell lines. The mRNA expression levels of these transcription factors where then compared against the p21 mRNA expression levels. Our results showed that none of the transcriptional regulators investigated demonstrated any obvious positive or negative correlation with the p21 mRNA expression levels throughout the panel (figure 3.8, section 3.4.1). To further address whether some of these potential regulators have a role in p21 transcriptional regulation of our melanoma cell panel, we used small molecular chemical inhibitors against the A375 and the SKMEL28 cell lines. Due to the large number of potential p21 regulators investigated, 4 genes (TBX2, AP-2α, c-Myc and MITF) were chosen for further analysis (figure 3.9, section 3.4.2). The A375 and the SKMEL28 cell lines were chosen as they represent both wild-type and mutated p53, respectively. Furthermore, both are $BRAF^{V600E}$ mutated and A375 contains low levels of MITF protein, while SKMEL28 has high levels of MITF protein (unpublished data). After analyzing our data we could not detect any solid correlation between p21 mRNA levels and the four potential regulators selected in either the A375 or the SKMEL28 cell line. In the SKMEL28 cell line, which is mutated for p53, but still have some p21 expression, we found indications of an inverse correlation between p21 mRNA expression and TBX2 after different inhibitor treatments. Nevertheless, due to the small changes in p21 mRNA levels after inhibitor treatments and with respect to the observed error bars (standard deviation values), this result needs further validation. Validation by the use of gain- and loss of function methods would contribute to confirm TBX2's role in p21 transcriptional regulation. The inhibitory effect of TBX2 upon the p21 promoter has also been described previously in the literature [111]. When comparing p21 mRNA levels with AP-2α and c-Myc after Plexxikon and UO126 treatments, we found a negative and a positive correlation, respectively. This is contradictory compared to previous

studies, describing AP-2α as an activator of p21 transcriptional regulation, while c-Myc have been found to be a repressor [28, 44]. In conclusion, this latter result clearly shows that loss and gain of function tools, which offer specificity towards the gene of interest, is required for verifying the role of each transcription factors that binds to the promoter. Moreover, the use of small molecular chemical inhibitors offers usually only unspecific screening that can contribute to find potential regulatory genes of interest. However, small molecular chemical inhibitors are an important tool when the aim is to disclose how pathway signaling contributes to p21 regulation, which is further discussed in the next chapter.

4.4 Signal pathway involved in p21 regulation

Previous reports suggest that p21 expression can be controlled transcriptionally, post-transcriptionally, translationally, post-translationally and by epigenetic mechanisms. In our study, we used small molecular chemical inhibitors against the MAPK- and cAMP pathway. The reason for this was to investigate how p21 expression is regulated by these pathways that are essential for melanoma development. Both the MAPK- and the cAMP pathway are often deregulated in melanoma by mutations in e.g. MCR-1 and $BRAF^{V600E}$. These mutations will again increase the risk for melanoma development. For the MAPK-pathway we used inhibitors against $BRAF^{V600E}$ (Plexxikon), MEK1/2 (UO126), and RSK1-4 (BI-D1870) in two metastatic cell lines, A375 and SKMEL28. Our results showed that p21 protein levels were down-regulated after Plexxikon and UO126 treatment in both cell lines. In contrast, BI-D1870 treatment did not seem to influence p21 protein levels significantly. This result was unexpected since all the inhibitors used, targeted the same signal pathway (MAPK). At the current stage we do not have any decent explanation for the observed result. The PKA inhibitor H-89 showed comparable effects upon p21 protein levels as the BI-D1870 inhibitor, or at best a minor up-regulation of p21 in the SKMEL28 cell line. When we investigated phospho-ERK, phospho-AKT and phospho-STAT1 protein levels and compared these levels against the p21 protein levels, none of these "key" pathway proteins correlated perfectly to p21 protein levels for all treatment combinations. However, all of them showed more or less good correlation with p21 protein levels when comparing only the single treatments (figure 3.10, section 3.5). The best correlation was however observed between p53 and p21 protein levels as previously shown. Of note, the MITF protein levels show a negative correlation with

p21 protein levels after single treatments in SKMEL28 (MITF positive cell line, in contrast to A375). This is in agreement with previous reports, showing the inhibitory effects of TBX2 (which is a MITF target) upon p21 transcriptional regulation in melanoma [112]. In conclusion, our results showed that down-regulation of phospho-ERK by e.g. Plexxikon results in decreased levels of p21 protein, while up-regulation of phospho-ERK by H-89 has the opposite effect. This is in agreement with other reports, showing induction of the senescence markers (p21 and p16) in e.g. melanocytes when the MAPK pathway is overstimulated [64, 94]. How p21 and senescence can be used as therapeutic approach is discussed in the next chapter.

4.5 p21 as a therapeutic target

p21 was originally identified as an inhibitor of cyclin-dependent kinases, a marker of cellular senescence and a mediator of p53 in growth suppression. p21 is required for appropriate cell cycle progression and plays a role in apoptosis, DNA repair, senescence, and induced pluripotent stem cell reprogramming. In fact, p21 was first identified as an overexpressed marker in senescent cells [113], to inhibit cell cycle progression. Several studies showed that p21 is up-regulated during oncogenic Ras-induced cellular senescence and inhibits Ras-induced transformation [114, 115]. It has been stated that the overexpression of p21, p53, pRB, or p16 is generally sufficient to induce a senescence growth arrest and consequent tumor suppression [116]. Activating the program of senescence in tumor cells seems an attractive approach to cancer treatment. Senescence-oriented therapeutic strategies may include development of drugs that will induce tumor cell senescence by up-regulating p21 (which, unlike p16, is almost never inactivated in tumors) or p21-inducible senescence-promoting genes [117, 118]. Identification of senescence-associated growth-inhibitory genes makes it possible to develop high-throughput screening systems for agents that induce such genes for instance p300 and c-Myc, which can regulate and arrest senescence respectively in cancer cells by manipulation of p21 [112, 117]. Thus, the elucidation of the biological aspects of tumor cell senescence offers plausible approaches for development of novel therapeutic strategies to stop the growth of tumor cells.

Conclusions

The present study showed that p21 mRNA expression was present in all cell lines in the melanoma cell panel. Epigenetic silencing of p21 therefore does not seem to play an important role in human melanoma cell lines. Our results revealed a strong correlation between p21 mRNA and protein levels; the exception was the LOX cell line. This result implies that post-transcriptional regulation by miRNA activity is less important in our cell panel. After screening the human melanoma cell panel for p21 expression at both mRNA and protein level, we compared expression levels against the disease stage and the mutational background. From these data we could not observe any correlation in expression between primary (RGP/VGP) and metastatic stages of the disease. In contrast, we detected a strong correlation between p21 expression and the mutational status of p53. This was further investigated by the use of various chemical inhibitors against the MAPK- and cAMP-pathways. These data showed that changes in p21 protein amount after treatment followed the changes detected in p53 protein amount. The latter result implies strong co-regulation between the two genes and is in agreement with previous reports. We also measured the expression levels of a number of transcription factors that previously been known to regulate p21 at the transcriptional level. However, when comparing these results against the p21 mRNA levels we could not detect any correlation. We then selected some of these genes for further manipulations by chemical inhibitors. Our results implied that TBX2 expression after treatment is negatively correlated with p21 in the SKMEL28 cell line. However, to verify this result, a more specific method involving loss- and gain of function of the particular gene of interest should be utilized. Although, many factors and mechanisms have been identified to regulate p21 expression, other factors are yet to be identified. A number of transcription factors have been found to bind to the p21 promoter, the role of each need to be further investigated to understand their effects upon p21 mRNA production.

Future perspectives

The results obtained in this study, raised new questions that would be interesting to pursue in the future. To what degree do p53 control p21 transcription in melanoma is still not fully understood. In mutated p53 cell lines we still detect p21 mRNA, but at a reduced level compared to normal p53. Does this mean that other transcription factors contribute to the transcriptional expression of p21, or can it be explained by other mechanisms? As known from the literature, mutant p53 is not the same as a missing p53. Mutant p53 have been found to function as an oncogene, the opposite of normal p53, which is a tumor-suppressor. Whether these new functions affect p21 mRNA transcriptional regulation is unknown. However, it would be interesting to investigate whether mutant p53 behaves like non-existing p53 in respect to p21 transcriptional regulation. Furthermore, the effect of each of the transcription factors and their co-factors that bind to the p21 promoter is unknown. To what extent do they control p21 in melanoma? To what degree is the promoter regulation cell-type specific, is it influenced by the microenvironment, or is it mainly controlled by the mutational status of the tumor cells. Due to the limited time span of this project many questions regarding p21 transcriptional regulation remain unanswered and further analysis and validation are necessary. For future investigations regarding the effect of the various transcriptional regulators of p21 transcription, molecular approaches like siRNA and mRNA transfections would be useful. With these tools it would be possible to study both gain- and loss of function of the gene of interest. Other relevant inquiries that should be addressed, is the importance of p21 in melanoma progression. Is manipulation of p21 a suitable target to control tumor progression? Is it possible to manipulate p21 to induce cell senescence in melanoma and exploit this inherited mechanism in a therapeutic setting?

REFERENCES

1. Stratton, M.R., P.J. Campbell, and P.A. Futreal, *The cancer genome.* Nature, 2009. **458**(7239): p. 719-24.
2. Greaves, M. and C.C. Maley, *Clonal evolution in cancer.* Nature, 2012. **481**(7381): p. 306-13.
3. Duffy, M.J., *The war on cancer: are we winning?* Tumour Biol, 2013. **34**(3): p. 1275-84.
4. Geller, J., et al., *Crafting a melanoma educational campaign to reach middle-aged and older men.* J Cutan Med Surg, 2006. **10**(6): p. 259-68.
5. Calabrese, P., S. Tavare, and D. Shibata, *Pretumor progression - Clonal evolution of human stem cell populations.* American Journal of Pathology, 2004. **164**(4): p. 1337-1346.
6. Hanahan, D. and R.A. Weinberg, *Hallmarks of cancer: the next generation.* Cell, 2011. **144**(5): p. 646-74.
7. Hanahan, D. and R.A. Weinberg, *The hallmarks of cancer.* Cell, 2000. **100**(1): p. 57-70.
8. Grande Sarpa, H., et al., *Prognostic significance of extent of ulceration in primary cutaneous melanoma.* Am J Surg Pathol, 2006. **30**(11): p. 1396-400.
9. Gilchrest, B.A., et al., *The pathogenesis of melanoma induced by ultraviolet radiation.* N Engl J Med, 1999. **340**(17): p. 1341-8.
10. Slipicevic, A. and M. Herlyn, *Narrowing the knowledge gaps for melanoma.* Ups J Med Sci, 2012. **117**(2): p. 237-43.
11. Vultur, A., J. Villanueva, and M. Herlyn, *Targeting BRAF in advanced melanoma: a first step toward manageable disease.* Clin Cancer Res, 2011. **17**(7): p. 1658-63.
12. Woodman, S.E., et al., *New strategies in melanoma: molecular testing in advanced disease.* Clin Cancer Res, 2012. **18**(5): p. 1195-200.
13. Rangel, J., et al., *Prognostic significance of nuclear receptor coactivator-3 overexpression in primary cutaneous melanoma.* J Clin Oncol, 2006. **24**(28): p. 4565-9.
14. Cancer Registry of Norway, C.i.N.-C.i., mortality, survival and prevalence in Norway., I.K. Larsen, Editor. 2013, Cancer Registry of Norway: Oslo.
15. Robsahm, T.E., et al., *Body mass index, physical activity, and colorectal cancer by anatomical subsites: a systematic review and meta-analysis of cohort studies.* Eur J Cancer Prev, 2013. **22**(6): p. 492-505.
16. *World Health Organisation. Health effects of UV radiation. 2013 [cited 2013 12.11]; Available from: http://www.who.int/uv/health/uv_health2/en/index1.html.*
17. Miller, A.J. and M.C. Mihm, Jr., *Melanoma.* N Engl J Med, 2006. **355**(1): p. 51-65.
18. Orgaz, J.L. and V. Sanz-Moreno, *Emerging molecular targets in melanoma invasion and metastasis.* Pigment Cell Melanoma Res, 2013. **26**(1): p. 39-57.
19. Eichler, A.F., et al., *The biology of brain metastases-translation to new therapies.* Nat Rev Clin Oncol, 2011. **8**(6): p. 344-56.
20. Damsky, W.E., L.E. Rosenbaum, and M. Bosenberg, *Decoding melanoma metastasis.* Cancers (Basel), 2010. **3**(1): p. 126-63.
21. *Hanahan, D.; Weinberg, R.A. The hallmarks of cancer. Cell 2000, 100, 57-70.*
22. Nguyen, D.X., P.D. Bos, and J. Massague, *Metastasis: from dissemination to organ-specific colonization.* Nat Rev Cancer, 2009. **9**(4): p. 274-84.
23. Lopez-Bergami, P., B. Fitchman, and Z. Ronai, *Understanding signaling cascades in melanoma.* Photochem Photobiol, 2008. **84**(2): p. 289-306.
24. Hocker, T.L., M.K. Singh, and H. Tsao, *Melanoma genetics and therapeutic approaches in the 21st century: moving from the benchside to the bedside.* J Invest Dermatol, 2008. **128**(11): p. 2575-95.

25. Garraway, L.A., et al., *Integrative genomic analyses identify MITF as a lineage survival oncogene amplified in malignant melanoma.* Nature, 2005. **436**(7047): p. 117-22.
26. Gray-Schopfer, V., C. Wellbrock, and R. Marais, *Melanoma biology and new targeted therapy.* Nature, 2007. **445**(7130): p. 851-7.
27. Jakob, J.A., et al., *NRAS mutation status is an independent prognostic factor in metastatic melanoma.* Cancer, 2012. **118**(16): p. 4014-23.
28. Bhatia, S., S.S. Tykodi, and J.A. Thompson, *Treatment of metastatic melanoma: an overview.* Oncology (Williston Park), 2009. **23**(6): p. 488-96.
29. Fidler, I.J., *The pathogenesis of cancer metastasis: the 'seed and soil' hypothesis revisited.* Nat Rev Cancer, 2003. **3**(6): p. 453-8.
30. Hoek, K.S., et al., *In vivo switching of human melanoma cells between proliferative and invasive states.* Cancer Res, 2008. **68**(3): p. 650-6.
31. Finn, L., S.N. Markovic, and R.W. Joseph, *Therapy for metastatic melanoma: the past, present, and future.* BMC Med, 2012. **10**: p. 23.
32. Uong, A. and L.I. Zon, *Melanocytes in development and cancer.* J Cell Physiol, 2010. **222**(1): p. 38-41.
33. Haluska, F.G., et al., *Genetic alterations in signaling pathways in melanoma.* Clin Cancer Res, 2006. **12**(7 Pt 2): p. 2301s-2307s.
34. Qin, J., et al., *Identification of a novel family of BRAF(V600E) inhibitors.* J Med Chem, 2012. **55**(11): p. 5220-30.
35. Marchesi, F., et al., *Triazene compounds: mechanism of action and related DNA repair systems.* Pharmacol Res, 2007. **56**(4): p. 275-87.
36. Ascierto, P.A., H.Z. Streicher, and M. Sznol, *Melanoma: a model for testing new agents in combination therapies.* J Transl Med, 2010. **8**: p. 38.
37. Chapman, P.B., et al., *Improved survival with vemurafenib in melanoma with BRAF V600E mutation.* N Engl J Med, 2011. **364**(26): p. 2507-16.
38. Sosman, J.A., et al., *Survival in BRAF V600-mutant advanced melanoma treated with vemurafenib.* N Engl J Med, 2012. **366**(8): p. 707-14.
39. Montagut, C. and J. Settleman, *Targeting the RAF-MEK-ERK pathway in cancer therapy.* Cancer Lett, 2009. **283**(2): p. 125-34.
40. Flaherty, K.T. and D.E. Fisher, *New strategies in metastatic melanoma: oncogene-defined taxonomy leads to therapeutic advances.* Clin Cancer Res, 2011. **17**(15): p. 4922-8.
41. Harper, J.W., et al., *The P21 Cdk-Interacting Protein Cip1 Is a Potent Inhibitor of G1 Cyclin-Dependent Kinases.* Cell, 1993. **75**(4): p. 805-816.
42. Shin, S.Y., et al., *The ETS family transcription factor ELK-1 regulates induction of the cell cycle-regulatory gene p21(Waf1/Cip1) and the BAX gene in sodium arsenite-exposed human keratinocyte HaCaT cells.* J Biol Chem, 2011. **286**(30): p. 26860-72.
43. Bunz, F., et al., *Requirement for p53 and p21 to sustain G2 arrest after DNA damage.* Science, 1998. **282**(5393): p. 1497-501.
44. Chan, T.A., et al., *Cooperative effects of genes controlling the G(2)/M checkpoint.* Genes Dev, 2000. **14**(13): p. 1584-8.
45. Charrier-Savournin, F.B., et al., *p21-Mediated nuclear retention of cyclin B1-Cdk1 in response to genotoxic stress.* Mol Biol Cell, 2004. **15**(9): p. 3965-76.
46. Phalke, S., et al., *p53-Independent regulation of p21Waf1/Cip1 expression and senescence by PRMT6.* Nucleic Acids Res, 2012. **40**(19): p. 9534-42.
47. Sestakova, B., L. Ondrusova, and J. Vachtenheim, *Cell cycle inhibitor p21/ WAF1/ CIP1 as a cofactor of MITF expression in melanoma cells.* Pigment Cell Melanoma Res, 2010. **23**(2): p. 238-51.

48. Vidal, M.J., et al., *Mutations and defective expression of the WAF1 p21 tumour-suppressor gene in malignant melanomas.* Melanoma Res, 1995. **5**(4): p. 243-50.
49. Gartel, A.L. and A.L. Tyner, *Transcriptional regulation of the p21((WAF1/CIP1)) gene.* Exp Cell Res, 1999. **246**(2): p. 280-9.
50. Kumar-Sinha, C., S. Kalyana-Sundaram, and A.M. Chinnaiyan, *SLC45A3-ELK4 chimera in prostate cancer: spotlight on cis-splicing.* Cancer Discov, 2012. **2**(7): p. 582-5.
51. Keld, R., et al., *The ERK MAP kinase-PEA3/ETV4-MMP-1 axis is operative in oesophageal adenocarcinoma.* Molecular Cancer, 2010. **9**.
52. Funaoka, K., et al., *Activation of the p21(Waf1/Cip1) promoter by the ets oncogene family transcription factor E1AF.* Biochemical and Biophysical Research Communications, 1997. **236**(1): p. 79-82.
53. Zhang, C., et al., *Ets-1 protects vascular smooth muscle cells from undergoing apoptosis by activating p21WAF1/Cip1: ETS-1 regulates basal and and inducible p21WAF1/Cip: ETS-1 regulates basal and inducible p21WAF1/Cip1 transcription via distinct cis-acting elements in the p21WAF/Cip1 promoter.* J Biol Chem, 2003. **278**(30): p. 27903-9.
54. Albanese, C., et al., *Transforming p21ras mutants and c-Ets-2 activate the cyclin D1 promoter through distinguishable regions.* J Biol Chem, 1995. **270**(40): p. 23589-97.
55. Bamberger, A.M., et al., *Expression pattern of the AP-1 family in endometrial cancer: correlations with cell cycle regulators.* Journal of Cancer Research and Clinical Oncology, 2001. **127**(9): p. 545-550.
56. Ropponen, K.M., et al., *p22/WAF1 expression in human colorectal carcinoma: association with p53, transcription factor AP-2 and prognosis.* Br J Cancer, 1999. **81**(1): p. 133-40.
57. Timchenko, N.A., et al., *Regenerating livers of old rats contain high levels of C/EBPalpha that correlate with altered expression of cell cycle associated proteins.* Nucleic Acids Res, 1998. **26**(13): p. 3293-9.
58. Chinery, R., et al., *Antioxidants enhance the cytotoxicity of chemotherapeutic agents in colorectal cancer: a p53-independent induction of p21WAF1/CIP1 via C/EBPbeta.* Nat Med, 1997. **3**(11): p. 1233-41.
59. Puri, P.L., et al., *P300 is required for MyoD-dependent cell cycle arrest and muscle-specific gene transcription.* Embo Journal, 1997. **16**(2): p. 369-383.
60. Perkins, N.D., et al., *Regulation of NF-kappaB by cyclin-dependent kinases associated with the p300 coactivator.* Science, 1997. **275**(5299): p. 523-7.
61. Herblot, S., P.D. Aplan, and T. Hoang, *Gradient of E2A activity in B-cell development.* Mol Cell Biol, 2002. **22**(3): p. 886-900.
62. Inoue, N., et al., *Lipid synthetic transcription factor SREBP-1a activates p21WAF1/CIP1, a universal cyclin-dependent kinase inhibitor.* Mol Cell Biol, 2005. **25**(20): p. 8938-47.
63. Li, D.W., et al., *P150(Sal2) is a p53-independent regulator of p21WAF1/CIP.* Molecular and Cellular Biology, 2004. **24**(9): p. 3885-3893.
64. Mori, K., et al., *A HIC-5- and KLF4-dependent mechanism transactivates p21(Cip1) in response to anchorage loss.* J Biol Chem, 2012. **287**(46): p. 38854-65.
65. Nyormoi, O. and M. Bar-Eli, *Transcriptional regulation of metastasis-related genes in human melanoma.* Clin Exp Metastasis, 2003. **20**(3): p. 251-63.
66. Xie, W., et al., *MDA468 growth inhibition by EGF is associated with the induction of the cyclin-dependent kinase inhibitor p21WAF1.* Anticancer Res, 1997. **17**(4A): p. 2627-33.
67. Gartel, A.L., et al., *Sp1 and Sp3 activate p21 (WAF1/CIP1) gene transcription in the Caco-2 colon adenocarcinoma cell line.* Oncogene, 2000. **19**(45): p. 5182-8.
68. Moustakas, A. and D. Kardassis, *Regulation of the human p21/WAF1/Cip1 promoter in hepatic cells by functional interactions between Sp1 and Smad family members.* Proceedings

of the National Academy of Sciences of the United States of America, 1998. **95**(12): p. 6733-6738.
69. Cao, H., et al., *Tbx1 regulates progenitor cell proliferation in the dental epithelium by modulating Pitx2 activation of p21.* Dev Biol, 2010. **347**(2): p. 289-300.
70. Fasano, C.A., et al., *shRNA knockdown of Bmi-1 reveals a critical role for p21-Rb pathway in NSC self-renewal during development.* Cell Stem Cell, 2007. **1**(1): p. 87-99.
71. Kitaura, H., et al., *Reciprocal regulation via protein-protein interaction between c-Myc and p21(cip1/waf1/sdi1) in DNA replication and transcription.* J Biol Chem, 2000. **275**(14): p. 10477-83.
72. Stepniak, E., et al., *c-Jun/AP-1 controls liver regeneration by repressing p53/p21 and p38 MAPK activity.* Genes Dev, 2006. **20**(16): p. 2306-14.
73. Chou, Y.T., et al., *CITED2 functions as a molecular switch of cytokine-induced proliferation and quiescence.* Cell Death and Differentiation, 2012. **19**(12): p. 2015-2028.
74. Neault, M., et al., *Ablation of PRMT6 reveals a role as a negative transcriptional regulator of the p53 tumor suppressor.* Nucleic Acids Research, 2012. **40**(19): p. 9513-9521.
75. Frey, M.R., et al., *Protein kinase C signaling mediates a program of cell cycle withdrawal in the intestinal epithelium.* J Cell Biol, 2000. **151**(4): p. 763-78.
76. Gil, J., et al., *Polycomb CBX7 has a unifying role in cellular lifespan.* Nature Cell Biology, 2004. **6**(1): p. 67-U19.
77. Demetrick, D.J., H. Zhang, and D.H. Beach, *Chromosomal mapping of the genes for the human CDK2/cyclin A-associated proteins p19 (SKP1A and SKP1b) and p45 (SKP2).* Cytogenetics and Cell Genetics, 1996. **73**(1-2): p. 104-107.
78. Wang, X., N.J. Hung, and R.H. Costa, *Earlier expression of the transcription factor HFH-11B diminishes induction of p21(CIP1/WAF1) levels and accelerates mouse hepatocyte entry into S-phase following carbon tetrachloride liver injury.* Hepatology, 2001. **33**(6): p. 1404-14.
79. Zheng, G. and Y.C. Yang, *ZNF76, a novel transcriptional repressor targeting TATA-binding protein, is modulated by sumoylation.* J Biol Chem, 2004. **279**(41): p. 42410-21.
80. Gottifredi, V., et al., *p53 down-regulates CHK1 through p21 and the retinoblastoma protein.* Mol Cell Biol, 2001. **21**(4): p. 1066-76.
81. Perez-Sanchez, C., V.S. Budhram-Mahadeo, and D.S. Latchman, *Distinct promoter elements mediate the co-operative effect of Brn-3a and p53 on the p21 promoter and their antagonism on the Bax promoter.* Nucleic Acids Res, 2002. **30**(22): p. 4872-80.
82. Choi, W.I., et al., *Proto-oncogene FBI-1 represses transcription of p21CIP1 by inhibition of transcription activation by p53 and Sp1.* J Biol Chem, 2009. **284**(19): p. 12633-44.
83. Coqueret, O., G. Berube, and A. Nepveu, *The mammalian Cut homeodomain protein functions as a cell-cycle-dependent transcriptional repressor which downmodulates p21(WAF1/CIP1/SDI1) in S phase.* Embo Journal, 1998. **17**(16): p. 4680-4694.
84. Tan, H.H. and A.G. Porter, *p21(WAF1) negatively regulates DNMT1 expression in mammalian cells.* Biochem Biophys Res Commun, 2009. **382**(1): p. 171-6.
85. Manzo, B.A., et al., *Helicobacter pylori regulates the expression of inhibitors of DNA binding (Id) proteins by gastric epithelial cells.* Microbes Infect, 2006. **8**(4): p. 1064-74.
86. Prince, S., et al., *Tbx2 directly represses the expression of the p21(WAF1) cyclin-dependent kinase inhibitor.* Cancer Research, 2004. **64**(5): p. 1669-1674.
87. Xie, X.L., et al., *2-Amino-3-methylimidazo[4,5-f]quinoline (IQ) promotes mouse hepatocarcinogenesis by activating transforming growth factor-beta and Wnt/beta-catenin signaling pathways.* Toxicol Sci, 2012. **125**(2): p. 392-400.
88. Bartel, D.P., *MicroRNAs: genomics, biogenesis, mechanism, and function.* Cell, 2004. **116**(2): p. 281-97.

89. Filipowicz, W., S.N. Bhattacharyya, and N. Sonenberg, *Mechanisms of post-transcriptional regulation by microRNAs: are the answers in sight?* Nat Rev Genet, 2008. **9**(2): p. 102-14.
90. Fontana, L., et al., *Antagomir-17-5p Abolishes the Growth of Therapy-Resistant Neuroblastoma through p21 and BIM.* Plos One, 2008. **3**(5).
91. Ivanovska, I., et al., *MicroRNAs in the miR-106b family regulate p21/CDKN1A and promote cell cycle progression.* Mol Cell Biol, 2008. **28**(7): p. 2167-74.
92. Kim, Y.K., et al., *Functional links between clustered microRNAs: suppression of cell-cycle inhibitors by microRNA clusters in gastric cancer.* Nucleic Acids Research, 2009. **37**(5): p. 1672-1681.
93. Li, G.R., et al., *Alterations in microRNA expression in stress-induced cellular senescence.* Mechanisms of Ageing and Development, 2009. **130**(11-12): p. 731-741.
94. Petrocca, F., et al., *E2F1-regulated microRNAs impair TGFbeta-dependent cell-cycle arrest and apoptosis in gastric cancer.* Cancer Cell, 2008. **13**(3): p. 272-86.
95. He, X.Y., et al., *Let-7a elevates p21(WAF1) levels by targeting of NIRF and suppresses the growth of A549 lung cancer cells.* Febs Letters, 2009. **583**(21): p. 3501-3507.
96. Bornstein, G., et al., *Role of the SCFSkp2 ubiquitin ligase in the degradation of p21Cip1 in S phase.* J Biol Chem, 2003. **278**(28): p. 25752-7.
97. Kim, G.Y., et al., *The stress-activated protein kinases p38 alpha and JNK1 stabilize p21(Cip1) by phosphorylation.* J Biol Chem, 2002. **277**(33): p. 29792-802.
98. Subramanyam, V., J. R, and M. Rafi, *Prevalence of overweight and obesity in affluent adolescent girls in Chennai in 1981 and 1998.* Indian Pediatr, 2003. **40**(4): p. 332-6.
99. Ng, H.H., et al., *MBD2 is a transcriptional repressor belonging to the MeCP1 histone deacetylase complex.* Nature Genetics, 1999. **23**(1): p. 58-61.
100. Davies, C., et al., *p53-independent Epigenetic Repression of the p21(WAF1) Gene in T-cell Acute Lymphoblastic Leukemia.* Journal of Biological Chemistry, 2011. **286**(43): p. 37639-37650.
101. *GE Healthcare Life Sciences. Detection Methods. 2014 [cited 2014 15.04]; Available from: http://www.gelifesciences.com/webapp/wcs/stores/servlet/catalog/en/GELifeSciences/products/detection-methods/.*
102. Mackenzie Ross, A.D., et al., *Senescence evasion in melanoma progression: uncoupling of DNA-damage signaling from p53 activation and p21 expression.* Pigment Cell Melanoma Res, 2013. **26**(2): p. 226-35.
103. Maelandsmo, G.M., et al., *Cyclin kinase inhibitor p21WAF1/CIP1 in malignant melanoma: reduced expression in metastatic lesions.* Am J Pathol, 1996. **149**(6): p. 1813-22.
104. Di Leonardo, A., et al., *DNA damage triggers a prolonged p53-dependent G1 arrest and long-term induction of Cip1 in normal human fibroblasts.* Genes Dev, 1994. **8**(21): p. 2540-51.
105. el-Deiry, W.S., et al., *WAF1, a potential mediator of p53 tumor suppression.* Cell, 1993. **75**(4): p. 817-25.
106. Weiss, J., et al., *Mutation and expression of the p53 gene in malignant melanoma cell lines.* Int J Cancer, 1993. **54**(4): p. 693-9.
107. Jung, Y.S., Y. Qian, and X. Chen, *Examination of the expanding pathways for the regulation of p21 expression and activity.* Cell Signal, 2010. **22**(7): p. 1003-12.
108. Fidler, I.J., *Biological heterogeneity of cancer: implication to therapy.* Hum Vaccin Immunother, 2012. **8**(8): p. 1141-2.
109. Michieli, P., et al., *Induction of WAF1/CIP1 by a p53-independent pathway.* Cancer Res, 1994. **54**(13): p. 3391-5.
110. Roskoski, R., Jr., *Signaling by Kit protein-tyrosine kinase--the stem cell factor receptor.* Biochem Biophys Res Commun, 2005. **337**(1): p. 1-13.

111. Alonso, S.R., et al., *Progression in cutaneous malignant melanoma is associated with distinct expression profiles - A tissue microarray-based study.* American Journal of Pathology, 2004. **164**(1): p. 193-203.
112. Senturk, S., et al., *Transforming growth factor-beta induces senescence in hepatocellular carcinoma cells and inhibits tumor growth.* Hepatology, 2010. **52**(3): p. 966-74.
113. Noda, A., et al., *Cloning of senescent cell-derived inhibitors of DNA synthesis using an expression screen.* Exp Cell Res, 1994. **211**(1): p. 90-8.
114. Michieli, P., et al., *Inhibition of oncogene-mediated transformation by ectopic expression of p21Waf1 in NIH3T3 cells.* Oncogene, 1996. **12**(4): p. 775-84.
115. Missero, C., et al., *The absence of p21Cip1/WAF1 alters keratinocyte growth and differentiation and promotes ras-tumor progression.* Genes Dev, 1996. **10**(23): p. 3065-75.
116. Campisi, J., *Aging, cellular senescence, and cancer.* Annu Rev Physiol, 2013. **75**: p. 685-705.
117. Roninson, I.B., *Tumor cell senescence in cancer treatment.* Cancer Res, 2003. **63**(11): p. 2705-15.
118. Roninson, I.B. and M. Dokmanovic, *Induction of senescence-associated growth inhibitors in the tumor-suppressive function of retinoids.* J Cell Biochem, 2003. **88**(1): p. 83-94.

APPENDIX A

Buffers and solutions used in the study

Table A1. *Complete growth medium supplements.*

Supplement	**Concentration**	**Per 500 ml RPMI 1640 without L-Glutamine**
Fetal bovine serum	10%	50 ml
glutaMAX	2 mM	5.5 ml of 200 mM stock

Table A2. *Freeze medium supplements.*

Supplement	**Concentration**	**Per 50 ml complete growth medium**
Fetal bovine serum	20%	5 ml
DMSO	10%	5 ml

Table A3. *Preparation of protein samples for gel electrophoresis.*

Compound	**Volume (µl)**
Sample	X
de-ionized water	to 6.5
NuPAGE LDS sample buffer (4X)	2.5
NuPAGE Reducing Agent (10X)	1
Total	10

Table A4. *Contents of wash buffer 0.1 % TBS-T (TBS with 0.1% Tween 20).*

Compound	**Volume (ml)**
5 M NaCl	27.5
1 M Tris-HCl PH 7.5	20
20 % Tween 20	5
ddH2O	To 1000

APPENDIX B

Real time PCR data

Table B1. *Primer sequences for qPCR.*

Gene	Forward primer (5'-3')	Reverse primer (5'-3')
CBX7	TGG GTT TCG GAC CTC TCT T	CGT CAT GGC CTA CGA GGA
CDC6	GTGTTGCATAGGTTGTCATC G	CCTGTTCTCCTCGTGTAAAAG C
CDKN1A (p21)	CGA-AGT-CAG-TTC-CTT-GTG-GAG	CAT-GGG-TTC-TGA-CGG-ACA-T
CITED2	CAG CAC ATA GAG GGG ACC TT	AGG GGA AAT AAA AGG GAA CG
c-Myc	TAACGTTGAGGGGCATCG	GCTGCTTAGACGCTGGATTT
ELK4	TGA ATG GCC CAT GAC TGT T	CAG TCC TGT TGC TCC CCT AA
EP300	AAA CAG CCA TCA CAG ACG AA	GAT CTG TGT CCT TCA CCA TGA G
ID2	GTT GTT GTT GTG CAA AGA ATA AAA G	TGT CAA ATG ACA GCA AAG CAC
ID3	CCT CCG GCA GGA GAG GTT	CAT CTC CAA CGA CAA AAG GAG
MITF-m	CAT-TGT-TAT-GCT-GGA-AAT-GCT-AGA	GCT AAA GTG GTA GAA AGG TAC TGC
PRMT6	CCC ACG TCC AGT ACC GTC T	ACC GCC TGG GTA TCC TTC
RPLPO	TCG-AAC-ACC-TGC-TGG-ATG-AC	CGC-TGC-TGA-ACA-TGC-TCA-AC
SALL2	ACC AGC TGA GCA GAA AGG TC	ATT GCA GCC TAG CCA AAA AG
SP1	TCC ACC TGC TGT GTC ATC AT	CTA TAG CAA ATG CCC CAG GT
SP3	GGT GAC GGC TGA GTG TCC	CAG CAGCAG CAA CAG CAC
TBP	GCC-CGA-AAC-GCC-GAA-TAT	CGT-GGC-TCT-CTT-ATC-CTC-ATG-A
TBX2	CACTAGTGGCGGGCAAAG	GCACATGCTGGCATCTCA
TBX3	ACT GCA GGG TGA GCT GTT TT	AAA AAT AGA CAA CAA CCC TTT TGC

TFAP2A (AP-2alpha)	AGG GGA GAT CGG TCC TGA	ACA TGC TCC TGG CTA CAA AAC
TFAP2C (AP-2gamma)	GGG GCT GTA GAG GTG CTG	CGA AGA GGA CTG CGA GGA

Primer efficiencies

a)

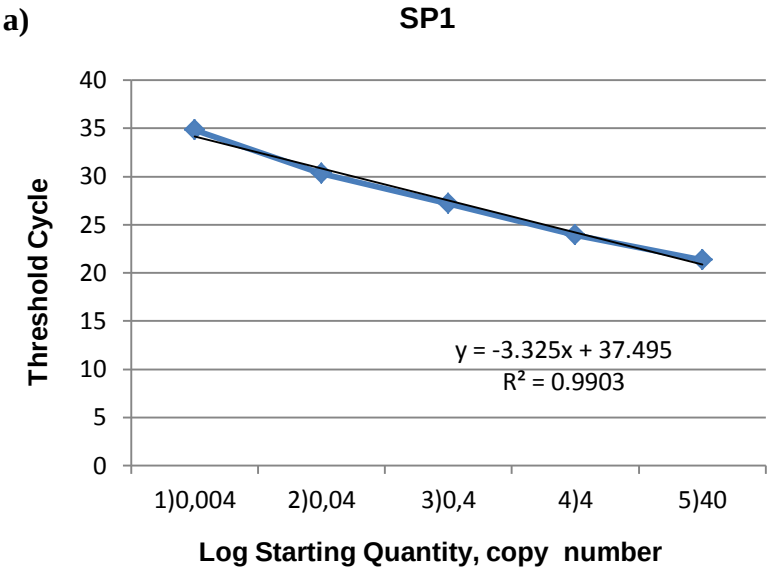

b)

Sample (ng/µl)	Ct mean
1) 0.004	34.8
2) 0.04	30.3
3) 0.4	27.2
4) 4	23.95
5) 40	21.35

Figure B2. *Generating a standard curve to assess reaction optimization. a) A standard curve was generated using a 10-fold dilution of the MEWO as a template amplified on the iCycler iQ real-time system. Each dilution was assayed in duplicate. The equation for the regression line and the R value are shown in the graph. b) Dilution series and the Ct-values.*

Amplification efficiency, E, is calculated from the slope of the standard curve using the following formula:

$E = 10^{-1/slope}$

Amplification efficiency is frequently presented as a percentage, that is, the percent of template that was amplified in each cycle:

% Efficiency = (E-1) × 100%

For the example shown in figure B2:

$E\ (SP1) = 10^{-(1/-3.325)} = 1.998$

% Efficiency (SP1) = (1.998-1) × 100% = 99.87%

At the end of each cycle, the amplicon copy number increased 1.998-fold, or 99.87% of the template that was amplified.

Table B3. *Primer efficiencies for qPCR.*

Gene	**Primer efficiency**
CDC6	98.03%
CITED2	100.08%
c-Myc	102.2%
ELK4	97.63%
EP300	101.99%
ID2	102.87%
MITF-m	93.8%
p21	95.2%
RPLPO	100.1%
SP1	99.87%
SP3	92.17%
TBP	96.7%
TBX2	105.35%
TBX3	101.99%
TFAP2A (AP-2alpha)	101.78%
TFAP2C (AP-2gamma)	98.43%

For the primers with Ct-value more than 33 in serially diluted samples, the efficiency was calculated after omitting Ct mean ≥ 33 and they need to be checked on another cell line in further experiments.

Western blotting data

Table B4. *Standard curve of reference protein calculations.*

Reference protein (µg)	Reference protein (µl)	ddH_2O (µl)
0	0	10
1	0.73	9.27
2	1.46	8.54
3	2.19	7.81
4	2.92	7.08
5	3.65	6.35

The average absorbance from triplicates was calculated the background absorbance was subtracted. Using linear regression from the standard curve, an equation was deduced that could be used to calculate the protein concentration of the samples (exemplified in figure B5).

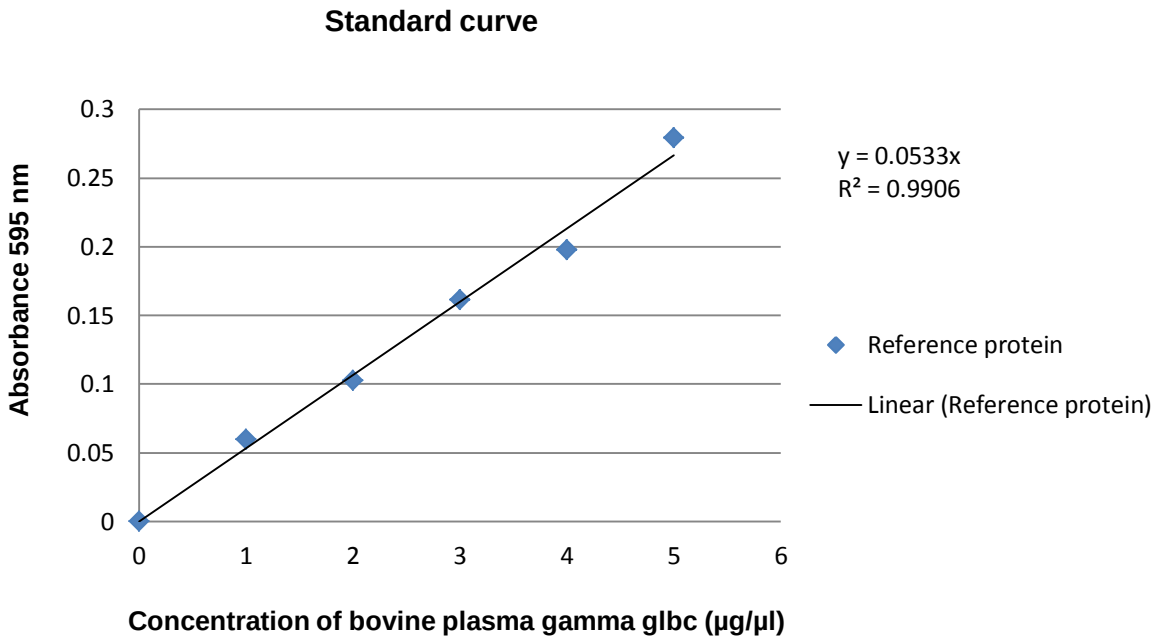

Figure B5. *A representative graph on standard curve for the calculation of protein concentrations. The measured absorbance is plotted as a function of the reference protein concentration. The equation is found by linear regression and is used to calculate protein concentrations of the samples. R^2 indicate how well the data fit into the linear regression line.*

APPENDIX C

Supplementary data

Control PLX4032 (Plexxikon) UO126 (MEK1/2)

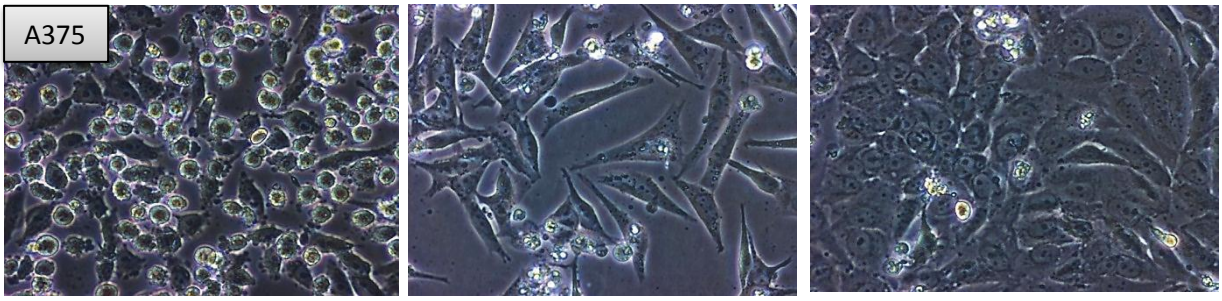

H-89 (PKA) BI-D1870 (RSK)

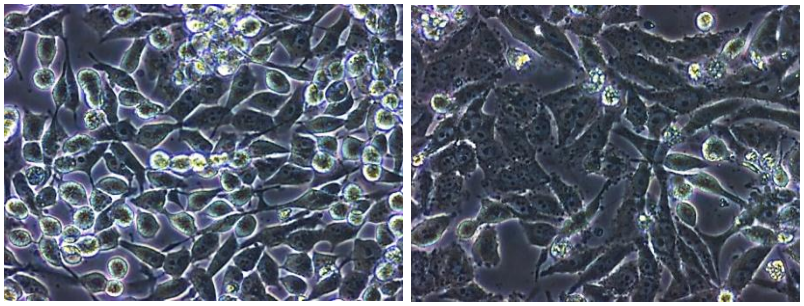

Control PLX4032 (Plexxikon) UO126 (MEK1/2)

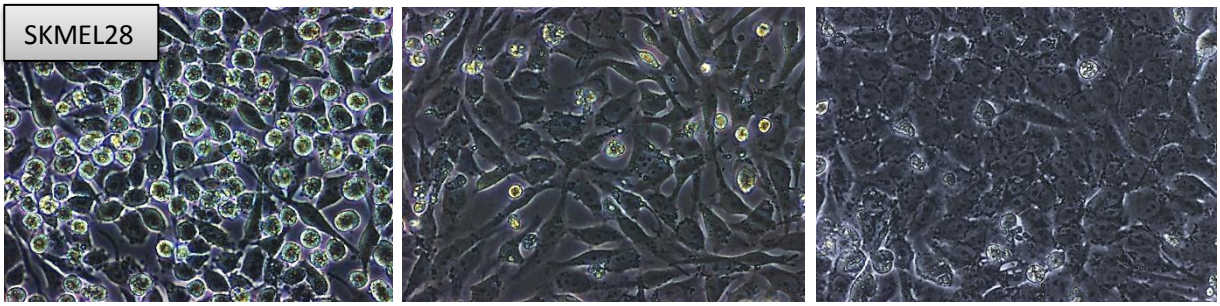

H-89 (PKA) BI-D1870 (RSK)

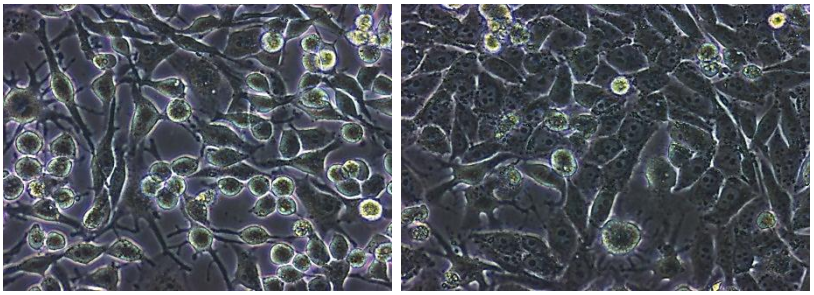

Figure C1. *Microscopy pictures of A375 and SKMEL28 cell lines when treated with 10 µM Plexxikon, MEK1/2, PKA, RSK inhibitors. The pictures shown are representative for three biological parallels.*

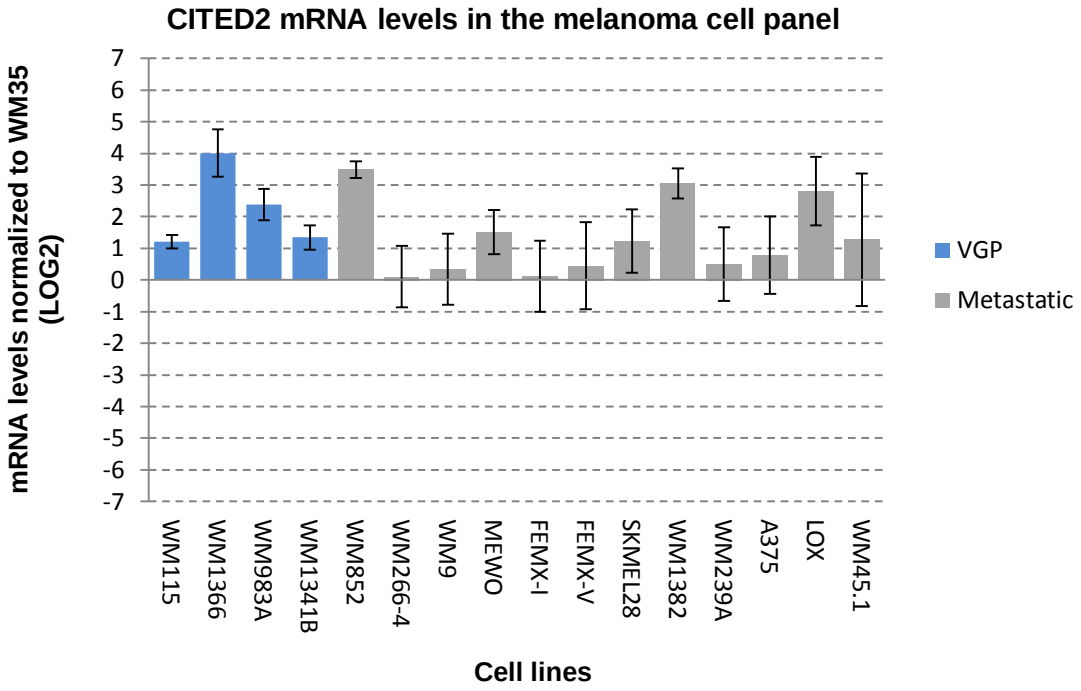

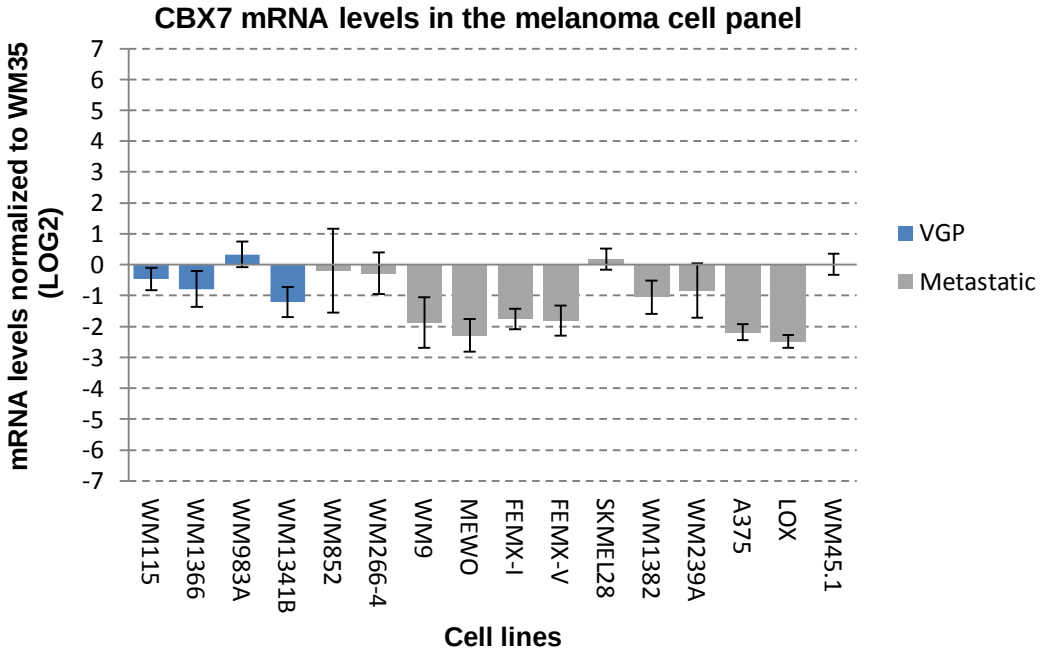

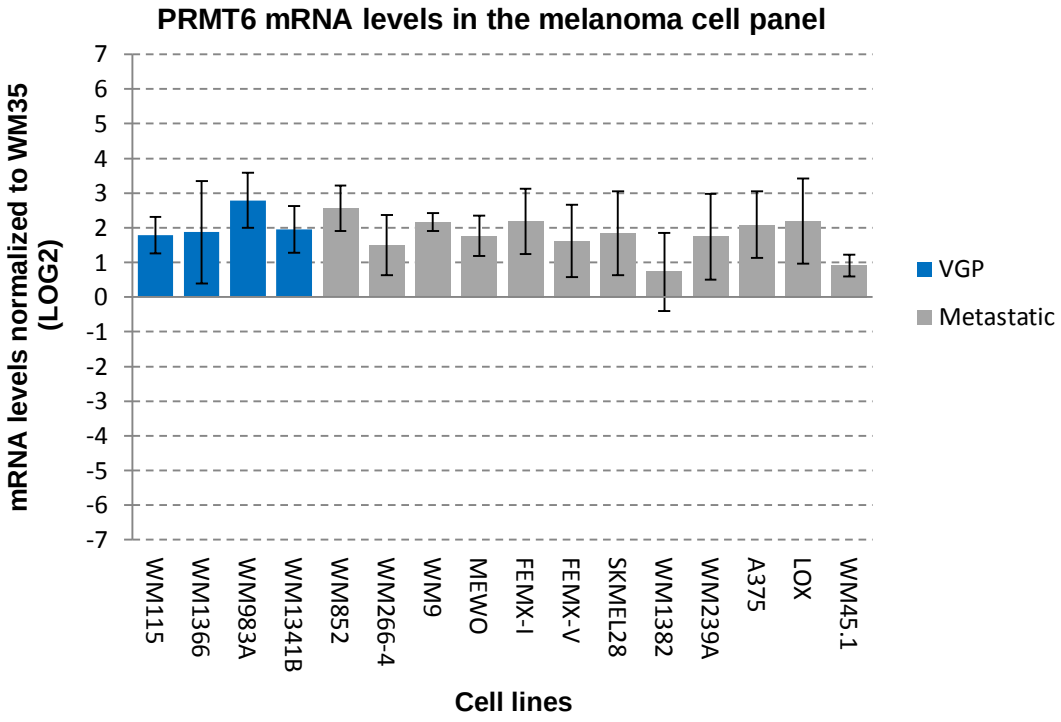
PRMT6 mRNA levels in the melanoma cell panel
mRNA levels normalized to WM35 (LOG2)
7
6
5
4
3
2
1
0
-1
-2
-3
-4
-5
-6
-7
WM115
WM1366
WM983A
WM1341B
WM852
WM266-4
WM9
MEWO
FEMX-I
FEMX-V
SKMEL28
WM1382
WM239A
A375
LOX
WM45.1
Cell lines
VGP
Metastatic

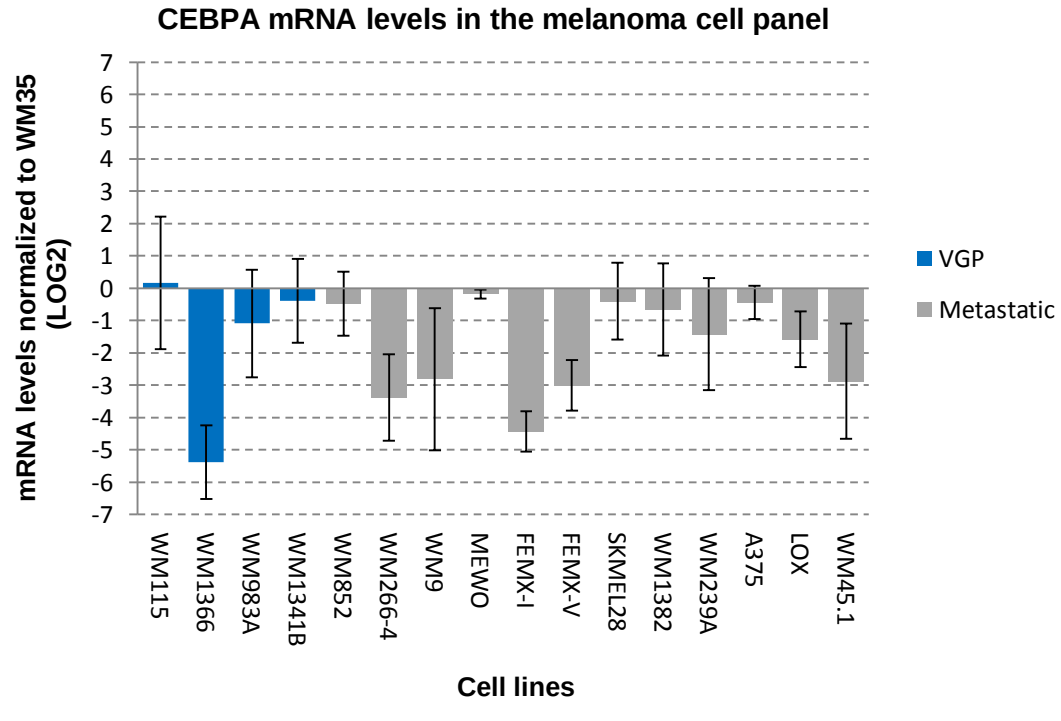
CEBPA mRNA levels in the melanoma cell panel
mRNA levels normalized to WM35 (LOG2)
7
6
5
4
3
2
1
0
-1
-2
-3
-4
-5
-6
-7
WM115
WM1366
WM983A
WM1341B
WM852
WM266-4
WM9
MEWO
FEMX-I
FEMX-V
SKMEL28
WM1382
WM239A
A375
LOX
WM45.1
Cell lines
VGP
Metastatic

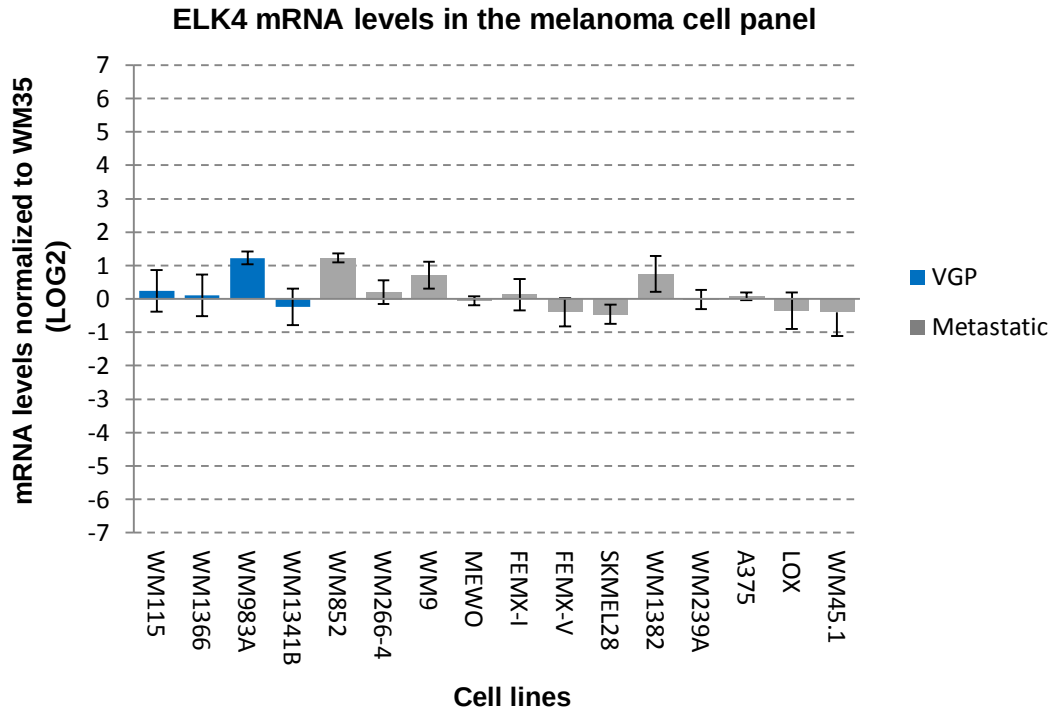
ELK4 mRNA levels in the melanoma cell panel
mRNA levels normalized to WM35 (LOG2)
7
6
5
4
3
2
1
0
-1
-2
-3
-4
-5
-6
-7
WM115
WM1366
WM983A
WM1341B
WM852
WM266-4
WM9
MEWO
FEMX-I
FEMX-V
SKMEL28
WM1382
WM239A
A375
LOX
WM45.1
Cell lines
VGP
Metastatic

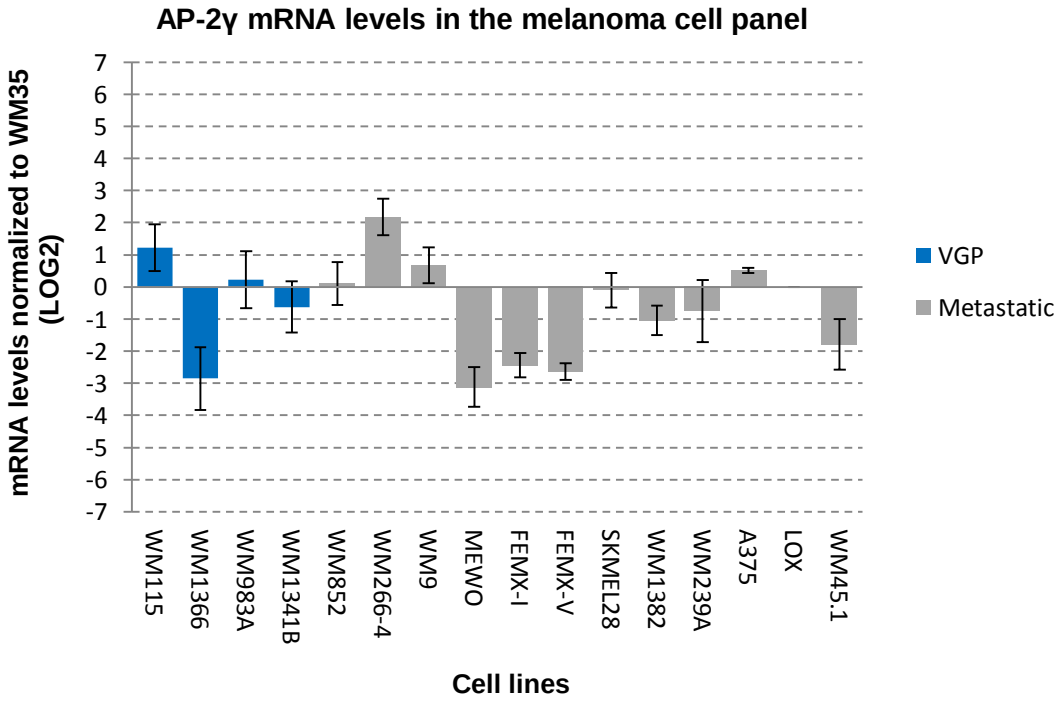
AP-2γ mRNA levels in the melanoma cell panel
mRNA levels normalized to WM35 (LOG2)
7
6
5
4
3
2
1
0
-1
-2
-3
-4
-5
-6
-7
WM115
WM1366
WM983A
WM1341B
WM852
WM266-4
WM9
MEWO
FEMX-I
FEMX-V
SKMEL28
WM1382
WM239A
A375
LOX
WM45.1
Cell lines
VGP
Metastatic

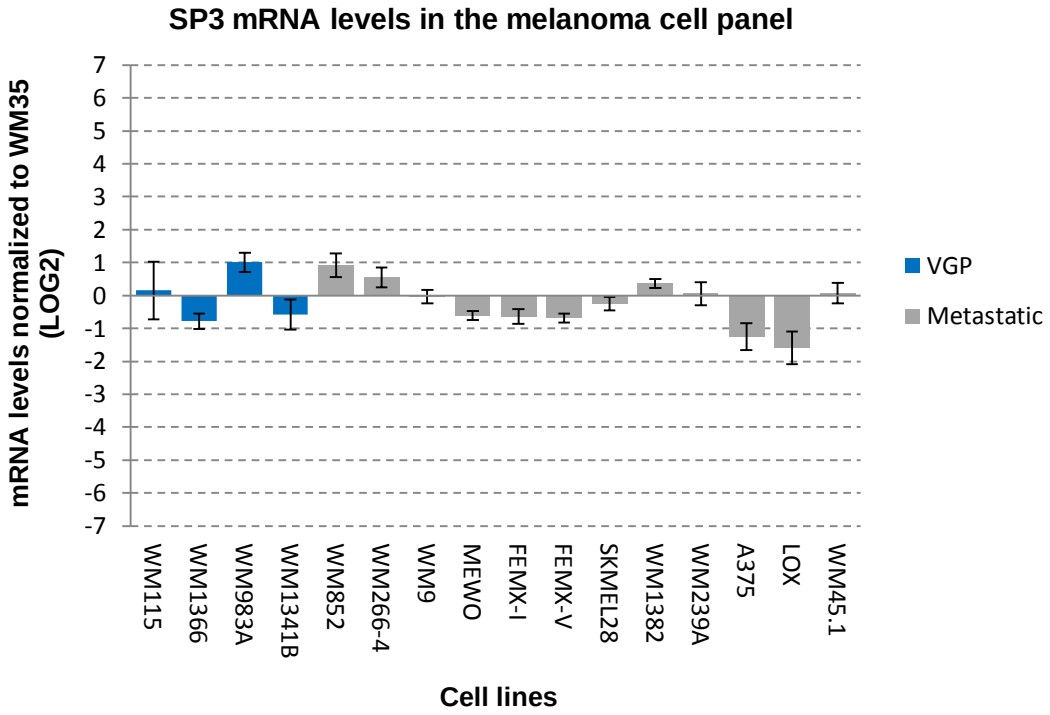
SP3 mRNA levels in the melanoma cell panel
mRNA levels normalized to WM35 (LOG2)
7
6
5
4
3
2
1
0
-1
-2
-3
-4
-5
-6
-7
WM115
WM1366
WM983A
WM1341B
WM852
WM266-4
WM9
MEWO
FEMX-I
FEMX-V
SKMEL28
WM1382
WM239A
A375
LOX
WM45.1
Cell lines
VGP
Metastatic

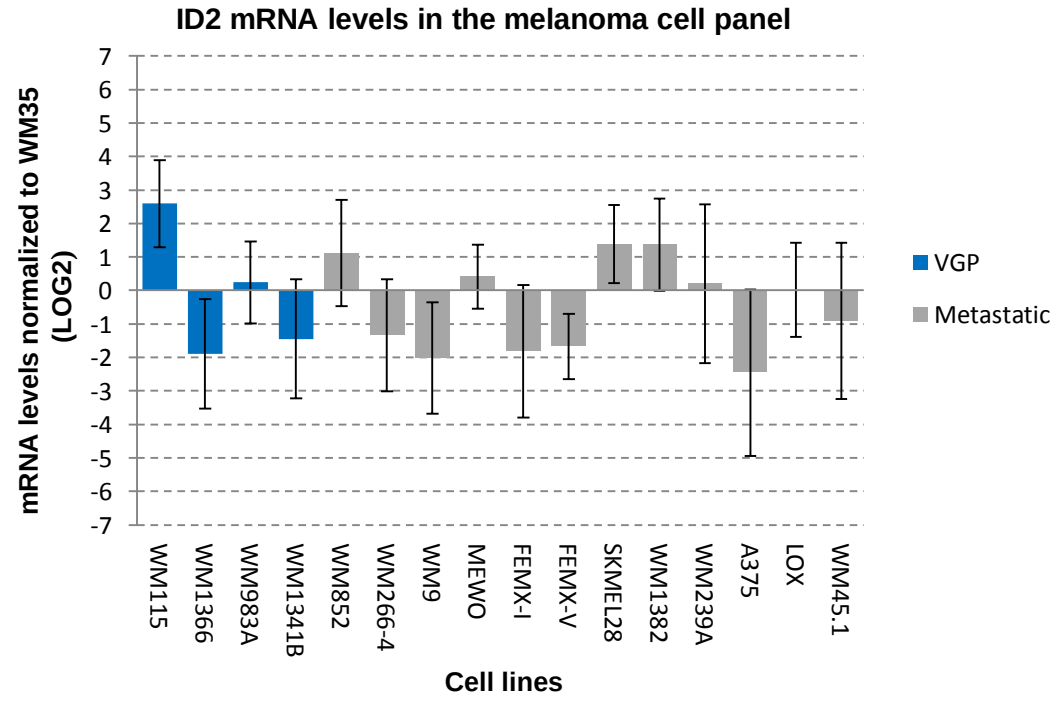
ID2 mRNA levels in the melanoma cell panel
mRNA levels normalized to WM35 (LOG2)
7
6
5
4
3
2
1
0
-1
-2
-3
-4
-5
-6
-7
WM115
WM1366
WM983A
WM1341B
WM852
WM266-4
WM9
MEWO
FEMX-I
FEMX-V
SKMEL28
WM1382
WM239A
A375
LOX
WM45.1
Cell lines
VGP
Metastatic

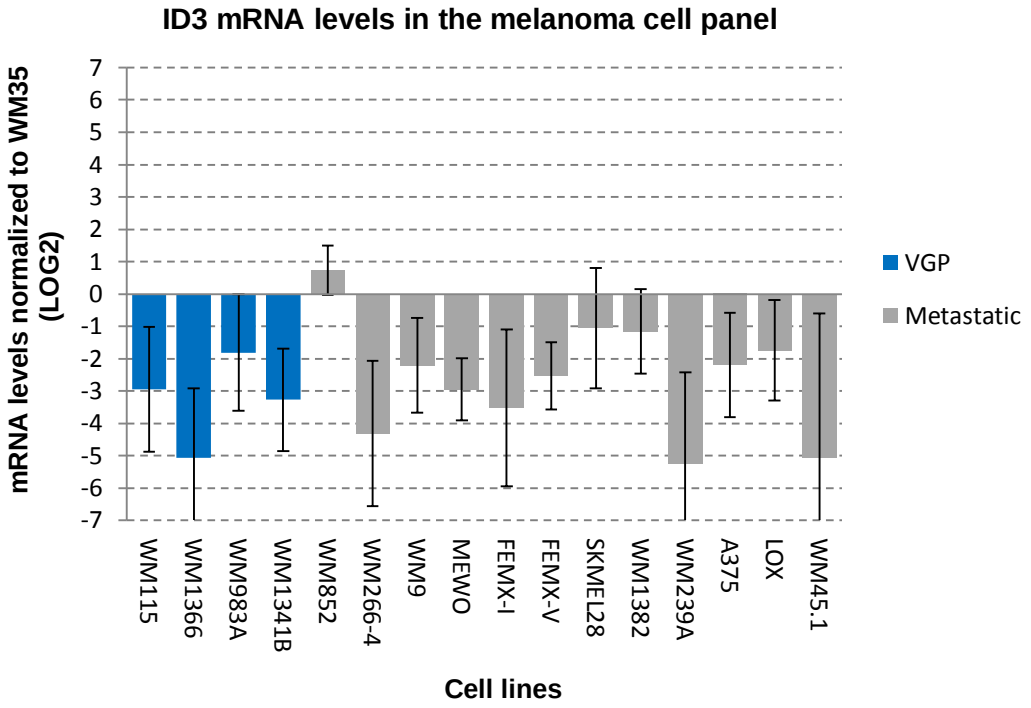
ID3 mRNA levels in the melanoma cell panel
mRNA levels normalized to WM35 (LOG2)
7
6
5
4
3
2
1
0
-1
-2
-3
-4
-5
-6
-7
WM115
WM1366
WM983A
WM1341B
WM852
WM266-4
WM9
MEWO
FEMX-I
FEMX-V
SKMEL28
WM1382
WM239A
A375
LOX
WM45.1
Cell lines
VGP
Metastatic

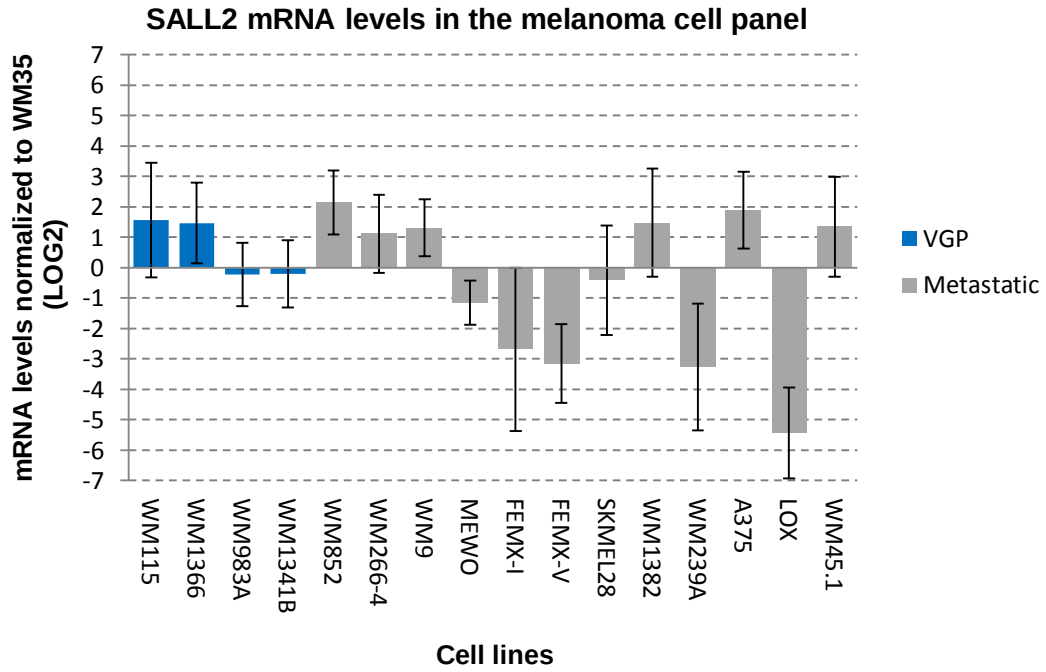
SALL2 mRNA levels in the melanoma cell panel
mRNA levels normalized to WM35 (LOG2)
7
6
5
4
3
2
1
0
-1
-2
-3
-4
-5
-6
-7
WM115
WM1366
WM983A
WM1341B
WM852
WM266-4
WM9
MEWO
FEMX-I
FEMX-V
SKMEL28
WM1382
WM239A
A375
LOX
WM45.1
Cell lines
VGP
Metastatic

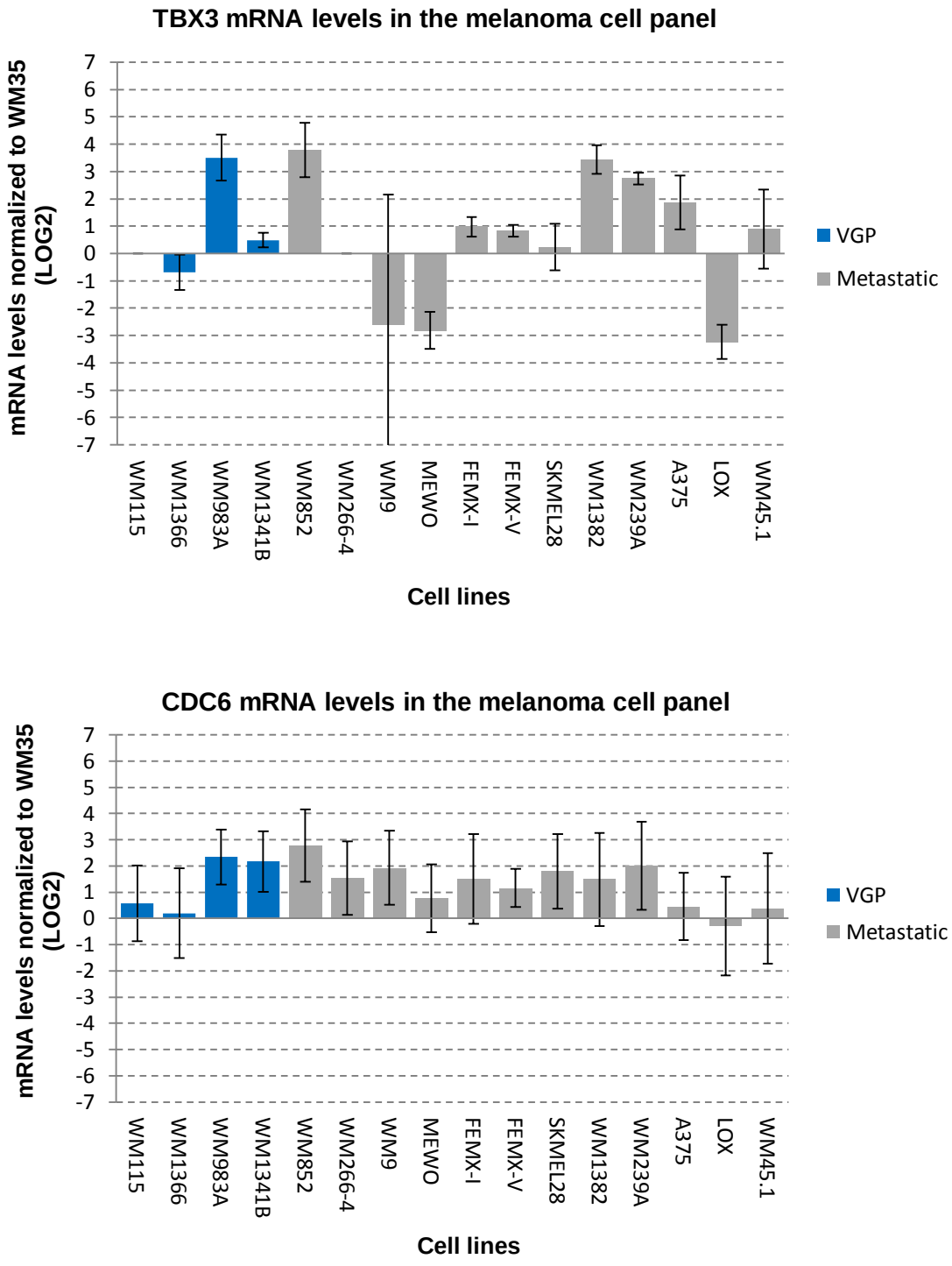

Figure C2. *Real-time RT-PCR data showing mRNA expression levels of CITED2, CBX7, PRMT6, CEBPA, ELK4, AP-2γ, SP-3, ID2, ID3, SALL2, TBX3, CDC6 in the melanoma cell panel. Data is presented as LOG2 and cell lines were normalized to WM35 (a cell line from the RGP stage). Blue bars represent VGP cell lines, while grey bars represent metastatic cell lines. Error bars represent standard deviation (SD) from three biological parallels.*